MicroRNAs as Specificity Determinants in Autoregulation of Nodulation

Dissertation

der Mathematisch-Naturwissenschaftlichen Fakultät

der Eberhard Karls Universität Tübingen

zur Erlangung des Grades eines

Doktors der Naturwissenschaften

(Dr. rer. nat.)

vorgelegt von

M. Sc. Caroline Wall

aus Ehingen

Tübingen

2022

Gedruckt mit Genehmigung der Mathematisch-Naturwissenschaftlichen Fakultät der Eberhard Karls Universität Tübingen.

Tag der mündlichen Qualifikation:	06.03.2023
Dekan:	Prof. Dr. Thilo Stehle
1. Berichterstatter/-in:	Prof. Dr. Katharina Markmann
2. Berichterstatter/-in:	Prof. Dr. Klaus Harter

Acknowledgements

I would like to thank my supervisor Professor Katharina Markmann, for the opportunity to work on such an interesting project. She helped me a lot with creative discussions and many suggestions and guided me through my whole journey as PhD student.

I would like to thank Marja Timmermans and Farid El Kasmi who were part of my TAC committee. They provided many helpful ideas and suggestions for my project.

I wish to thank Moritz Sexauer for his great help during the first analysis of small RNA sequencing. Furthermore, his expertise and help in many experimental problems was highly appreciated.

Next, I would like to thank Ulrike Herzog. Without her help in genotyping hundreds of plants, my project would not have been possible.

Special thanks go to Hemal Bhasin who was in the lab when I started my PhD. She helped me with the first steps in the lab and more than once solved experimental problems. What I know today I have learned from her.

Many thanks go to my group members Maria Schön, Martin Hack, Michael Mauch, Adrián Vojtassák and Elena Roitsch for a great working atmosphere.

I wish to thank Jennifer Jaufmann, Sruthi Sunil and Alexandra Ehinger. Their encouragement and help in scientific discussions provided several solutions to problems I have faced.

Special thanks goes to Johanna Schröter and the whole team of gardeners, for providing so much help with seed harvest.

Further, I would like to thank Caterina Brancato for her great help in whole plant transformation.

Last, I would like to thank Felix Lössl. He always listened to my problems and gave me support whenever I doubted myself. Without his aid, this whole journey would not have been possible.

Abstract

Under N-limiting soil condition legumes display a fitness advantage, because the plants can acquire nitrogen with help of nitrogen fixing rhizobia inducing symbiosis. During symbiosis a specialized organ called nodule is developed, which is energy intense for the plant. Therefore, a tightly regulated feedback loop termed autoregulation of nodulation (AON) is essential to balance nodule number. One important factor in AON is the shoot-derived inhibitor, which accumulates in AON activated leaf tissue and systemically moves to the roots inhibiting further nodulation. Here we show that *Lotus japonicus* miR171c fulfills SDI criteria like dependence on the receptor-like kinase gene *HYPERNODULATION ABERRANT ROOT FORMATION 1* (*HAR1*), expression in shoot phloem and systemic travel. miR171c is further shown to be involved in nitrate mediated inhibition of nodulation.

Using small RNA sequencing, we show that *Lotus japonicus* miR171c is highly expressed in AON activated (CLE-RS3 OX) and dramatically reduced in AON-inhibited (*har1-3*) plants. miR171c is specifically expressed in shoot phloem cells and systemically travels to the roots. miR171c loss-of-function (ko) mutants generated using CRISPR/Cas9-technology revealed that miR171c is not only involved in AON but also in nitrate dependent inhibition of nodulation. Specifically, miR171c ko plants are insensitive to nitrate-dependent inhibition of nodulation, developing nodules despite high nitrate concentration. In contrast, miR171c overexpression (ox) plants partially inhibit nodulation and are hypersensitive to nitrate application. Moreover, miR171c is systemically and locally induced in shoots and roots upon nitrate as well as rhizobia treatment. Nitrate and rhizobia induced miR171c in the shoot is *HAR1* dependent. Taken together, our data show that miR171c fulfills key SDI criteria and acts in both rhizobia- and nitrate dependent inhibition of nodulation.

Zusammenfassung

Unter N-limitierenden Bodenverhältnissen haben Leguminosen einen Fitnessvorteil. Die Pflanzen nehmen Stickstoff mit Hilfe von stickstofffixierenden Rhizobien auf, welche eine Symbiose induzieren. Während der Symbiose muss ein spezialisiertes Organ (Knöllchen) entwickelt werden; dieser Prozess ist jedoch sehr energieaufwendig. Daher ist eine streng regulierte Rückkopplungsschleife wie die Autoregulation der Knöllchenbildung (AON) unerlässlich, um die Anzahl der Knöllchen zu regulieren. Ein wichtiger Faktor bei AON ist der aus dem Spross stammende Inhibitor, der sich in AON-aktiviertem Blattgewebe anreichert und sich systemisch zu den Wurzeln bewegt. Hierdurch wird weitere Knöllchenbildung gehemmt. Hier zeigen wir, dass *Lotus japonicus* miR171c die SDI-Kriterien wie *HYPERNODULATION ABERRANT ROOT FOTMATION 1* (HAR1) -Abhängigkeit, Expression im Sprossphloem und systemische Wanderung erfüllt und auch an der Nitrat-vermittelten Hemmung der Knöllchenbildung beteiligt ist.

Mittels RNA-Sequenzierung zeigen wir, dass *Lotus japonicus* miR171c in AON-aktivierten Pflanzen (CLE-RS3 OX) stark exprimiert und in AON-inhibierten Pflanzen (*har1-3*) dramatisch reduziert wird. miR171c wird spezifisch in Spross-Phloemzellen exprimiert und wandert systemisch zu den Wurzeln. miR171c knockout Mutanten generiert durch CRISPR/Cas9 zeigen, dass miR171c nicht nur an der AON, sondern auch an der nitratabhängigen Hemmung der Nodulation beteiligt ist. miR171c KO Pflanzen sind unempfindlich gegenüber der Nitrat-abhängigen Inhibierung der Knöllchenbildung und entwickeln trotz hoher Nitratkonzentration Knöllchen. Überexpression von miR171c führt hingegen zu einer teilweisen Hemmung der Knöllchenbildung und die Pflanzen zeigen zudem eine Hypersensitivität auf Nitratzugabe. Darüber hinaus wird miR171c sowohl bei Nitrat- als auch bei Rhizobienbehandlung systemisch und lokal im Spross und der Wurzel induziert. Nitrat- und Rhizobien-induziertes miR171c im Spross ist HAR1-abhängig. Zusammengenommen erfüllt miR171c die SDI-Kriterien und wirkt in der AON, wie auch in der nitratabhängigen Hemmung der Knöllchenbildung.

List of abbreviations

Abbreviation	Definition
AM	Arbuscular Mycorrhiza
AON	Autoregulation of Nodulation
ARF	Auxin Response Factor
CRISPR	Clustered Reg. Interspaced Short Palindromic Repeats
D	Days
DCL	Dicer-like
dpi	Days Post Inoculation/Infection
GUS	Beta-glucuronidase
gRNA	guide RNA
KO	knockout
Lj; Lotus	*Lotus japonicus*
M. loti	*Mesorhizobium loti*
OX	overexpression
MIR	miRNA gene
miRNA	Micro RNA
Mt; Medicago	*Medicago truncatula*
phasiRNA	phased siRNA
pUBQ1	LjUbiquitin1 promoter
SDI	Shoot Derived Inhibitor
Seq	Sequencing
siRNA	short interfering RNA
sRNA	small RNA
SSAP	Sequence-Specific Amplification Polymorphism
STTM	Short Tandem Target Mimic

Table of contents

List of figures

List of tables

List of supplemental figures

1 Introduction

1.1. Legumes form symbiotic interactions in their roots

The development and growth of plants is dependent on the uptake of minerals from the soil. Nutrients that limit plant performance are mainly nitrogen (N) and phosphorus (P), which are important for the plant as elements for essential amino acids, nucleic acids and chlorophyll. Legumes like *Lotus japonicus* that form symbiosis with fungi or bacteria display a fitness advantage in specific soil environments where nitrogen and phosphorus are scarce. *Lotus japonicus* can form symbiotic interactions with arbuscular mycorrhiza (AM) fungi in order to efficiently acquire phosphorus as well as nitrogen from the soil. During nodulation symbiosis with rhizobial bacteria, aerial di-nitrogen is fixed in specialized organs called nodules. In both associations, the interaction between plant and symbiont is mutually beneficial if well-balanced, where the symbiont facilitates access to nitrogen or phosphorus, and the plant in exchange provides photosynthesis products as well as mineral nutrients.

More than 80% of land plants are able to establish AM symbiosis (Parniske, 2008) but only a defined group of plants have evolved the capacity to perform root nodule symbiosis (RNS). Both symbioses share common genes that are dually required for AM and RNS. The signal transduction taking place in AM and RNS with shared genes is called "common symbiotic pathway" (Catoira et al., 2000). Based on the common symbiotic signaling that occurs directly after perception of symbionts, it is suggested that RNS has evolved from AM (Duc et al., 1989; Markmann and Parniske, 2009; Wang et al., 2010). The resemblance of signal molecules like Nod factors in RNS and Myc factors in AM, support the idea of a co-opted symbiosis system (Spaink et al., 1991; Maillet et al., 2011).

Root nodule symbiosis starts with secretion of plant flavonoids which trigger the production of specific signaling molecules (Nod factors) secreted from the rhizobia. In *Lotus japonicus*, the respective symbiont is called *Mesorhizobium loti.* The plant is able to recognize the signal and triggers a cascade of downstream responses. Rhizobia can enter the plant cell via crack entries in the root epidermis or intracellularly through root hairs forming infection threads (IT). The plant starts transcriptional reprogramming of the cortex cells, leading to nodule formation. Rhizobia invade the developing nodules and form symbiosomes, where nitrogen fixation

takes place. *Lotus japonicus* and soybean for example form two different types of nodules that are termed "determinate" and "indeterminate", respectively. Determinate nodules in *Lotus japonicus* are of spherical shape and lack a persistent nodule meristem. Plants like *Medicago truncatula* or soybean which develop "indeterminate" nodules display a persistent nodule meristem which shows similarity to lateral roots development (Crespi and Frugier, 2008).

1.2. Initiation of root nodule symbiosis

Under N-limiting soil condition the legume plants release metabolites so called "flavonoids" (Liu and Murray, 2016). These root exudates confer host specificity to compatible rhizobial symbionts (Bolaños-Vásquez and Werner, 1997). Flavonoids can interact with the rhizobial NodD protein, a transcription factor which triggers the production of lipochitooligosaccharide Nod factors (Peters et al., 1986; Lerouge et al., 1990). In *Lotus japonicus* Nod factors are perceived and bound by NOD FACTOR RECEPTOR (NFR)1 and 5 (Limpens et al., 2003; Madsen et al., 2003). *nfr1* and *nfr5* mutants do not show any morphological changes like root hair deformation or root hair curling when inoculated with rhizobia, suggesting that NFR1 and NFR5 are essential for the initial signal transduction after NOD factor perception (Madsen et al., 2003; Radutoiu et al., 2003). NFR1 and 5 are receptor kinases with three extracellular lysin motif domains (LysM) that form homo- and heteromeric complexes at the plasma membrane (Broghammer et al., 2012; Moling et al., 2014). However NFR5 can also interact with a plasma membrane leucine-rich repeat receptor like kinase (LRR-RLK) namely the symbiotic receptor kinase SYMRK (Stracke et al., 2002). SYMRK interacts with SYMRK INTERACTING PROTEINS (SIPs) and PLANT U BOX PROTEN (PUB1) and forms together with NFR1 and 5 the NOD-factor receptor complex which induces downstream signaling (Zhu et al., 2008; Chen et al., 2012; Yuan et al., 2012; Wang et al., 2013a). Apart from lipochitooligosaccharides, exopolysaccharides (EPS) are secreted from rhizobial symbionts ensuring the recognition of compatible rhizobia (Breedveld et al., 1993; Cheng and Walker, 1998). In *Lotus japonicus* EXOPOLYSACCHARIDE RECEPTEOR (EPR) 3 binds EPS directly and is able to distinguish between EPS variants (Kawaharada et al., 2015). Truncated EPS inhibits infection, suggesting that EPR3 serves as a second step control mechanism allowing only compatible rhizobia to promote infection (Kawaharada et al., 2015).

1.3. Nod factor signaling

After Nod factor perception, changes in ion flux occur, leading to depolarization of the cell membrane. Here the nuclear and perinuclear calcium concentration undergoes oscillating fluctuations, which is called calcium spiking. Apart from NFR1/5 and SYMRK, calcium spiking requires the ion channels CASTOR and POLLUX (Ané et al., 2004; Imaizumi-Anraku et al., 2005), CNGC (Cyclic nucleotide gated channel) a/b/c (Charpentier et al., 2016) and three nucleoporins NUP85 (Kanamori et al., 2006), NUP133 (Saito et al., 2007), and NENA (Groth et al., 2010). *Castor* and *pollux* mutants do not form nodules, suggesting that calcium spiking is required as a mediator for nodule organogenesis (Charpentier et al., 2008). Calcium oscillations in the cell are perceived by the calcium– calmodulin kinase CCAMK (Tirichine et al., 2006). CCAMK interacts with CYCLOPS (Yano et al., 2008), and induces downstream gene expression. It has been shown that auto-active versions of CCAMK and CYCLOPS induce spontaneous nodules (snf: spontaneous nodule formation) in the absence of rhizobia (Tirichine et al., 2006; Yano et al., 2008; Singh et al., 2014). CCAMK and CYCLOPS appear to act as crosstalk factors to form the connection between infection thread formation and nodule organogenesis.

Once the root hairs entrap compatible rhizobia and trigger the development of ITs, cell divisions of the root pericycle and cortex enable nodule primordia formation (Oldroyd et al., 2011). Nodules in *Lotus japonicus* emerge from the middle and outer cortex (Hadri et al., 1998). In order to generate different nodule tissues, anticlinal and periclinal cell divisions are required (Xiao et al., 2014).

Cytokinins are regulators of cell divisions. Cytokinin is perceived by the receptor LOTUS HISTIDINE KINASE 1 (LHK1) (Murray et al., 2007; Tirichine et al., 2007) LHK1A and LHK3 (Held et al., 2014). The gain of function mutation of LHK1 results in spontaneous formed nodules in the absence of rhizobia, however the loss of function mutants *lhk1* show hyperinfected root hairs without the ability to form nodules (Murray et al., 2007; Tirichine et al., 2007). LHK1 activates the GRAS-type transcriptions factors NODULATION SIGNALLING PATHWAY (NSP) 1 and NSP2 (Kaló et al., 2005; Smit et al., 2005; Heckmann et al., 2006; Murakami et al., 2006). In the presence of rhizobia, *nsp2* mutants do not show any morphological changes like root hair curling, infection thread formation or cortical cell

divisions necessary for nodule formation displaying the importance of NSP2 for downstream signaling (Heckmann et al., 2006; Murakami et al., 2006). NSP2 together with CYCLOPS and NSP1 activate ETHYLENE RESPONSIVE FACTOR REQUIRED FOR NODULATION 1 (ERN1) (Kawaharada et al., 2017a; Kawaharada et al., 2017b). In *ern1* mutants, bacterial entry via ITs into the root epidermis is abolished and nodule primordia are uninfected, displaying a role for coordination of IT formation and nodule primordia development (Cerri et al., 2017; Kawaharada et al., 2017a). NSP2 together with NSP1 are acting as heterodimers and induce the expression of NIN (NODULE INCEPTION) (Schauser et al., 1999; Hirsch et al., 2009), which is a key player in IT formation as well as nodule organogenesis. NIN targets the nuclear factor Y (NF-Y) A1 and NF-YB1 belonging to transcription factors which are involved in nodule meristem maintenance (Soyano et al., 2013).

1.4. Infection specific signaling pathway

To allow entry of rhizobia into the plant cell, the formation of infection threads is required (Van Spronsen et al., 1994). Therefore, the cell wall needs to degrade. The pectate –lyase encoding gene NPL is able to degrade polygalacturonic acids and pectin and therefore induces cell wall degradation (Xie et al., 2012). In *npl* plants, infections fail to progress from infection foci in curled root hair into normally developed ITs (Xie et al., 2012). Several membrane trafficking proteins like FLOT2, FLOT4 and SYMREM allow membrane remodeling. Silencing of FLOT4 and SYMREM1 causes IT elongation defects and loss of IT stability and polarity (Haney and Long, 2010; Lefebvre et al., 2010). These proteins are essential for plasma membrane invagination and inward extension (Haney and Long, 2010; Lefebvre et al., 2010). The growth of the IT towards the nodule cortex is accomplished by the "infectosome" (Liu et al., 2019). This exocyst complex comprises the protein VAPYRIN as well as LIN (LUMPY INFECTION) and EXO70 H4 (EXOCYST subunit H4) (Pumplin et al., 2010; Murray et al., 2011; Liu et al., 2019). Mutations in any of these proteins affect polar growth of IT (Liu et al., 2019).

Moreover, cytoskeletal rearrangements are required for the correct root hair tip growth and infection thread development (Timmers, 2008). Members of the SCAR/WAVE complex like NAP1 and PIR1 affect actin assembly, which is important for the extension of filaments and

therefore cell growth of IT (Yokota et al., 2009). *nap1* and *pir1* mutants have much less infection threads; the rare ITs that form are abnormal, indicating their essential role in the early infection events (Yokota et al., 2009). To ensure a correct infection process, several transcriptional changes occur. LAN (LACK OF ACOMMODATION) is required for root hair IT formation. *lan* mutants only rarely develop Its, however intercellular rhizobial invasions do occur (Suzaki et al., 2019). LAN, which is involved in the recruitment of RNA polymerase II (Suzaki et al., 2019), and AGO5 (ARGONAUTE5) encoding an argonaute protein contribute to correct symbiont accommodation and root hair bending (Reyero-Saavedra et al., 2017).

Several phytohormones have important functions in early infection events. Ethylene acts as negative regulator for both infection thread formation and nodule organogenesis (Penmetsa and Cook, 1997; Oldroyd et al., 2001). The *Lotus japonicus* double mutant *ein2aein2b* (ETHYLENE INSENSITIVE 2: EIN2) defective in ethylene perception shows a hypernodulating and hyperinfected phenotype (Miyata et al., 2013; Reid et al., 2018). Auxin was shown to positively regulate infection, and mutations in MtARF16a (AUXIN RESPONSE FACTOR 16: ARF 16) reduce the number of infection events in *Medicago truncatula* (Breakspear et al., 2014). Cytokinin is essential for IT formation. The loss of function mutant *lhk1* shows hyperinfected root hair but fails cortical cell divisions required for nodule formation (Murray et al., 2007).

1.5. Autoregulation of nodulation

Lotus japonicus displays a fitness advantage compared to non-symbiotic plants because the plant is not dependent on nitrogen occurrence in the soil. However, the plant needs to control the nodule number, otherwise too many resources are spent on feeding the rhizobia with photosynthesis products and mineral nutrients. This control mechanism is called "Autoregulation of Nodulation" (AON) (Figure 1). AON is a fine-tuned long-distance signaling pathway where signals from emerging nodules travel to the shoot, where they induce shoot-to-root signals that suppress further nodulation (Caetano-Anollés and Gresshoff, 1991).

After the initial rhizobial infection events, several CLE (CLAVATA3/EMBRYO SURROUNDING REGION-RELATED) peptides (Reid et al., 2011) are produced in the root tissue. Certain CLE-peptides undergo a modification by PLENTY, an arabinosyltransferase, which is an essential step for nodulation inhibition (Okamoto et al., 2013; Hastwell, 2018; Yoro et al., 2019). *plenty* mutants are hypernodulating and exhibit short roots (Yoro et al., 2019). Interestingly, CLE-RS1 and CLE-RS2 overexpression suppressed the hypernodulation phenotype in *plenty* but not CLE-RS3, suggesting the involvement of PLENTY in arabinosylation of CLE-RS3 (Yoro et al., 2019). CLE-RS1 and CLE-RS2 are directly induced by NIN after inoculation with rhizobia (Schauser et al., 1999; Okamoto et al., 2009; Soyano et al., 2014), however CLE-RS3 induction mainly requires LHK1 (Miri et al., 2019). After travelling through the xylem to the shoot, CLE-peptides are perceived by a homodimeric or heterodimeric receptor complex (Krusell et al., 2002a; Nishimura et al., 2002; Okamoto et al., 2009). One key component of this complex is HAR1 (HYPERNODULATION ABERRANT ROOT FORMATION1) (Wopereis et al., 2000; Krusell et al., 2002a; Nishimura et al., 2002), a leucine-rich-repeat receptor-like kinase. *har1* mutants display a hypernodulation phenotype where nodules cover almost the entire root, accompanied by abnormal root development (Wopereis et al., 2000). Overexpression of CLE-RS1, CLE-RS2 and CLE-RS3 was shown to inhibit nodulation in a HAR1 dependent manner (Okamoto et al., 2009; Nishida et al., 2016). It is suggested that other shoot transmembrane proteins like CLAVATA2, CORYNE and KLAVIER additionally act as part of the CLE peptide receptor complex because mutations in those genes also lead to a hypernodulating phenotype (Oka-Kira et al., 2005; Miyazawa et al., 2010; Krusell et al., 2011; Crook et al., 2016). Perception of CLE-peptides by HAR1 induces the repression of miR2111 (Tsikou et al., 2018). Overexpression of miR2111 results in an increase of ITs as well as nodule number, suggesting miR2111 as positive regulator of symbiosis (Tsikou et al., 2018). miR2111 is expressed in the shoot and travels systemically through the phloem to the root tissue (Tsikou et al., 2018) where it targets TML (TOO MUCH LOVE), a kelch repeat-containing F-box protein (Takahara et al., 2013). TML is suggested to be involved in the proteasomal degradation of target proteins (Takahara et al., 2013). *tml* mutants are hypernodulating similar to *har1* (Takahara et al., 2013). A functional *TML* gene is also required for the suppression of nodulation caused by CLE-RS1 and CLE-RS2 (Takahara et al., 2013). In double mutants of *tml* and the gain of function mutant LHK1 (*snf2*) it could be shown that

TML inhibits nodule organogenesis induced by the LHK1-mediated cytokinin signaling (Takahara et al., 2013). Moreover, in *lhk1* mutants the accumulation of CLE-RS1 and CLE-RS3 is reduced suggesting the importance of LHK1-mediated cytokinin as an early AON signal (Tsikou et al., 2018).

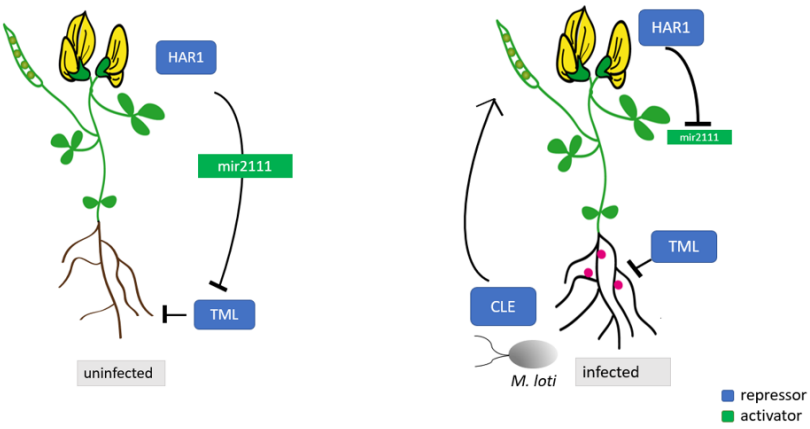

Figure 1: Autoregulation of Nodulation in *Lotus japonicus*.

In an uninfected state HAR1 mediates the expression of miR2111 which in turn targets TML, enabling the susceptibility for symbiosis. Once the plant is infected with *Mesorhizobium loti*, CLE peptides are produced which interact with HAR1 in the shoot. HAR1 suppresses miR2111, TML accumulates and inhibits further nodulation.

1.6. Nitrate dependent inhibition of nodulation

Apart from rhizobial Nod factor signals, nodulation is also suppressed by nitrogen availability in the soil (Carroll et al., 1985). That helps legume plants to balance nodule formation and -suppression depending on the nitrogen concentrations. The source of nitrogen seems to be important, as nitrate and ammonia display a strong inhibitory effect on nodule development, while urea does not (Dart and Wildon, 1970; Vigue et al., 1977). Nitrate application has various effects on RNS, such as inhibition of flavonoid production, early infection events and nodule growth (Streeter and Wong, 1988; Carroll and Mathews, 2018). Furthermore, nitrate suppresses nitrogen fixation activity and accelerates senescence (Coronado et al., 1995; Matamoros et al., 1999). In split root experiments it could be shown that nodule formation is inhibited in nitrate treated as well as in mock treated roots, suggesting a nitrate-mediated local and systemic response (Cho and Harper, 1991; Yashima et al., 2003; Jeudy et al., 2010).

Phytohormones appear to be associated with nitrate-induced control of RNS. Nitrate application increased the levels of ethylene in afalfa roots (Caba et al., 1998). In addition, the nitrate induced inhibition of nodulation can be partially suppressed by aminoethoxyvinylglycine, an inhibitor of ethylene biosynthesis (Ligero et al., 1991). In soybean

it was shown that auxin levels rise when plants are inoculated with rhizobia; however this effect can be inhibited by nitrate application (Caba et al., 2000). Moreover, cytokinin is involved in nitrate-mediated regulation of nodulation. In *Lotus japonicus* it could be shown that the cytokinin degradation mutant *ckx3 (*CYTOKININ OXIDASE/DEHYDROGENASE 3) is hypersensitive to nitrate dependent inhibition of nodulation (Reid et al., 2016).

Nitrogen regulation of nodulation acts immediately as it was shown that nitrate application suppresses the expression of *NIN* within 24h (Barbulova et al., 2007). Nitrate activates a number of CLE peptides in *Lotus japonicus* like CLE-RS2, CLE-RS3 and CLE40 (Nishida et al., 2016). CLE-RS2 is induced by a NIN-like transcription factor (NLP) which is activated through nitrate and accumulates in the nucleus (Nishida and Suzaki, 2018). Mutations in *LjNLP1* and *LjNLP4* showed insensitivity to nitrate application (Nishida and Suzaki, 2018; Nishida et al., 2021). Further, nitrate-induced CLE-RS2 expression was completely abolished in *Ljnlp1*/*Ljnlp4* double mutants suggesting a role in nitrate-mediated control of root nodule symbiosis and gene expression (Nishida et al., 2021). Interestingly, rhizobia-induced target genes of NIN, like EPR3, NF-YA1 and NF-YB1 are downregulated in *Ljnlp1*/*Ljnlp4* mutants, assuming an upstream repression of these genes (Nishida et al., 2021). NLP4 directly binds to the NBS/NRE (NIN-binding nucleotide sequence/nitrate-responsive cis-element) of CLE-RS2 promoter to which NIN also binds (Nishida et al., 2021). Upon nitrate application, CLE-RS2 promoter is mainly activated trough NLP4 inducing a strong inhibition of nodulation (Nishida et al., 2021) Nishida et al (2020) propose a model in which NIN and NLP4 compete for specific binding elements within the promoter of positive and negative regulators of symbiosis. Besides *nlp* and *cle-rs2* mutants, nodule number of *har1* also is unaffected by nitrate (Nishida and Suzaki, 2018; Nishida et al., 2020; Nishida et al., 2021) assuming HAR1 participation in nitrate mediated signaling. Interestingly, *tml* mutants do show nitrate responsiveness, suggesting other HAR1 downstream factors involved in nitrate mediated control of RNS (Nishida et al., 2020).

1.7. The shoot-derived inhibitor

AON in *Lotus japonicus* is a complex multicomponent-system that is not yet fully understood. Several genes and, more recently a miRNA have been discovered that play key roles in AON signaling. However, one key component that remains unidentified is the so called "shoot-derived inhibitor" (SDI). It has been postulated that there has to be a shoot signal that blocks further nodulation by travelling from the shoot to the root via phloem (Delves et al., 1986; Delves et al., 1987; Delves et al., 1992). The first evidence for the existence of an SDI came from interspecies heterografts, where WT scions placed on hypernodulating mutant stocks induced inhibition of nodule formation (Delves et al., 1987). Then in 2010, the SDI was investigated using of a petiole feeding assay (Lin et al., 2010). WT leaf extracts were fed into the petiole of a hypernodulating mutant, and possible effects on the root nodulation phenotype were investigated. Indeed it could be shown that WT leaf extracts contain inhibitors that suppress nodulation (Lin et al., 2010). With help of mutants and different rhizobial strains it was shown that SDI is dependent on rhizobial presence, functional Nod factors and the activity of HAR1 (Lin et al., 2010). To further investigate the properties of SDI, different treatments of WT leaf extracts were performed. SDI appeared to be heat, proteinase K and ribonuclease A stable with a molecular mass below 1000 Da (Lin et al., 2010).

Cytokinin was thought to qualify as SDI candidate because elevated iPRP, intermediates in cytokinin biosynthesis, were measured in shoots of AON-induced plants (Sasaki et al., 2014). Moreover, when 6-benzylaminopurine (BAP: synthetic cytokinin) was applied to cotyledons via surface cut, BAP travels from the shoot to the root and inhibits nodulation (Sasaki et al., 2014). However in Heckmann et al. (2011) it was shown that plants grown on agar plates containing BAP, spontaneously induce nodule primordia (Heckmann et al., 2011). In addition, a gain of function mutation in LHK1, which acts as cytokinin receptor, triggers spontaneously formed nodules (Tirichine et al., 2007). Cytokinin is involved in many developmental processes in the plant, and might not confer the specificity needed to act as SDI. We hypothesized that the criteria proposed by Lin et al. (2010) might be suitable for miRNAs. Plant miRNAs are capable of cell-to-cell as well as systemic movement through the plant (Benkovics and Timmermans, 2014; Sarkies and Miska, 2014; Skopelitis et al., 2018). In phloem sap the lead and lag strand of miRNA duplexes were both detected (Pant et al., 2009),

suggesting that miRNAs systemic travel may occur in the form of a 3'-methylated duplex resistant to degradation. The mode of action of miRNAs is based on sequence complementarity and therefore highly specific, supporting miRNAs as suitable SDI candidates.

One miRNA that was shown to be involved in AON as mobile factor was miR2111 (Tsikou et al., 2018). With shootless root and grafting experiments it could be shown that miR2111 travels from shoot to root as a mobile systemic signal (Tsikou et al., 2018). However it was shown that upon rhizobia inoculation, miR2111 levels decrease in a HAR dependent manner (Okuma et al., 2020). Overexpression of miR2111 leads to increased number of nodules and knockout mutants of miR2111 show a decrease in nodule numbers (Okuma et al., 2020). Based on these findings miR2111 acts as a positive regulator of symbiosis, and therefore does not qualify as potential SDI.

1.8. miRNA maturation

miR2111 has been uncovered as systemic mobile signal which is essential in the AON pathway (Tsikou et al., 2018). Like other miRNAs, miR2111 has a specific target, the F-box Kelch-repeat Gene *TML*, that it posttranscriptionally regulates. By targeting *TML* mRNA and reducing its levels, miR2111 is thought to enable the plant to enter into symbiotic associations (Tsikou et al., 2018). As the initiation of RNS requires miRNA-mediated inhibition of the repressor gene *TML*, miRNAs are essential in the regulation of legume-rhizobial symbiosis.

MicroRNAs (miRNAs) are a class of small non-coding RNAs that act as major post-transcriptional and transcriptional regulators in both animals and plants. Many processes are influenced by miRNAs, like plant development or biotic/abiotic stress responses. miRNAs consist of 19-24 nucleotides, and many regulate their target mRNAs post-transcriptionally. Most plant *MIR* genes are located in intergenic regions and can be regulated by their own promoter (Jones-Rhoades et al., 2006).

miRNAs are transcribed from *MIR* genes by DNA-dependent RNA Polymerase II (PoI II) (Kurihara and Watanabe, 2004). Splicing of the 5'cap and 3'polyadenylation are necessary modifications in order to form the primary transcript (pri-miRNA) (Kurihara and Watanabe,

2004; Kim et al., 2011). Pri-miRNAs form a partially complementary hairpin structure and are further processed by several protein complexes. Dicer-like 1 (DCL1) together with HYPONASTIC LEAVES (HYL1) and SERRATE (SE) enable the transition from pri-miRNA to the precursor miRNA (pre-miRNA) transcript by removing the 5'cap and 3' poly (A) tail (Kurihara and Watanabe, 2004; Kurihara et al., 2006; Dong et al., 2008). The miRNA precursor is then cleaved by DCL1, releasing the miRNA double-stranded duplex form (Vazquez et al., 2004). Methylation of the 3' end of the miRNA duplex (miRNA/miRNA*) by HUA ENHANCER 1 (HEN1) prevents uridylation and therefore degradation (Li et al., 2005; Yu et al., 2005). HASTY, the plant homolog of exportin-5, transports the miRNA duplex into the cytoplasm where the miRNA* is degraded (Park et al., 2005). The mature miRNA is then loaded into ARGONAUTE1 (AGO1) which forms together with other proteins the RNA induced silencing complex (RISC). Among the 10 AGO proteins in *Arabidopsis thaliana*, each AGO has certain binding preferences for small RNAs (Mi et al., 2008; Montgomery et al., 2008; Takeda et al., 2008). AGO1, which is acting in the miRNA pathway, has a preference for 5' uridine as the initial nucleotide (Mi et al., 2008). Furthermore, AGO1 prefers mRNA targets with central mismatches (Zhu et al., 2011). The RISC complex induces cleavage or translational repression of mRNAs (Baumberger and Baulcombe, 2005). mRNA cleavage is induced by the PIWI domain of AGO1 which has an endonuclease activity (Farazi et al., 2008). Lots of plant mRNAs however undergo translational inhibition where the translation initiation as well as the movement to ribosomes is inhibited (Brodersen et al., 2008; Iwakawa and Tomari, 2013).

1.9. Important miRNAs in nutrient homeostasis and the symbiosis context

miRNAs control a variety of different plant processes. From developmental changes to pathogen responses, miRNAs have great impact on plant adaptation to various stimuli. Especially in response to different nutrient concentrations, miRNAs serve as a quick and efficient response factor to modulate downstream signaling.

In soybean it was reported that several miRNAs respond to nitrogen starvation stress (Wang et al., 2013b). Gma-miR1510, gma-miR171, gma-miR482 are upregulated in shoot and root

tissue under long term nitrogen starvation (Wang et al., 2013b). In *Lotus japonicus*, miR2111 levels decrease when nitrate is applied (Tsikou et al., 2018). In common bean, miR396 is upregulated in leaf tissue and miR1508 levels increase in root tissue under nitrogen deficiency (Valdés-López et al., 2010). Besides nitrogen, phosphorus is also an essential macronutrient and phosphorus deficiency limits plant growth and development. miR399 is strongly induced under phosphorus deficiency in alfalfa whole plants (Li et al., 2018) and common bean (Valdés-López et al., 2010). miR399 targets a phosphate transporter and high-affinity inorganic phosphate transporter gene, which enables phosphorus uptake (Li et al., 2018).

Some miRNAs have been shown to play major roles in symbiosis. miRNAs regulate different stages of symbiosis like infection thread formation, nodule development and nodule functioning.

One example for a miRNA upregulated early during infection is miR172 in *Lotus japonicus* (Holt et al., 2015). It was shown that the expression level of miR172 is increased in root tissue at 3 days post inoculation with rhizobia compared to non-infected roots (Holt et al., 2015). miR172 abundance regulation is dependent on rhizobia and Nod factor presence, and is expressed in cells directly associated with the infection process. (Holt et al., 2015). miR172 targets APETALA2-like transcription factors, that control the floral organ identity and flowering (Yamashino et al., 2013) but also have a role in nodule development and senescence (Nova-Franco et al., 2015).

During rhizobial infection, the interplay of hormones like auxin and cytokinin is essential. miR160 targets AUXIN RESPONSE FACTOR (ARF) 10, ARF16 and ARF17 which are key players in auxin signaling. An early increase in miR160 accumulation can be observed in *Medicago truncatula* 12 hours post infection (hpi) (Bustos-Sanmamed et al., 2013). Overexpression of miR160 showed reduced nodulation, hypersensitivity to auxin and hyposensitivity to cytokinin (Bustos-Sanmamed et al., 2013; Nizampatnam et al., 2015). miR160 therefore controls the homeostasis between auxin and cytokinin.

Also during nodule primordia formation miRNAs have significant impact. In *Medicago truncatula* it was shown that miR166 regulates the expression of HOMEODOMAIN LEUCINE ZIPPER (HD-ZIP) III genes, which are involved in nodule meristem initiation and the

formation of vascular bundles (Boualem et al., 2008). Furthermore the miR166-HD-ZIP III node controls root architecture like lateral root density (Boualem et al., 2008).

Combier et al. (2006) demonstrated the importance of the miR169-NF-YA1 (HAP2) node in the persistence of the nodule meristem in (indeterminate) *M. truncatula* nodules. NF-YA1 RNAi roots and miR169a overexpressing roots show delayed nodulation and nodule growth arrest (Combier et al., 2006). miR169a overexpression and knockdown of *NF-YA1* roots also show a dwarfed phenotype because of the inability to fix nitrogen (Combier et al., 2006). Further in NF-YA1 knockdown roots, nodules do not show a spherical but rather a round shape like in determinate nodules (Combier et al., 2006). NF-YA1 as well as miR169a are expressed in the infection and meristematic zone and therefore assumed to be important for the differentiation and maintenance of nodule meristem (Combier et al., 2006). Moreover it was demonstrated that overexpression of miR169c and CRISPR/CAS-9 mediated knockout of NF-YA-C in soybean results in inhibition of nodulation (Xu et al., 2021). Constructs of miR169c STTM (short tandem target mimic) and NF-YA-C OX leading to an increased amount of nodules and confirm the distinct roles of miR169 as negative and NF-YA-C as positive regulator of symbiosis (Xu et al., 2021). Interestingly, gma-miR169c regulation seems to be dependent on nitrate concentrations. In treatments where higher nitrate concentrations was applied, miR169c was upregulated; NF-YA-C however is mainly controlled by rhizobial presence (Xu et al., 2021). The gma-miR169-NFYA–C module seems to be involved in the control of nodulation in an N-dependent manner.

A further miRNA involved in root endosymbiosis is miR171. In *Medicago truncatula*, miR171h is strongly upregulated in roots during both AM and rhizobia mediated nodulation (Lauressergues et al., 2012; Devers, 2019). Overexpression of mtr-miR171h leads to reduced colonization of mycorrhiza and decreased amount of nodules compared to wild type plants (Lauressergues et al., 2012; Devers, 2019). In *Lotus japonicus*, miR171c is not only expressed in roots and nodules during infection but also in leaf tissue (De Luis et al., 2012). Experiments with *snf* mutants showed a link to infection but not organogenesis, as miR171c is upregulated only in the presence of rhizobia (De Luis et al., 2012). The miR171c isoform in *Lotus japonicus* displays 2-3 nucleotide polymorphism in the mature sequence compared to the other 4 members of the miR171 family (De Luis et al., 2012). miR171c specifically targets NSP2, a GRAS-type transcription factor which is essential for symbiosis establishment (Kaló et al.,

2005; Heckmann et al., 2006; De Luis et al., 2012). Interestingly, in *Medicago truncatula NSP2* levels in nodules increase from 1 d to 7 d post inoculation, while in *Lotus japonicus* nodules, *NSP2* levels gradually decrease after 8 d, suggesting different roles of the miR171-NSP2 node in determinate and indeterminate nodules (Kaló et al., 2005; Heckmann et al., 2006).

Aims

The aim of this project was to test the hypothesis that miRNAs may act as shoot-derived inhibitors in symbiosis. In an unbiased global approach, small RNA sequencing was performed to identify small RNAs and their respective targets meeting the SDI criteria. One candidate miRNA displaying a combination of properties qualifying it as SDI candidate is miR171c. In order to analyze miR171c as possible SDI, root nodulation phenotypes, using stable lines, were investigated. Furthermore, potential local and systemic responses of miR171c during nitrate and rhizobial treatment were analyzed.

2 Results and discussion

2.1. Identification of SDI like miRNAs using small RNA sequencing

In order to identify possible SDI candidates, we performed comparative sRNA sequencing of selected plant genotypes/-treatment combinations where SDI candidates are expected to show specific differential abundance patterns. To this end, plants that are AON activated (CLE-RS3 OX) or AON inhibited (*har1-3*) were included. Overexpression of CLE-RS3 OX induces inhibition of nodulation (Nishida et al., 2016), and in such AON activated samples, an accumulation of SDI is expected. *har1-3* mutants represent plants where no SDI accumulation is expected as it was shown in Lin et al. (2010) that SDI levels in shoots are *HAR1* dependent. Further, WT plants transformed with empty vector constructs were included. WT (Gifu) plants serve as nontransgenic control group. Since SDI candidates are hypothesized to accumulate in leaf tissue, leaves harvested at 14 days post inoculation were used for sequencing (Table 1).

Table 1: Plants used for RNA seq

Genotype	**Inoculation with *M. loti* (MAFF)**	**Expected SDI level**
CLE-RS3 OX	+	++
har1-3	-	-
WT empty vector	+	+
WT empty vector	-	-
WT	+	+
WT	-	-

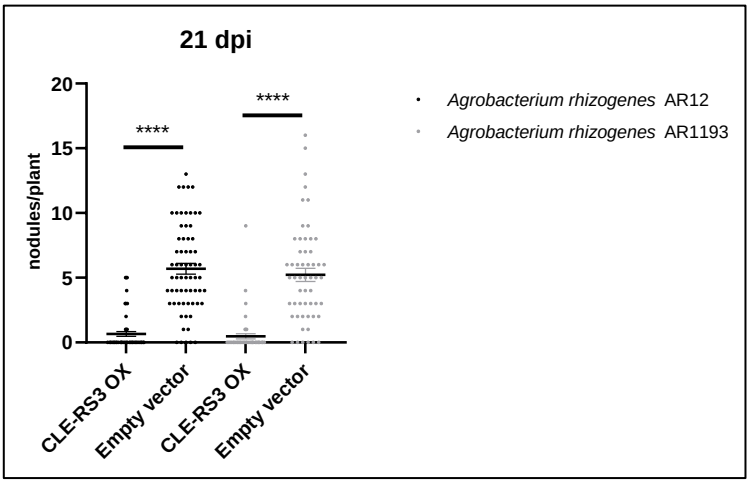

Figure 2: CLE-RS3 OX inhibits nodulation.

Nodules were counted at 21 dpi. Plants were transformed with *A. rhizogenes* strains AR12 or AR1193. At least 55 plants were used for each construct. Centerlines and error bars show the mean with SEM. Students t-test with ****=p<0.0001 are shown.

In a pre-experiment (Figure 2), CLE-RS3 OX constructs were tested to confirm that overexpression of CLE-RS3 indeed inhibits nodulation. In all inoculation experiments *M. loti* strain MAFF303099 was used. Two strains of *Agrobacterium rhizogenes*, namely AR12 and AR1193 were tested for possible difference in transformation efficiency. In both tested strains, overexpression of CLE-RS3 leads to inhibition of nodulation compared to the empty vector control (Figure 2). The number of over-transformant plants where transgenic hairy roots do not develop properly was higher when transformed with AR1193. Therefor the follow-up experiments were performed with *Agrobacterium rhizogenes* strain AR12.

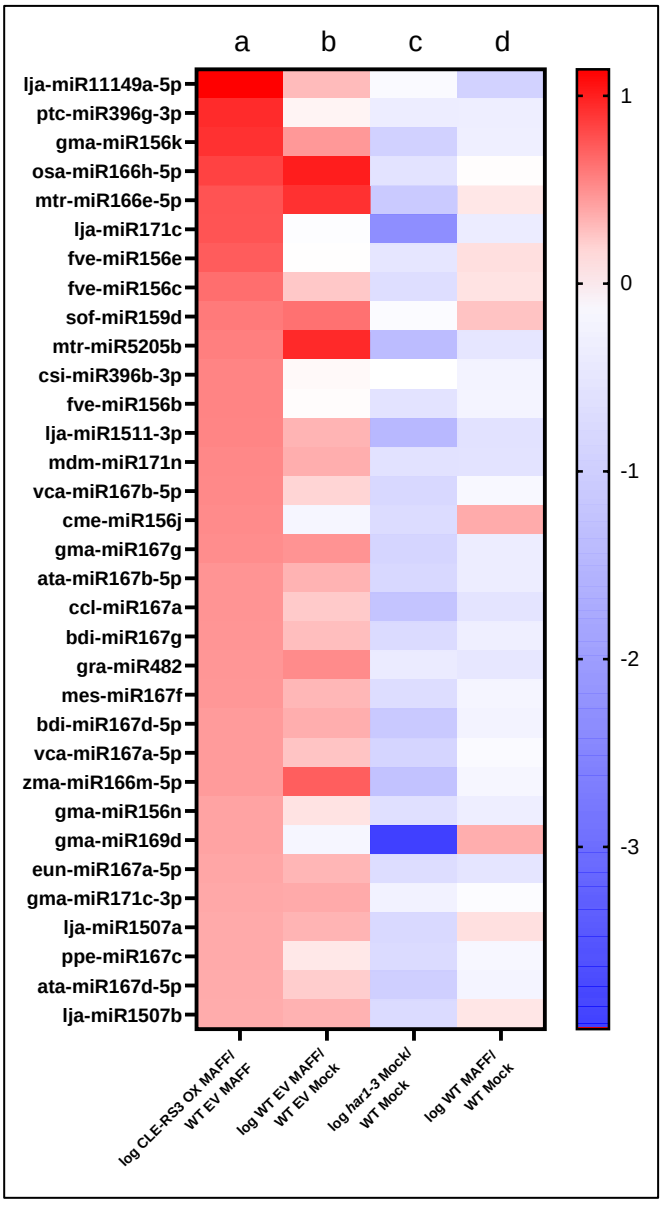

After successful confirmation of constructs, the experiment was repeated and after 14 dpi leaf tissue was harvested and total RNA was extracted and sent for small RNA sequencing (GeneXPro). For each experimental setup, two biological replicates were analyzed. The libraries were sequenced on an Illumina NextSeq500 instrument. Duplicate reads were eliminated based on the UMI using an in-house software (GenXPro). The reads were hereafter annotated to the "Lotus Japonicus" entries in the "miRbase": all non-annotated reads where hereafter annotated to all miRBase (v22) "plant" entries. Small RNA transcripts were quantified and pairwise

Figure 3: **Heatmap of 33 differentially expressed miRNAs**.

miRNAs were mapped against miRbase (v22). The heatmap shows miRNAs sorted as log2FC of relative CLE-RS3 OX MAFF/WT EV MAFF (**a**), WT EV MAFF/ WT EV Mock (**b**), *har1-3* Mock/ WT Mock (**c**), WT MAFF/WT Mock (**d**). Additionally, CLE-RS3 OX transcript abundance was sorted (log2FC>0). For inoculation *M. loti* strain MAFF 303099 was used.

comparisons were performed using DESeq2 (Love et al., 2014a; Love et al., 2014c) for p-value calculation of differentially expressed small RNAs. The mapped miRNAs were listed and sorted in cooperation with Moritz Sexauer (Supplemental table 1). The normalized sequence abundance values of CLE-RS3 OX samples were sorted such that transcript abundance is > 20, then the mean of normalized values from both biological replicates was calculated.

The relative transcripts levels were calculated as quotients for particular reads as follows: CLE-RS3 OX MAFF/WT EV MAFF (a), WT EV MAFF/ WT EV Mock (b), *har1-3* Mock/ WT Mock (c), WT MAFF/WT Mock (d). Then log2FC of the relative transcript abundance was calculated. Additionally, upregulated small RNA transcript levels in CLE-RS3 OX plants were displayed with log2FC>0. Candidate SDI miRNAs are predicted to display an abundance pattern which is high in CLE-RS3 OX plants (a) and low in *har1-3* (c) plants (Table 1). Out of 33 differentially expressed miRNAs (Figure 3, Supplemental Table S1), four were analyzed further.

Candidate miRNA analysis

SDI properties proposed by Lin et al. (2010) include (a) high abundance in shoot tissue upon inoculation, (b) HAR1 dependence, and (c) the ability to travel from shoot to root. Additionally, the specific miRNA target is expected to act as symbiosis activator. Therefore, upregulation in CLE-RS3 OX and downregulation of transcripts in *har1-3* plants are the main criteria for SDI. miR171c is highly abundant in CLE-RS3 OX plants (Figure 3a) and lowly abundant in *har1-3* plants (Figure 3c). No expression difference could be observed in inoculated plants carrying the empty vector (Figure 3b). Less abundance was displayed in inoculated WT plants (Figure 3d). On this basis, miR171c appears as a suitable SDI candidate. It was shown that miR171c is expressed in leaf tissue upon inoculation (De Luis et al., 2012). Further, overexpression of miR171h in *Medicago truncatula* reduces colonization with arbuscular mycorrhizal fungi and nodulation (Lauressergues et al., 2012; Devers, 2019). NSP2, which is required for rhizobial infection, is the target of miR171c and represents an activator for root nodules symbiosis. Therefore, miR171c appears as suitable SDI candidate and was further analyzed.

miR169 represents further an interesting SDI candidate. The abundance levels of a small RNA (named Lj-miR169d) mapping to gma-miR169d were high in CLE-RS3 OX plants (Figure 3a)

and low in *har1-3* plants (Figure 3c). No transcript level difference was observed in plants carrying the empty vector (Figure 3b). In inoculated WT plants (Figure 3d) miR169d levels were higher than in *har1-3* plants. The small RNA (Lj-miR169d) mapped to gma-miR169d appears to be dependent on HAR1 and is highly abundant in AON activated (Figure 3a) plants. miR169 targets NF-YA1, a transcription factor that is important in maintenance and differentiation of the nodule meristem (Combier et al., 2006). Overexpression of miR169 leads to reduced nodulation in soybean (Xu et al., 2021). As negative regulator of symbiosis, miR169 fits in the SDI category.

Two further miRNAs mapping to mtr-miR5205b and lja-miR1511 show high levels in inoculated CLE-RS3 OX (Figure 3a) and WT empty vector plants (Figure 3b). In *har1-3* plants (Figure 3c) miRNAs mapped to mtr-miR5205b and lja-miR1511 levels are low. In inoculated WT plants (Figure 3d) lower abundance levels of both miRNAs are observable. miR5205 is present in *Phaseolus vulgaris* (Han et al., 2014) and in tubers of potato (Din et al., 2014). In wheat, it was shown that the miR5205 family targets several proteins involved in disease resistance but also metabolism (Han et al., 2013). In *Arabidopsis thaliana,* miR5205 is important in abiotic stress responses like drought, salinity or cold stress by targeting a CBS domain containing protein (Kushwaha et al., 2009). miR1511 targets ALUMINUM SENSITIVE PROTEIN 3 and therefore is involved in aluminum tolerance of *Phaseolus vulgaris* plants (Ángel Martín-Rodríguez et al., 2021). In soybean, it was shown that miR1511 targets the 60S ribosomal protein L4 (RPL4) (Luo et al., 2012). However not much is known about the active role of miR5111 and miR5205 in legumes, and it will be interesting to investigate possible roles and functions in the context of symbiosis.

To confirm the sequencing data, qPCR analysis of miR171c and miR169bc from a repeated experiment with the same conditions was performed (Figure 4) and values were compared to the normalized reads obtained from RNA seq. Pre-experiments and predictions were performed with miR169bc and therefore RT and qPCR primer were optimized for that specific isoform. Therefore qPCR analysis was performed for miR169bc, however in future studies miR169d will be analyzed as well.

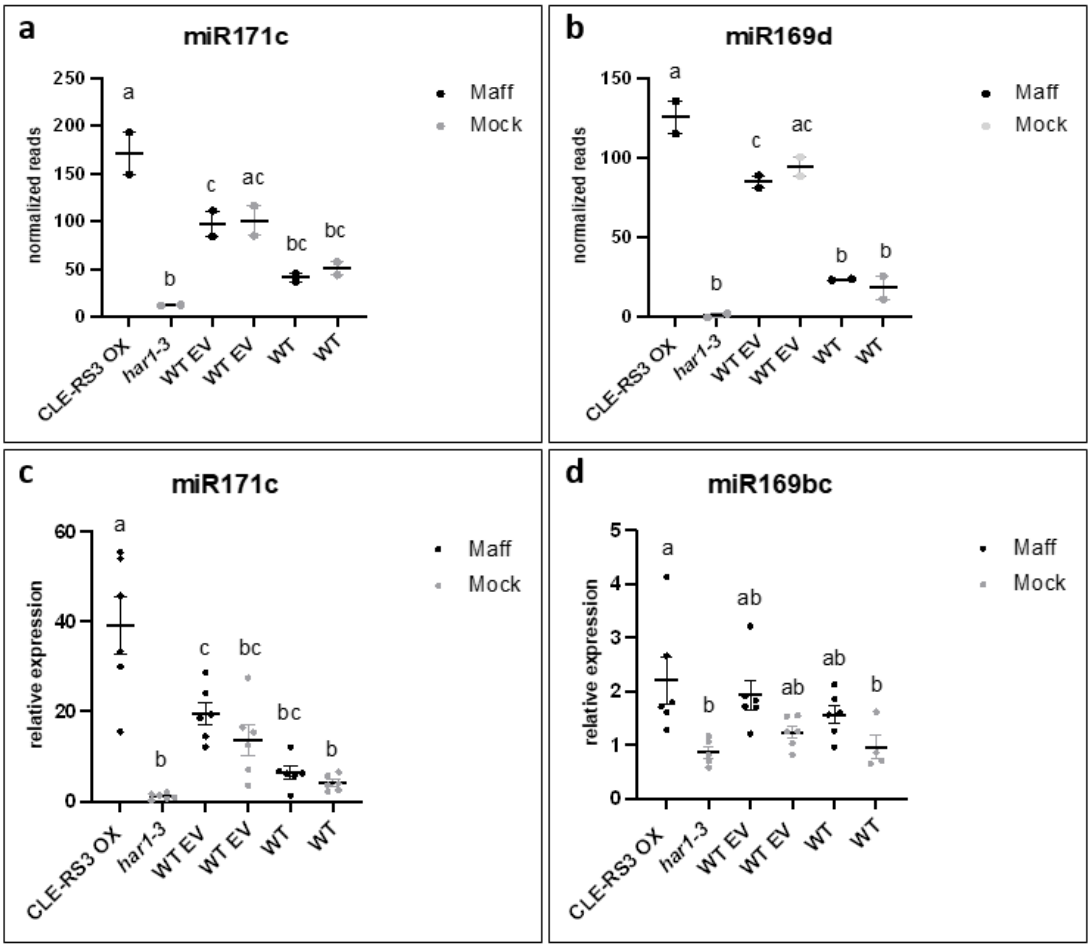

Figure 4: Normalized reads and relative expression levels of two SDI candidates: miR171c and miR169.

a, b: Normalized reads of miR171c and miR169d. **c, d**: Relative expression levels of miR171c and miR169bc. Leaf tissue were harvested at 14 dpi. For inoculation *M. loti* strain MAFF303099 was used. Several genotypes and treatments were used: Hairy roots of CLE-RS3 ox, *har1-3* mutants, wild type plants with and without transformed empty vector (EV) in hairy roots. Centerlines and error bars show the mean with SEM, *har1-3* =1. Two-way ANOVA was performed followed by Tukey's test. $p<0.05$, significantly different values are marked with different letters.

Normalized reads from RNA seq (Figure 4a, b) as well as qPCR data (Figure 4c, d) of miR171c, miR169d and miR169bc are shown. miR169bc in *Lotus japonicus* shows high sequence similarity to miR169d (Supplemental figure S1). miR171c reads and qPCR transcript levels are increased in CLE-RS3 OX plants and decreased in *har1-3* plants (Figure 4a, c). No difference in miR171c abundance levels can be observed between WT empty vector inoculated and WT empty vector Mock treated plants (Figure 4a). However, inoculated plants carrying the empty vector (Figure 4c) show higher miR171c abundance levels than mock treated empty vector plants. No difference is observable between WT Mock and WT inoculated plants (Figure 4a, c).

Abundance levels of miR169d are strongly increased in CLE-RS3 OX plants (Figure 4b), however the abundance levels of miR169bc in CLE-RS3 OX plants based on qPCR-data (Figure 4d) show intermediate increase. Weak miR169bc expression (Figure 4d) and low miR169d abundance levels (Figure 4b) can be observed in *har1-3* plants. WT empty vector plants that are mock treated show higher abundance levels than inoculated empty vector plants (Figure 4b). However, abundance levels of miR169bc based on qPCR-data (Figure 4d) are not significantly different between inoculated and mock treated empty vector plants. Between inoculated and mock treated WT plants no difference in abundance levels of miR169d and miR169bc could be observed (Figure 4b, d).

Discussion

The datasets gained from small RNA sequencing represent a resource tool to investigate possible SDI candidates that are specifically upregulated in the shoot. Overexpression of CLE-RS3 inhibits nodulation (Figure 2) and leads to hyperactivated AON response in plants, where potential SDI candidates accumulate. Based on their strong transcript accumulation in shoots of plants overexpressing CLE-RS3 in their roots (Figure 4), miR171c and miR169d display good SDI candidates. Moreover, the observed low abundance levels of miR171c and miR169d in *har1-3* support this hypothesis (Lin et al., 2010). The newly identified miRNA miR169d shows higher increased abundance levels in CLE-RS3 OX plants than miR169bc. Although miR169bc is present in sequencing data, abundance levels are intermediate. miR169d however displayed increased abundance levels in all tested conditions, with the exception in *har1-3* plants (Figure 4b). Both miR171c and miR169 have targets that act as symbiosis activators namely *NSP2* and *NF-YA1.* By inhibiting a symbiosis activator, these miRNAs can potentially interfere with the onset of nodulation. *nsp2* knockout are non-nodulating (Kaló et al., 2005) and in soybean it was shown that knockout of *NF-YA-C* leads to inhibition of nodulation (Xu et al., 2021) demonstrating the role as symbiosis activator.

miR171 and miR169 were found in phloem sap of *Brassica napus* (Buhtz et al., 2008) indicating potential systemic shoot to root mobility. In Li et al. (2021) it was shown with interspecific heterografts that certain miRNAs move from shoot to root, and members of the miR171 and miR169 family were found among them (Li et al., 2021). The dataset contains further

interesting candidates that may potentially be involved in SDI activity. Therefore, the dataset can also be used to study other small RNAs like tasiRNAs or phasiRNAs, which are potentially involved in the AON signaling pathway.

Overall, the transcript levels of miR171c (Figure 4c), show a similar pattern like the normalized reads of miR171c (Figure 4a). Abundance levels of miR169d show a stronger response to the different plant genotypes and treatments than miR169bc (Figure 4b, d). However, in both SDI candidates the reads/transcript levels in EV plants were significantly higher than in non-transgenic WT plants, indicating a strong influence of *Agrobacteria rhizogenes* presence and/or *Agrobacterium rhizogenes*-mediated transgenic tissue. It might be possible that the increased levels of miR171c and miR169d and miR169bc are part of the pathogen defence response of the plant. In Arabidopsis, it was shown that members of the miR169 family are involved in defence responses triggered by *Ralstonia solanacearum* (Hanemian et al., 2016). Furthermore, in rice, miR169 negatively regulates immunity against the Blast Fungus *Magnaporthe oryzae* (Li et al., 2017). miR171 is not known to be involved in pathogenic-derived defence responses so far. However, agrobacteria mediated hairy roots could display an altered metabolism in the root tissue and therefore be involved in the high accumulation of miR171c and miR169bc.

One other difficulty displays the identification of specific isoforms with qPCR. miR171c does display a specific shift of nucleotides along the precursor backbone and can therefore be specifically detected in qPCR analysis because it can be distinguished between the other members of the miR171 family. However, miR169bc does not show much nucleotide difference to the other members of the family (Supplemental figure S1). It cannot be excluded that other miR169 isoforms were detected (Figure 4d). Additionally, miR169d needs to be examined via qPCR to confirm the results obtained from small RNA sequencing.

2.2. Investigation of miR171c as possible SDI candidate

2.2.1. The *MIR171c* promoter is active in the vascular system

Although expression of mature miR171c was observed in shoots as well as in roots (De Luis et al., 2012) the promoter activity of the *MIR171c* locus in *Lotus japonicus* has not been examined so far. To qualify as SDI, promoter activity of miR171c should be present in the vascular system of the plant, especially in the shoot phloem, which has been proposed to be a prerequisite for systemic transport of miRNAs (Skopelitis et al., 2018). Therefore, stable plants expressing a 3kb upstream region of the *MIR171c* locus fused to the *GUS*/*uidA* reporter gene were generated.

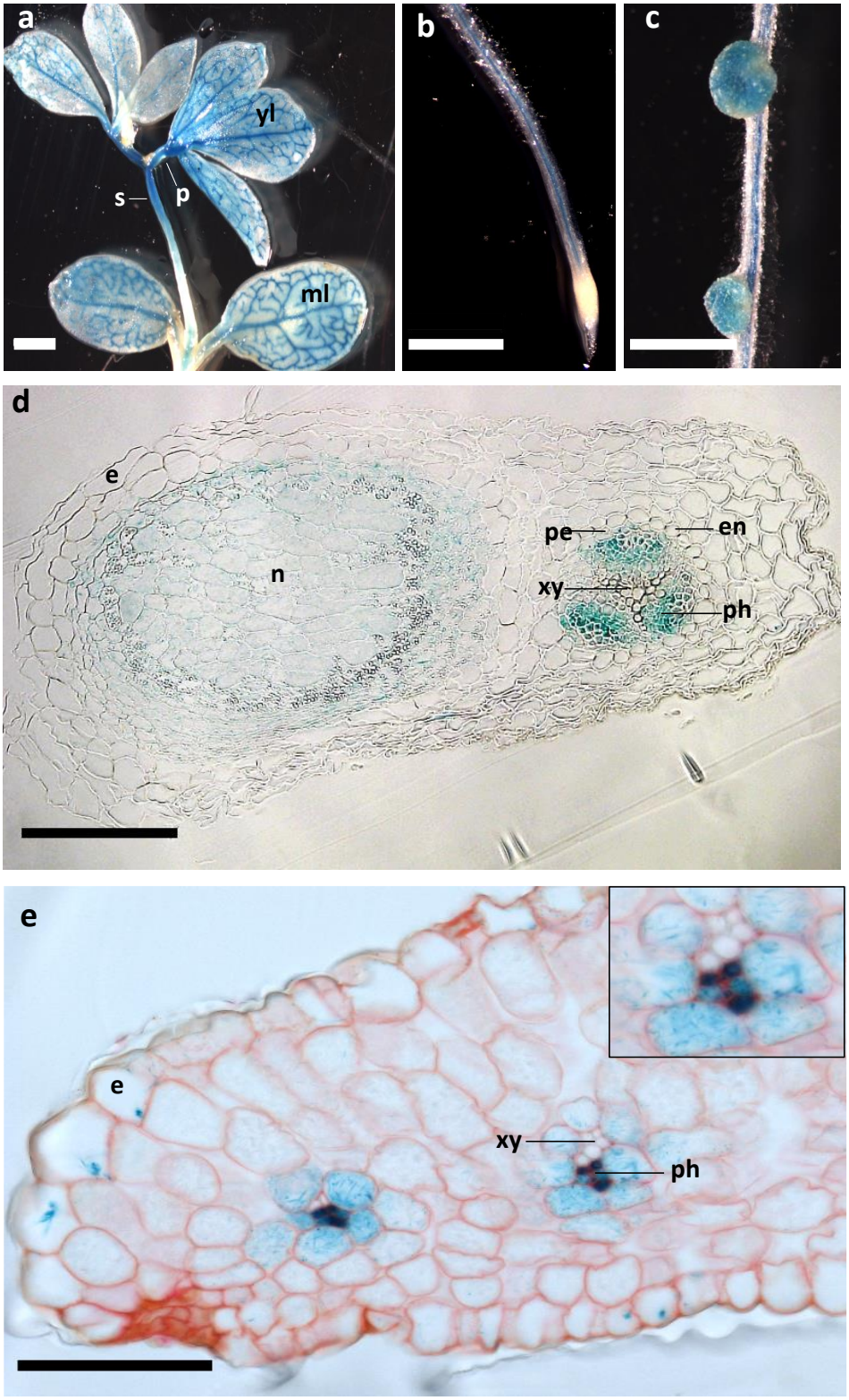

Figure 5: ***pMIR171c::GUS*** **expression is present in the vasculature.**

a-e: GUS activity in *pMIR171c::GUS* expressing plants (14 days). GUS activity in leaf veins (**a**), root stele (**b**) and nodules (**c**). Semi-thin sections of nodules display GUS activity in nodule and phloem of vascular bundle (**d**). GUS expression is present in phloem of semi-thin sections of leaf (**e**). ml: mature leaf, yl: young leaf, p: petiole, s: stem, e: epidermis, n: nodule, pe: pericycle, en: endodermis, xy: xylem, ph: phloem. Scale bar a, c: 1 mm, b: 0, 5 mm, d, e: 100 µm.

pMIR171c::GUS activity is present in vasculature of the plant (Figure 5). GUS staining is visible in leaf veins of mature and young leaves (Figure 5a), as well as in the root central cylinder (Figure 5b) and nodules (Figure 5c). Semi-thin sections of nodules (Figure 5d), reveal strong GUS staining in phloem tissue of root vascular bundles and intermediate staining in nodule. Notably, strong GUS staining is evident in phloem cells of leaf vascular bundle (Figure 5e).

Discussion

Systemic movement of miRNAs is thought to be achieved through their expression in leaf phloem cells (Skopelitis et al., 2018). GUS staining is evident in leaf phloem of semi-thin sections (Figure 5e), suggesting that *MIR171c* is strongly expressed in this tissue. This suggests systemic mobility, an important prerequisite for potential SDI activity. The *pMIR171c::GUS* analysis suggests that miR171c is expressed in both shoots and roots. In shoots, *MIR171c* promoter activity is visible exclusively in leaf vascular bundle, specifically in phloem cells (Figure 5e), whereas xylem is GUS free. In *pMIR2111::GUS* studies, similar GUS signals were observed. Promoter activity of miR2111 was observed in phloem cells of leaf veins, suggesting the synthesis of miR2111 in shoot tissue, and systemic mobility to its root specific target *TML* (Tsikou et al., 2018). Grafting experiments confirmed miR2111 systemic mobility (Okuma et al., 2020; Sexauer et al., 2022 unpublished). However, miR2111 is predominantly produced in shoots (Tsikou et al., 2018), whereas miR171c is synthesized in shoot as well as in roots (Figure 5a-e). Other miRNAs for which systemic travel has been proposed are miR399 and miR395, which are upregulated in response to phosphate and sulfur starvation, respectively (Aung et al., 2006; Kawashima et al., 2009). Both, miR399 and miR395 are expressed in the vasculature of shoots and roots indicating that systemic shoot-root travel of miRNAs can take place simultaneously to a local expression in roots.

In roots of *pMIR171c::GUS* plants (Figure 5b-d), GUS signal is present in the stele and in nodules. Semi-thin sections confirm strong GUS activity in phloem of root vascular bundle and weakly in central nodule cells (Figure 5d). Infection and symbiosis dependent induction of miR171c was previously shown (De Luis et al., 2012), and elevated transcript levels were observed when plants were inoculated with rhizobia compared to mock treated controls, suggesting that miR171c activity is linked to rhizobial infection (De Luis et al., 2012) and may

have a local role in symbiosis development in roots. Devers (2019) investigated how different nutritional and symbiotic conditions affect *pMIR171h::GUS* activity (*Medicago truncatula* miR171h is homologous to miR171c in *Lotus japonicus*) in hairy roots (Devers, 2019). Under phosphate sufficiency and nitrogen starvation, plants inoculated with rhizobia (+P-N+Nod) showed GUS signal only in nodules; however no signal was observed in the root central cylinder (Devers, 2019). These findings differ from our observations (Figure 5d), where a strong GUS signal was evident in root phloem of *pMIR171c::GUS* expressing *L. japonicus* plants, however *Medicago truncatula* hairy roots were treated with 1 mM Phosphate whereas *Lotus japonicus* plants grew on 0.5 mM Phosphate, which could explain the difference in GUS signal. *Medicago truncatula* plants which were treated with nitrate however, showed a strong GUS signal in central cylinder whether or not they were inoculated with arbuscular mycorrhiza (Devers, 2019). Overall, *Medicago truncatula* hairy roots display GUS signal in root central cylinder when treated with nitrate but GUS signal is absent when plants are grown under phosphate sufficiency and rhizobial presence (Devers, 2019). *Lotus japonicus* plants however display strong GUS signal in root vasculature under nitrate deficiency. The differences in promoter activity of miR171c and miR171h might be because of the different types of nodulation (determinate and indeterminate), it is possible that miR171c and miR171h play distinct roles in gene regulation. Moreover, the differences in transformation ((Devers, 2019) used hairy root transformation; Figure 5: stable lines) might play a role in the distinct promoter patterns. However, it would be interesting to examine like in Devers (2019) the promoter activity pattern of miR171c in *Lotus japonicus* under different nutrient conditions as well as mycorrhizal colonization. That might give more specific insights into the nutrient- and symbiont-dependent changes in promoter activity of *L. japonicus* miR171c and possible differences between the species.

2.2.2. miR171c KO plants are insensitive to nitrate dependent inhibition of nodulation

In order to analyze the nodulation phenotype of miR171c KO plants, CRISPR-CAS 9 mediated knockout lines were generated. Two guide RNAs were designed, which target the sequences of the mature miR171c as well as miR171c*, leading to a 393 bp deletion in the precursor sequence. In previous experiments, miR171c KO plants inoculated with *M. loti* (MAFF 303099) did not show differences in nodule number compared to wild type plants (Gifu). Devers (2019) observed, significant induction of *pMIR171h::GUS* in *Medicago truncatula* when plants were treated with nitrate (Devers, 2019). We therefore applied nitrate in form of 5 mM KNO_3 to miR171c KO plants in order to test whether miR171c is involved in nitrate-induced inhibition of nodulation.

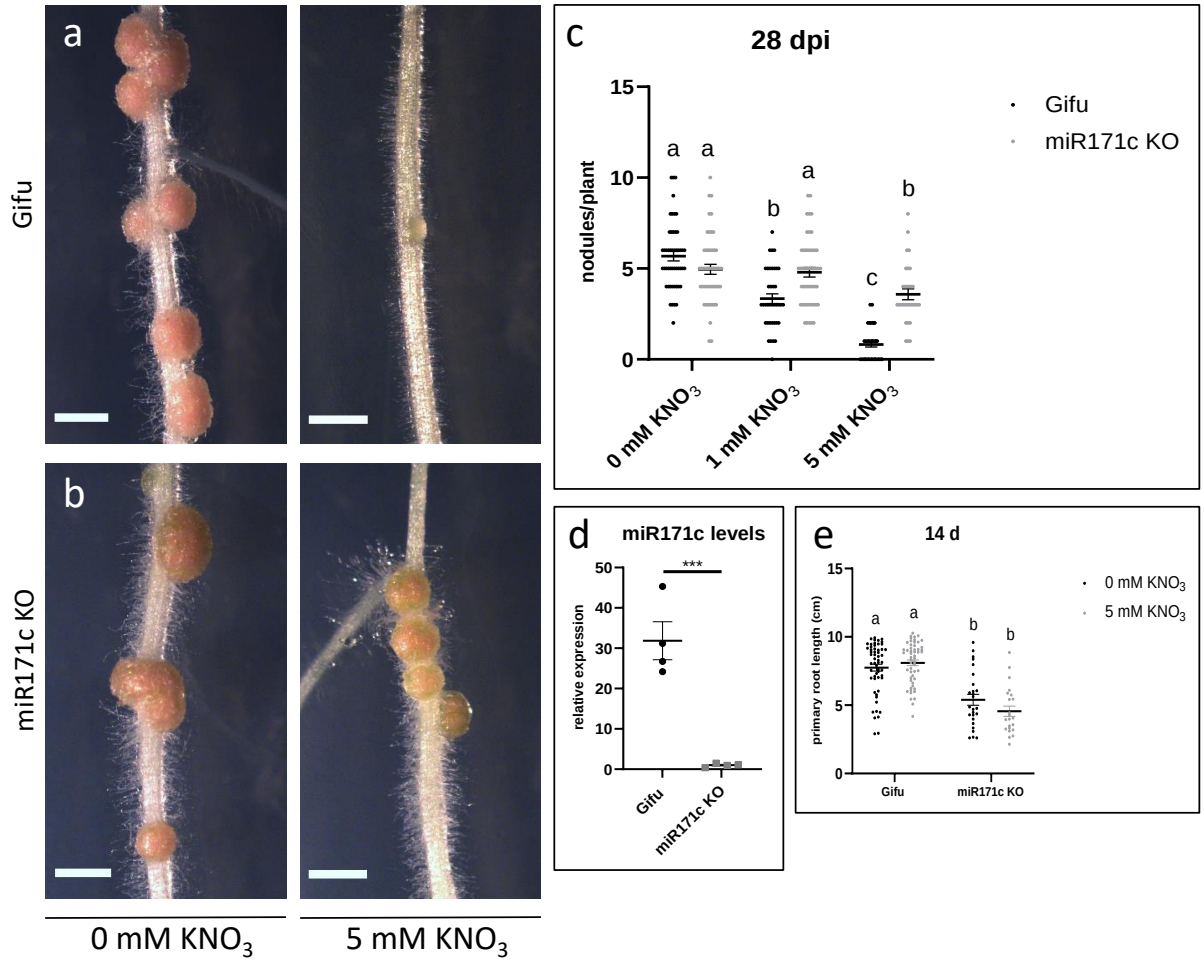

Figure 6: miR171c is required for nitrate-dependent regulation of nodulation.

a-b: Nodule number of wild type (Gifu) and miR171c KO under different nitrate conditions. Plants were grown on B&D media containing 0 mM or 5 mM KNO_3, pictures were taken 14 dpi, scale bar: 1 mm. **c**: Nodule number of wild type (Gifu) and miR171c KO under different nitrate conditions. Plants were grown on B&D media containing 0 mM, 1 mM or 5 mM KNO_3, at least 31 plants of two independent experiments were used for each nitrate conditions, nodules were counted after 28 d. **d**: miR171c transcript abundance in wild type (Gifu) and miR171c KO. Mature miR171c levels were measured with qPCR from whole seedlings (pool of 4 seedlings are 1 replicate), plants were grown on B&D plates and harvested after 10 d, miR171c KO =1. **e**: Primary root length of wild type (Gifu) and miR171c KO. Plants were grown on B&D plates with 0 mM or 5 mM KNO_3, primary root length was measured after 14 d, at least 22 roots of two independent experiments were measured for each condition. Two-way ANOVA was performed followed by Tukey's test. $p<0.05$, significantly different values are displayed with different letters. Centerline and error bars display the mean with SEM. Student's t-test ***= $p>0.001$.

Wild type (Gifu) and miR171c KO plants were grown on B&D plates supplied with 0 mM, 1 mM or 5 mM KNO_3 (Figure 6a-c). Gifu plants show inhibition of nodulation when grown on 5 mM KNO_3 (Figure 6a, c). Gifu plants develop rare nodule primordia (Figure 6a) as well as mature nodules under high nitrate conditions, but the number of mature nodules is

dramatically decreased (Figure 6c). In contrast, miR171c KO plants fail to show normal nitrate dependent inhibition of nodulation (Figure 6a and c). They still develop mature nodules when exposed to 5 mM KNO_3 (Figure 6b) and after 28 days, only a mild decrease in nodule number is visible (Figure 6c). qPCR tests confirmed that the levels of mature miR171c in miR171c KO plants are strongly reduced compared to wild type plants (Figure 6d). miR171c KO plants show shorter primary roots than Gifu plants under 0 mM and 5 mM KNO_3 (Figure 6e). However, neither Gifu plants nor miR171c KO plants show a nitrate dependent primary root response. miR171c KO plants further displayed delayed germination and development. Germination was delayed for about 3 days compared to Gifu, and the plants take longer to develop cotyledons. Taken together, miR171c KO plants are insensitive to nitrate dependent inhibition of nodulation and show additional developmental disorders that seem independent of nitrate availability.

2.2.3. miR171c OX plants partially inhibit nodulation and are hypersensitive to nitrate

In *Medicago truncatula* it was demonstrated that overexpression of miR171h leads to inhibition of nodulation as well as reduction of arbuscular mycorrhizal colonization (Devers, 2019). To investigate the nodulation phenotype of miR171c overexpression in *Lotus japonicus*, stable lines were generated carrying the construct *pUBQ1::miR171c*. After successful genotyping, two homozygous overexpression plants (miR171c OX #4 and miR171c OX #35) were isolated and characterized using an sequence-specific amplification polymorphism (SSAP) (Syed and Flavell, 2006) approach.

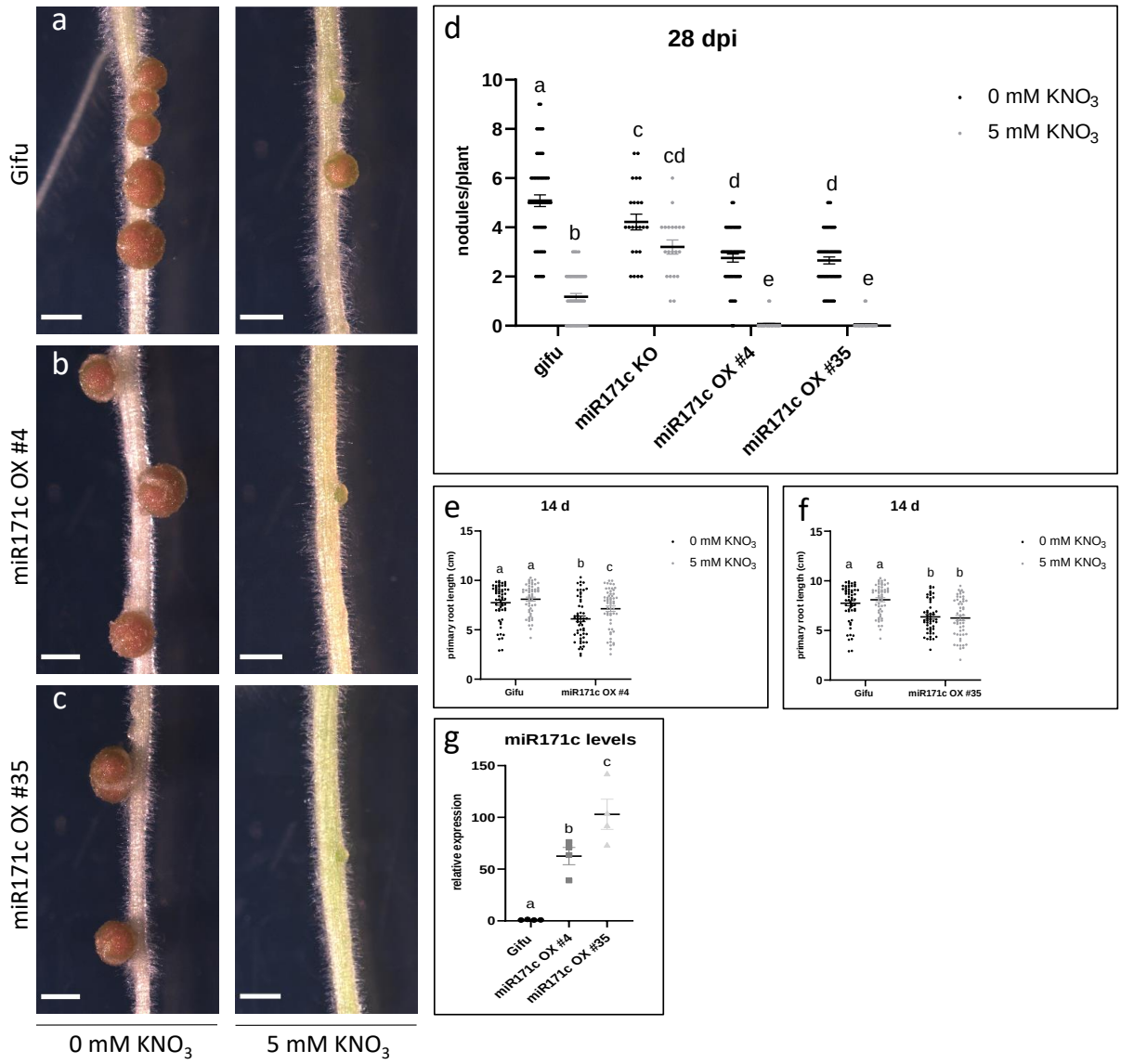

Figure 7: miR171c OX plants partially inhibit nodulation and are hypersensitive to nitrate.

a-c: Nodule number of wild type (Gifu), miR171c OX #4 and miR171c OX #35 under different nitrate conditions. Plants grew on B&D media containing 0 mM or 5 mM KNO_3, pictures were taken 14 dpi, scale bar: 1mm. **d:** Nodule number of wild type (Gifu), miR171c KO, miR171c OX #4 and miR171c OX #35 under different nitrate conditions. Plants were grown B&D media containing 0 mM or 5 mM KNO_3, nodules were counted after 28d, at least 52 plants of two independent experiments were used for each condition. **e-f**: Measured primary root length of wild type (Gifu), miR171c OX #4 and miR171c OX #35. Plants were grown on B&D media containing 0 mM or 5 mM KNO_3, primary root length was measured after 14 d, at least 51 roots of two independent experiments were measured for each treatment. **g:** miR171c abundance levels of wild type (Gifu), miR171c OX #4, and miR171c OX #35. Mature miR171c levels were measured with qPCR from whole seedlings (pool of 4 seedlings are 1 replicate), plants were grown on B&D plates and harvested after 10 d, Gifu =1. Two-way ANOVA was performed followed by Tukey's test. $p<0.05$, significantly different values are displayed with different letters. Centerline and error bars display the mean with SEM.

Under nitrogen starvation (0 mM KNO_3), miR171c OX plants show partial inhibition of nodulation compared to WT plants (Figure 7 a-d). When 5 mM KNO_3 was applied however, both homozygous miR171c overexpression lines (miR171c OX #4 and miR171c OX #35) show a hypersensitive reaction (Figure 7a-d). miR171c OX plants displayed no mature nodules under 5 mM KNO_3, whereas WT plants develop mature nodules but significantly fewer compared to 0 mM KNO_3 (Figure 7a-d). The same tendencies in nodule number were observed at earlier time points (14 and 21 days post inoculation, Supplemental figure S2). Consistently, miR171c KO plants grown under the same conditions showed insensitivity to nitrate dependent inhibition of nodulation (Figure 7d).

Dependent of nitrogen supply, miR171c OX plants displayed a shorter primary root length than WT plants (Figure 7e-f). miR171c OX #4 plants showed a nitrate dependent response in that primary root length increases when plants are grown under 5 mM KNO_3 compared to 0 mM KNO_3 (Figure 7e). However WT plants as well as miR171c OX #35 did not show a difference in primary root length when grown under 5 mM KNO_3 compared to nitrate starvation conditions (Figure 7e-f). qPCR confirmed an overabundance of mature miR171c in miR171c OX #4 and miR171c OX #35 lines compared to wild type plants (Figure 7g). miR171c OX#4 displayed 50-fold higher and miR171c OX#35 100-fold higher miR171c abundance than WT (Figure 7g). miR171c OX plants respond developmentally to applied nitrate, which leads to strong shoot development with increased leaf size and green color, whereas miR171c KO plants hardly respond (Supplemental figure S3). Unlike miR171c KO plants, miR171c OX plants (#4 and #35) showed normal germination. Overall, miR171c OX plants show partial inhibition of nodulation and are overly sensitive to nitrate supply leading to strong reduction of nodulation.

Discussion

miR171c KO plants display a nitrate dependent phenotype. According to the SDI hypothesis, a hypernodulation phenotype in SDI KO plants is expected because of the lacking inhibitor. However, no difference between WT and miR171c KO plants are visible in regard to nodule number under 0 mM KNO_3. miR171c transcript levels were hardly detectable in these plants, therefore a full knockout is assumed (Figure 6d). The fact that nodulation was similar in

miR171c KO and WT plants under low nitrate conditions suggests the existence of one or more miR171c independent SDI molecule(s) which prevail under these conditions. Then loss of one inhibitor among others would not change significantly the phenotype. miR171c KO plants displayed germination problems and delayed overall development. In plate experiments where miR171c KO plants were compared between 0 mM and 5 mM (without *M. loti* MAFF303099) it could be observed that miR171c KO plants do not show bigger shoots and increased leaf size with dark green color when 5 mM KNO_3 was applied (Supplemental Figure S3). That also indicates that miR171c KO plants are not able to either sense nitrate supply or process those information in downstream signaling cascades.

miR171c OX plants displayed a partial inhibition of nodulation, and when nitrate was applied these plants showed a stronger reduction of nodulation than WT. According to the SDI hypothesis, miR171c OX plants should lead to inhibition of nodulation. However, these plants develop nodules but nodule number is reduced by half compared to WT. The miR171c levels in miR171c OX #4 are 50-fold and in OX #35 100-fold increased which might be not enough to induce a full symbiosis inhibition. However it is more likely that other factors like miRNAs or transcription factor which are part of SDI are involved in rhizobia-triggered AON. In miR171c OX plants however it was observable that these plants react more sensitively to nitrate than WT. miR171c OX plants did not develop any nodules when grown on 5 mM KNO_3 and responded much more strongly than WT, where usually still occasional nodules appear. miR171c OX plants did not have any germination problems or in general developmental issues in contrast to miR171c KO plants. In addition, when seedlings were grown on plate with 0 mM or 5 mM KNO_3 (without *M. loti* MAFF303099) it could be observed that these plants can sense and process nitrate supply because of bigger leaf size and green color (Supplemental figure S3).

From those observations, of miR171c KO and miR171c OX it can be assumed that miR171c has a function in nitrate-responsive development and nitrate-triggered AON. Two NIN-like proteins namely LjNLP4 and LjNLP1 (Nishida and Suzaki, 2018; Nishida et al., 2018; Lin et al., 2021; Nishida et al., 2021) have been shown to play a major role in nitrate mediated inhibition of nodulation. Knockout plants of *nlp4* and *nlp1* do not respond to nitrate supply and therefor show no reduction in nodule number (Nishida and Suzaki, 2018; Nishida et al., 2018; Lin et al., 2021; Nishida et al., 2021). To further investigate the role of miR171c in nitrate signaling,

crossings of *nlp1* and/or *nlp4* with miR171c KO could reveal if miR171c and both NLP act in the same pathway and might lead to an additive phenotype. Another possibility would be to test transcript levels of miR171c in *nlp* mutants and vice versa test NLP transcript level in miR171c KO plants to examine which factor lies upstream and affects the other. So far, overexpression of NLP proteins in legumes has been performed in context of LjNF-YB gene expression but not in context of nitrate-induced inhibition of nodulation (Nishida et al., 2021). It is possible that overexpression of NLP leads to a similar phenotype like in miR171c OX plants. Interestingly, cytokinin mutants like *ipt4* display an overly sensitive nitrate phenotype (Lin et al., 2021) comparable to miR171c OX plants. With qPCR analysis in miR171c OX plants the transcript levels of several IPTs could be examined to investigate if IPT levels are changed and therefor dependent on miR171c. Investigating NLPs and miR171c and their respective phenotype, also in the context of cytokinin regulation, might lead to further insights into nitrate-mediated inhibition of nodulation.

2.2.4. miR171c-dependent nitrate responsiveness of symbiosis is shoot controlled

miR171c KO plants show a nitrate insensitive phenotype when inoculated with *M. loti* (Figure 6). Since in *Lotus japonicus* miR171c is present in both shoots and roots, the question arises which miRNA population is responsible for the phenotype observed in miR171c KO mutants. Therefore grafting experiments were performed. Scion and rootstock of two genotypes (WT and miR171c KO) were swapped with the other genotype, respectively. Successfully grafted plants were then inoculated with *M. loti* and grown on 5 mM KNO_3.

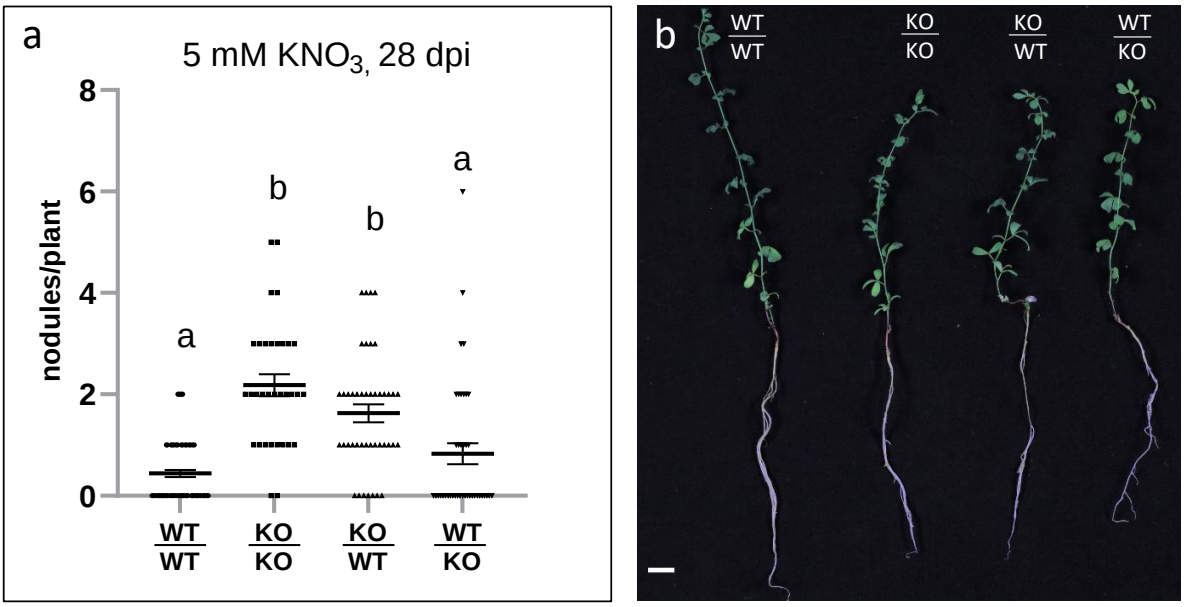

Figure 8: **Shoot miR171c is responsible for nitrate insensitivity in miR171c KO plants.**

a: Nodule counts on grafted plants inoculated with *M. loti* (MAFF303099) and grown on 5 mM KNO_3. Nodules were counted after 28d. At least 33 plants of 4 independent experiments were evaluated for each scion/rootstock combination. **b**: Representative, successfully grafted plants, harvested after 28 dpi, scale bar: 1 cm. Two-way ANOVA was performed followed by Tukey's test. $p<0.05$, significantly different values are indicated by different letters. Centerline and error bars display the mean with SEM.

4 weeks after inoculation, plants were harvested and nodules counted (Figure 8a, b). In WT/WT grafts, the nodule number was low when plants grew on 5 mM KNO_3. KO/KO plants however are insensitive to nitrate dependent nodule inhibition and consistently, the nodule number was higher than in WT/WT plants (Figure 8a). KO/WT plants showed similar amount of nodules as KO/KO, whereas WT/KO grafts displayed a similar number of nodules as WT/WT. Taken together, the results suggest that the shoot population of miR171c is required and sufficient for the nitrate insensitivity in miR171c KO plants in a systemic way.

Discussion

Grafting experiments of WT and miR171c KO plants clearly demonstrated systemic mobility of miR171c, and shoot-derived miR171c was determined as main factor in conferring nitrate insensitivity displayed by miR171c KO plants, and was both necessary and sufficient to induce it. These results indicate that under high nitrate concentrations, miR171c is produced in shoots and travels systemically to the root where it activates downstream signaling leading to the reduction of nodule numbers. Although from the grafting experiments it is assumed that the shoot-derived miR171c is the main factor for the nitrate insensitive nodulation phenotype of miR171c plants, it cannot be excluded that root-derived miR171c also possess a function in that regard. Natural nodule number variation does occur in WT plants, and few nodules still develop under high nitrate concentrations. The same nodule number variation can be observed in miR171c KO plants. Therefore, high number of replicates are needed to confirm quantitative differences in nodulation phenotypes. Furthermore, grafting experiments as such are difficult to perform because many plants do not merge when scion and rootstock are put in place. However at least 33 grafted plants of 4 independent experiments were evaluated (Figure 8), strongly indicating the involvement of systemic shoot miR171c in nitrate-mediated nodule inhibition.

2.2.5. miR171c is induced systemically and locally upon nitrate and *M. loti* treatment

Graftings experiments (Figure 8) showed that nitrate induces miR171c in *L. japonicus* shoots, which then travels to the root and triggers nitrate-dependent inhibition of nodulation. To gain further insights in local and systemic regulation of miR171c by nitrate as well as rhizobial inoculation, split root experiments were performed. To this end, primary roots of seedlings were removed to induce secondary root growth. Plants were then placed on agarpatches containing 0 mM or 5 mM KNO_3 or were inoculated with *M. loti* (MAFF303099). Then shoot and root tissue was harvested separately for qPCR-based determination of expression levels.

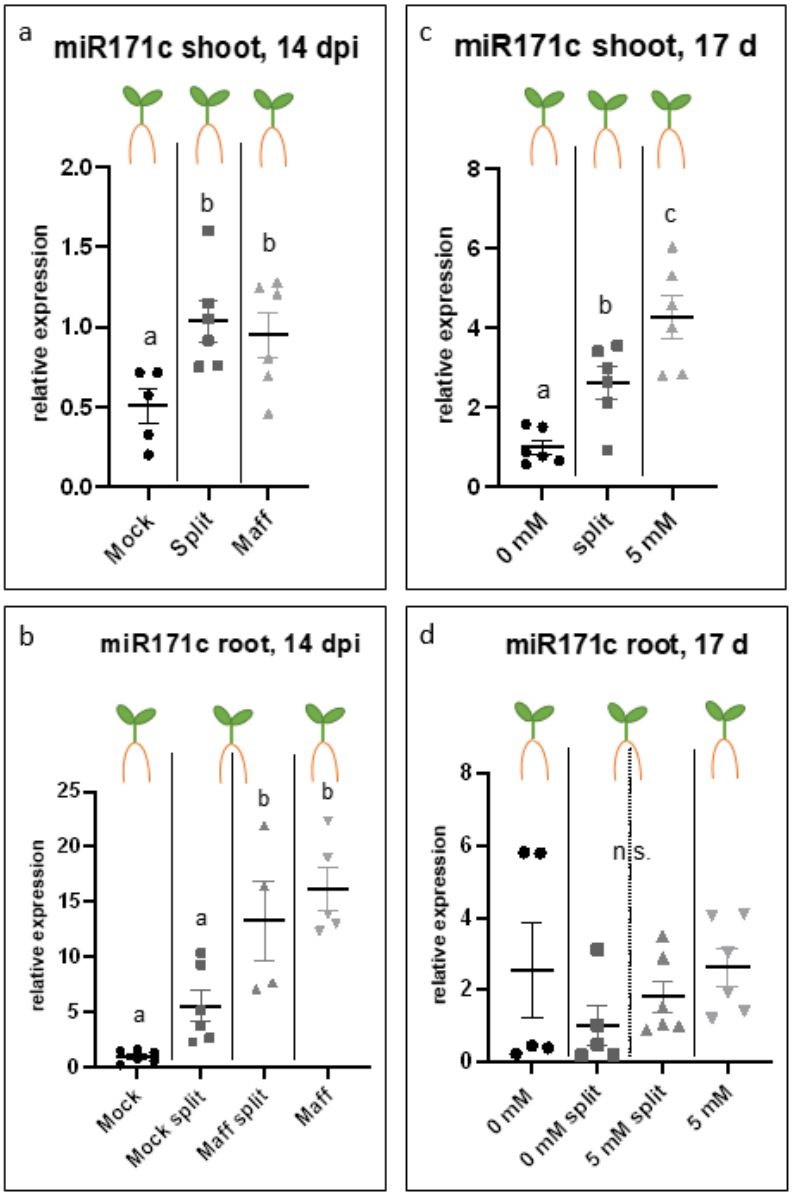

Figure 9: miR171c levels are higher in nitrate and *M. loti* treated roots as well as shoots compared to mock treated tissues.

a, b: Relative miR171c expression levels in shoots and roots in *M. loti* treated split roots. Plants were grown on B&D agar patches where one part was inoculated with *M. loti* (MAFF 303099). Harvest of shoot and root tissue was after 14 dpi. **c, d**: Relative miR171c expression levels in shoots and roots in nitrate treated split roots. Plants were grown on B&D agar patches containing 0 mM or 5 mM KNO_3. Harvest of shoot and root tissue was after 17 d. At least 4 biological replicates are shown. Centerlines and error bars show the mean with SEM, 0mM/Mock =1. Two-way ANOVA was performed followed by Tukey's test. $p<0.05$, significantly different values are indicated by different letters.

miR171c was induced in shoots of plants with *M. loti* treated split roots as well as in shoots of *M. loti* treated control roots compared to shoots in mock treated split roots (Figure 9a). miR171c levels in roots were higher in both split roots (mock split and *M. loti* split) as well as in control

M. loti roots than in mock treated roots (Figure 9b). Higher miR171c levels were observed in shoots of plants with split roots and in 5 mM KNO_3 control shoots (Figure 9c). No significant differences of miR171c levels could be observed in roots treated with different nitrate levels, however the tendencies suggest a nitrate- dependent increase of miR171c in split roots as well as in 5 mM KNO_3 control roots (Figure 9d). Increase of miR171c in shoots in both nitrate and *M. loti* treated plants compared to Mock and 0 mM KNO_3 control shoots indicates systemic miR171c induction (Figure 9a, c). miR171c levels in *M. loti* treated split roots (Mock split and *M. loti* split) were similar to miR171c levels in control roots (Mock and *M. loti*) suggesting a local response of miR171c to rhizobia in roots (Figure 9c). Increase of miR171c in split roots (0 mM split and 5 mM split) as well as in 5 mM KNO_3 control roots compared to 0 mM KNO_3 treated roots, points to a local response of miR171c to nitrate in roots (Figure 9d).

Shoots of *M. loti* treated plants (shoots of plants with split roots and *M. loti* control shoots) appear slightly bigger than control shoots under Mock conditions (Supplemental figure S4a). In nitrate treated plants (0 mM split, 5 mM split, and 5 mM control) shoots are bigger and develop enlarged dark green leaves compared to plants grown on 0 mM KNO_3 agar patches Supplemental figure S4b). Taken together, the results show that nitrate and *M. loti* treatment induces a systemic response in shoots as well as a local response in roots.

Discussion

It has been shown that plants display a systemic response when treated with rhizobia and nitrate sources (Suzuki et al., 2008; Jeudy et al., 2010). However, the involvement of miR171c in AON and nitrate signaling has not been shown. In split root experiments, local and systemic responses to specific treatments can be analyzed. The local response in roots can be observed when roots have direct access to nutrients. It was shown that *Medicago truncatula* roots respond to nutrients locally by branching and lateral and primary root growth (Jeudy et al., 2010). Roots respond to specific nutrient stimuli without direct contact, indicating that systemic signaling takes place (Cho and Harper, 1991; Yashima et al., 2003; Jeudy et al., 2010). The roots in contact send signals to the shoot, which in turn triggers systemic signal travel to the roots. The induction of miR171c in shoots upon nitrate and *M. loti* treatment is a strong indication for systemic response (Figure 9a, c). In split roots of *M. loti* treated plants (Mock split and *M. loti*

split, Figure 9b) increase of miR171c levels are similar to transcript levels of the respective control conditions (Mock and *M. loti*) indicating a local response. Intermediate levels of miR171c in split roots (Mock split and *M. loti* split) would point to a systemic response of miR171c to rhizobia. However, it is possible that a strong rhizobia-mediated local response of miR171c overpowers a possible weaker systemic response in shoots (Figure 9a, b). In nitrate treated plants miR171c levels in roots increased (0 mM split, 5 mM split, 5 mM control; Figure 9c, d). However if a nitrate-mediated local response of miR171c is present it is difficult to interpret, because of data variation and lack of statistical significance.

The difference in shoot appearance between *M. loti* and nitrate treated plants (Supplemental figure S4) could be due to the different time period plants need for nitrogen incorporation. Plants that grow directly on media supplied with nitrate can sense and take up nitrate resulting in the development of big green shoots (Supplemental figure S4b). However, in *M. loti* treated plants, the development of pink nodules takes between 10 and 14 days explaining the smaller shoots compared to nitrate treated plants. However, the split root system needs improvement. We faced technical difficulties when analyzing roots exposed to nutrient stress (in both *M. loti* and nitrate treatment), where RNA quality was compromised. In addition, the optimal harvest time point needs to be further addressed. The harvest time point of 14 days for *M. loti* treated plants is sufficient to observe mature nodule development and rhizobia-triggered miR171c induction. In split root experiments where plants were treated with nitrate, 14 days as harvest time point is not sufficient to observe nitrate-mediated miR171c induction, however 21 days resulted in starved (0 mM KNO_3 agar patches) and therefore stressed plants leading to poor RNA quality. In nitrate treated split roots (Figure 9c, d), harvest was performed after 17 days but also here problems occurred with partial RNA degradation due to aged, nutrient-stressed tissue. Once these problems are solved, split roots provide insights in systemic and local responses of plants to different stimuli. Overall, nitrate and rhizobia treatment induce upregulation of miR171c in shoots and roots. Although in both conditions (nitrate and rhizobia treatment) systemic and local induction of miR171c could be observed, our data suggest a stronger systemic response of miR171c to nitrate treatment, whereas rhizobia induced miR171c display a stronger local response.

2.2.6. Systemic induction of miR171c by nitrate and *M. loti* is dependent on *HAR1*

Lin et al. (2010) showed that SDI is HAR dependent. In order to test if miR171c is HAR1 dependent, wild type (Gifu) and *har1-3* plants were grown on plates and infected with *M. loti*, or on media which was supplied with 5 mM KNO_3, as well as under control conditions. After 3 and 14 days shoot and root tissue was harvested and RNA extraction was performed with subsequent qRT-PCR.

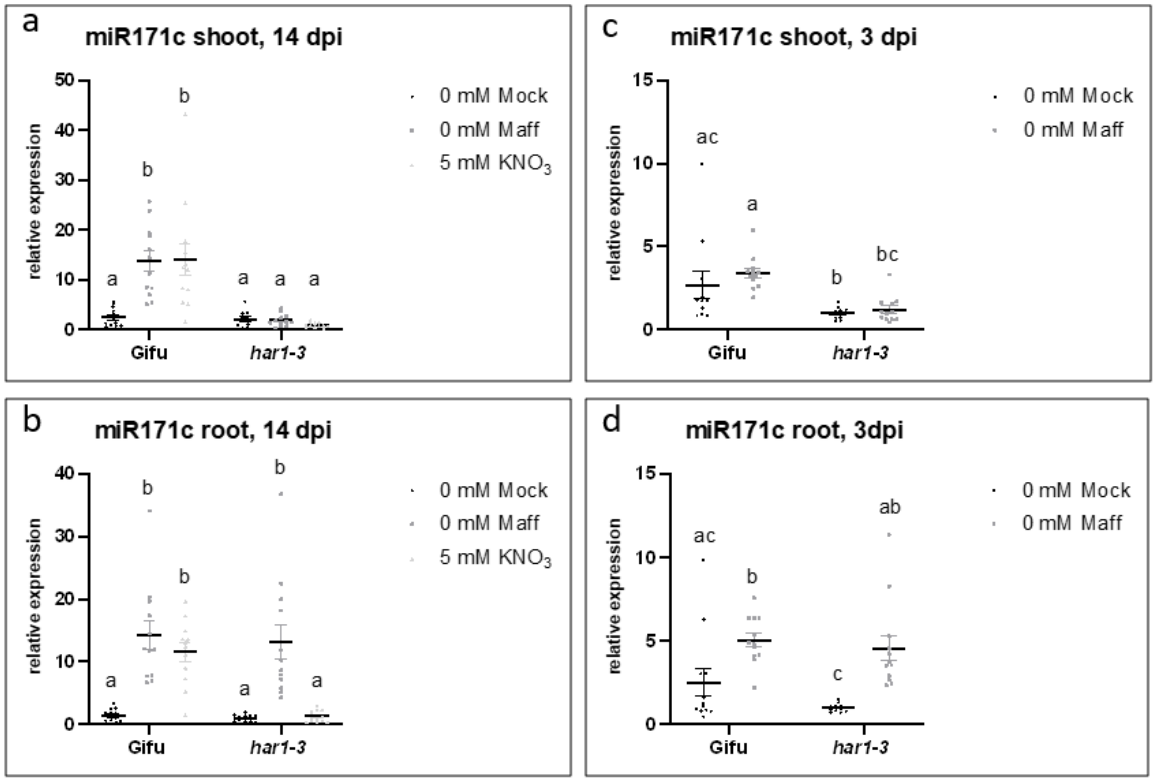

Figure 10: Rhizobia and nitrate induced miR171c in shoot tissue is HAR1 dependent.

a, b: Expression levels of miR171c in shoots and roots after 14d. Plants were grown on B&D plates supplied with 0 mM or 5 mM KNO_3 or infected with *M. loti* (MAFF303099). Shoot and root tissue was harvested after 14d. At least 11 biological replicates of two independent experiments are shown. **c, d:** Expression levels of miR171c in shoots and roots after 3 d. Plants were grown on B&D plates under mock conditions or infected with *M. loti* (MAFF303099). Harvest was performed after 3 dpi. At least 11 biological replicates of two independent experiments are shown. Centerlines and error bars show the mean with SEM, *har1-3* 5 mM KNO_3/*har1-3* 0 mM Mock =1. Two-way ANOVA was performed followed by Tukey's test. $p<0.05$, significantly different values are indicated by different letters.

miR171c was induced by nitrate as well as rhizobia in wild type shoots compared to mock conditions (Figure 10a). In *har1-3* mutants however no induction of miR171c triggered by nitrate or *M. loti* in shoot tissue could be observed (Figure 10a). Wild type roots showed increased miR171c levels when treated with 5 mM KNO_3 or rhizobia compared to mock

conditions (Figure 10b). In *har1-3* roots *M. loti* induced upregulation of miR171c could be observed, however nitrate-mediated miR171c induction was absent (Figure 10b).

In order to investigate if rhizobia triggered induction of miR171c (Figure 10a, b) is dependent on nodule primordia development, wild type (Gifu) and *har1-3* plants were harvested at 3 days post inoculation, preceding traceable nodule organogenesis. *M. loti* induced miR171c levels in wild type shoots could be observed (Figure 10c). *M. lot* induced miR171c levels in *har1-3* shoots were absent (Figure 10c). miR171c levels in wild type and *har1-3* roots increased when treated with *M. loti* compared to mock conditions (Figure 10d). Taken together, nitrate induced miR171c is dependent on HAR1. However, rhizobia induced miR171c is dependent on HAR1 in shoots but not in roots. Rhizobia induced miR171c in wild type and *har1-3* roots is not dependent on nodule primordia.

Discussion

HAR1 is one major factor controlling nodule number in rhizobia triggered as well as nitrate triggered AON. In inoculated *har1-3* mutants, roots are hypernodulating (Wopereis et al., 2000). Furthermore, *har1-3* plants fail to respond to nitrate, displaying the important role HAR1 has in AON and nitrate dependent inhibition of nodulation (Nishida and Suzaki, 2018; Nishida et al., 2020; Nishida et al., 2021). Moreover, *HAR1* dependency of SDI was postulated (Lin et al., 2010). miR171c induction in shoots is dependent on *HAR1*, fulfilling one requirement to serve as SDI. The question arises how *HAR1* controls induction of miR171c in response to rhizobia and nitrate.

Nitrate-induced miR171c levels in shoots and roots appear to be *HAR1* dependent (Figure 10a, b). However if root levels of miR171c are of local or systemic origin, and whether they depend on root or shoot HAR1 needs to be further addressed. One approach to solve this question might be via graftings using *har1-3* mutants and miR171c KO plants. In miR171c KO/WT grafts treated with nitrate, it could be analyzed if root miR171c levels depend on shoot expression of miR171c. Moreover, WT/*har1-3* grafts could give insights into whether root miR171c levels depend on root or shoot *HAR1* under nitrate sufficient conditions.

Shoot miR171c is *HAR1* dependent upon *M. loti* treatment (Figure 10a) however root miR171c is *HAR1* independent (Figure 10b). The induction of root miR171c might be a local response to rhizobia presence and therefore *HAR1* independent. To gain further insights in miR171c induction in roots, a shootless root experiment could be performed (Tsikou et al., 2018). If rhizobia mediated induction of miR171c occurs in shootless roots, miR171c is probably induced locally in roots and not dependent on shoot factors.

Rhizobia-mediated induction of miR171c is not dependent on nodule primordia presence (Figure 10c, d). After 3 days post inoculation, miR171c is induced in roots of wild type and *har1-3* plants indicating a very early response to rhizobia presence. These findings are in line with results of Holt (2014), where miR171c induction was present after 3 days post inoculation.

Local and systemic response of miR171c to nitrate treatment and rhizobia presence could be observed. HAR1 controls miR171c induction in shoots upon nitrate and rhizobia treatment. However if HAR1 acts alone or together with other shoot receptor-like kinases like CORYNE, KLAVIER or CLAVATA2 (Oka-Kira et al., 2005; Miyazawa et al., 2010; Krusell et al., 2011; Crook et al., 2016) needs to be further addressed. Examination of miR171c expression levels upon nitrate and rhizobia treatment in *coryne* (Crook et al., 2016), *klavier* (Oka-Kira et al., 2005; Miyazawa et al., 2010) or *clavata 2* (Krusell et al., 2011) mutants could reveal a possible involvement of these receptor-like kinases.

2.2.7. A general shoot inhibitor might control miR171c levels in roots

miR171c is induced in root tissue upon rhizobia treatment independently of HAR1 (Figure 10b). In order to examine if rhizobia-dependent miR171c induction in root tissue is still present without possible shoot factors, a shootless root experiment was performed. To this end, wild type (Gifu) plants were grown on B&D plates for 11 days. The shoot was cut and removed and the remaining roots were infected with *M. loti* immediately or transferred to plates containing 5 mM KNO_3. After 3 days roots were harvested.

In control roots (uncut) miR171c levels increased upon *M. loti* and nitrate treatment (Supplemental figure S5). In cut (shootless) roots, the transcript levels of miR171c were in general higher than in control roots (uncut). miR171c transcript levels were 20-fold higher in

mock cut roots compared to mock uncut roots. Upon both, *M. loti* and nitrate treatment slightly higher miR171c levels in cut roots compared to cut mock roots were observed. This is consistent with combined root- and shoot- regulation of root miR171c levels. Overall, cut roots display in general higher miR171c levels than uncut roots, which may indicate the presence of a shoot factor involved in inhibiting miR171c accumulation in roots.

Discussion

The shootless root experiment was performed to examine if unknown shoot factors are responsible for the induction of miR171c in *M. loti* treated roots (Figure 10b). Surprisingly, transcript levels of miR171c in cut roots are in general increased compared to control (uncut) roots (Supplemental figure S5) indicating that shoot factors might be involved in the regulation of root miR171c levels. In order to test for potential shoot factors acting as miR171c regulators, the same shootless root experiment should be repeated with several mutants like *coryne*, *klavier* and *clavata2* included (Oka-Kira et al., 2005; Miyazawa et al., 2010; Krusell et al., 2011; Crook et al., 2016). Potential interaction partners of HAR1 like CORYNE, KLAVIER or CLAVATA2 (Oka-Kira et al., 2005; Miyazawa et al., 2010; Krusell et al., 2011; Crook et al., 2016) could be involved in shoot mediated miR171c signaling, because these mutants are part of AON and also display a hypernodulating phenotype. The examination of this potential shoot factor will give further insights in the specificities of a general shoot inhibitor of miR171c.

2.2.8. *pMIR171c::GUS* activity in roots is independent of shoot miR171c presence

miR171c induction upon *M. loti* treatment in roots was shown to be independent of HAR1 (Figure 10b). In nitrate treated plants however neither shoot nor root miR171c induction could be observed (Figure 10b). One possibility might be that shoot-derived miR171c may act as possible inductor of root MIR171c resulting in a positive feedback-loop. In order to examine if the 3kb upstream region of the *MIR171c* locus (fused to the *GUS*/*uidA* reporter gene) is active in roots without miR171c presence in shoots, graftings with wild type (Gifu), *pMIR171c::GUS* and miR171c KO plants were performed. As negative control served WT/WT (scion/rootstock) grafts. WT/*pMIR171c::GUS* grafts served as positive control to compare grafted miR171c

KO/*pMIR171c::GUS* plants with. After 3 weeks, plants were stained with X-Gluc staining buffer to investigate the GUS signal in the roots.

No GUS signal was observable in WT/WT grafts (Supplemental figure S6). WT/*pMIR171c::GUS* grafts displayed GUS signal in the root stele. miR171c KO/*pMIR171c::GUS* plants equally showed a clear GUS signal in the root vasculature. Thus, promoter activity of miR171c in the roots does not require shoot miR171c presence.

Discussion

GUS signal was visible in miR171c KO/GUS plants, indicating that the 3kb promoter fragment of miR171c in roots is not dependent on shoot presence of miR171c (Supplemental figure S6). These findings are in line with rhizobia-triggered induction of root miR171c independently of shoot miR171c presence in *har1-3* mutants (Figure 10b). miR171c KO/*pMIR171c::GUS* grafts were grown on mock conditions (without nitrate and *M. loti*). It would be interesting to examine promoter activity of miR171c KO/*pMIR171c::GUS* grafts in roots under different nutritional conditions. Thus, miR171c promoter activity in roots without shoot miR171c influence could reveal root specific promoter activity profiles to different stimuli like nitrate or rhizobia.

2.2.9. 3 kb promoter fragment of *NSP2* and *NSP3* is not functional

Degradome sequencing and 5'RACE revealed that miR171c targets the scarecrow-like GRAS transcription factor NSP2, which is necessary for nodulation (Branscheid et al., 2011; De Luis et al., 2012). Furthermore miR171c also targets a close homolog of NSP2 with high amino acid similarity level (66%); NSP3. The function of NSP2 and its mutant phenotypes were extensively studied, however not much is known about the function of NSP3. Therefore hairy roots expressing the *GUS*/*uidA* reporter gene driven by 3kb region upstream of *NSP3* were generated to study the promoter activity under mock and inoculated (3 dpi and 14 dpi) conditions. Furthermore, *pNSP2::GUS* constructs were included to compare the similarities or differences of the promoter activity to NSP3.

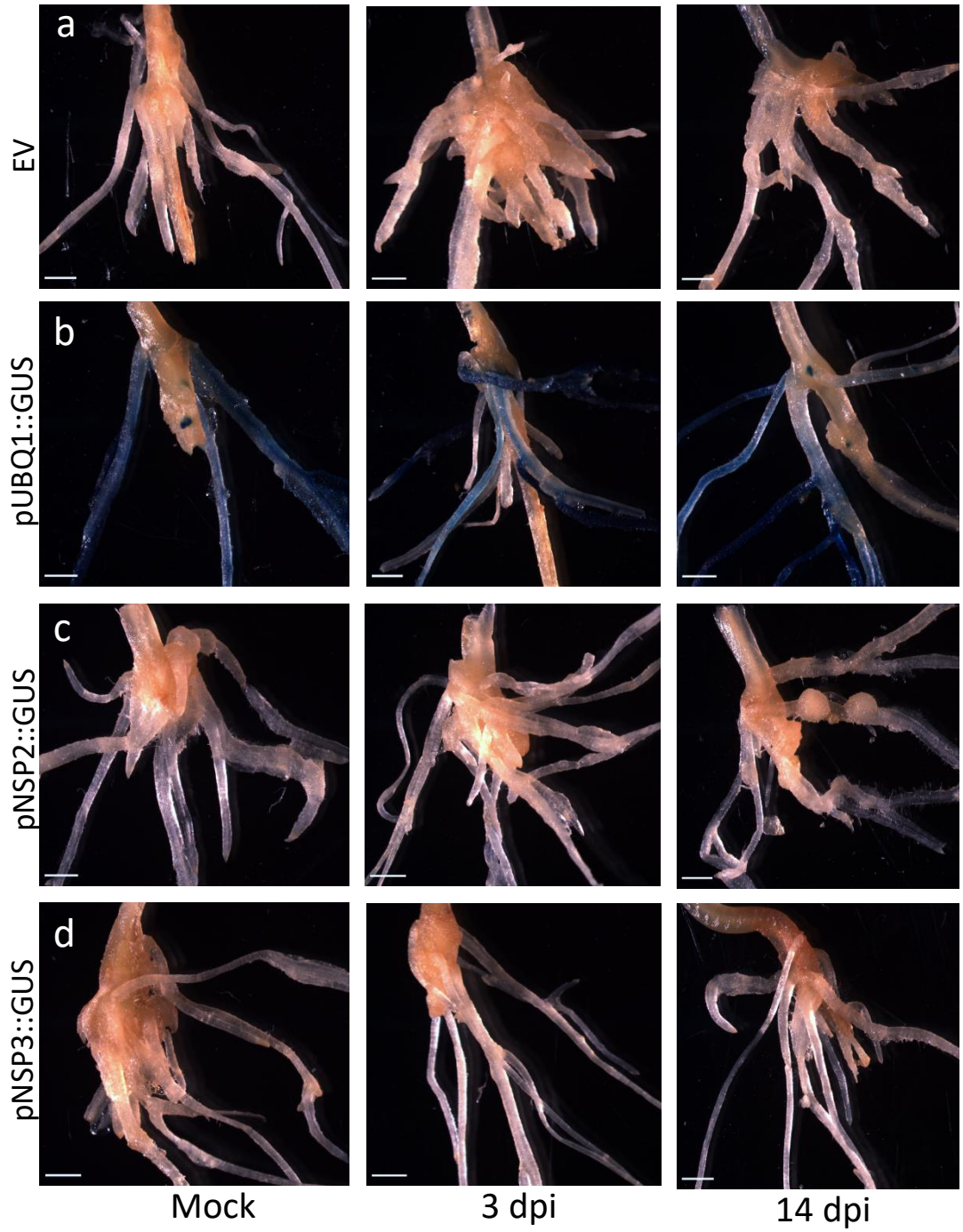

Figure 11: 3 kb promoter fragment of *NSP2* and *NSP3* is not functional.

a-d: Hairy roots expressing empty vector (EV) or the *GUS/uidA* reporter gene driven by *pUBQ1*, or a 3 kb promoter fragment of *NSP2* or *NSP3* are shown. Plants were transformed with *Agrobacterium rhizogenes* AR1193 carrying the constructs empty vector (EV) (**a**), *pUBQ1::GUS* (**b**), *pNSP2::GUS* (**c**) or *pNSP3::GUS* (**d**). Plants were either mock treated or inoculated with *M. loti* (MAFF303099, 3 dpi and 14 dpi). GUS staining was performed after 4 weeks. Scale bar: 1 mm.

No GUS signal was visible in hairy roots expressing the empty vector (EV, Figure 11a). Hairy roots expressing *pUBQ1::GUS*, serving as positive control showed clear GUS signal (Figure 11b). In hairy roots carrying *pNSP2::GUS* and *pNSP3::GUS*, no GUS signal was visible in any of the applied conditions (Mock, 3 dpi and 14 dpi). 3000 bp upstream of *NSP2* and *NSP3* were used for these promoter studies, which are probably not sufficient to drive traceable expression.

2.2.10. *nsp3-1* mutants display impaired nodulation and reduced nitrate sensitivity

In order to study possible nodulation phenotypes of *nsp3* mutants, in previous experiments *nsp3* mutants were isolated using a TILLING approach (Perry et al., 2009; Holt, 2014). *nsp3-1* mutants and wild type (Gifu) plants were grown on 0 mM and 5 mM KNO_3 and nodules were counted (14, 21 and 28 dpi).

nsp3-1 plants showed less nodules under 0 mM KNO_3 compared to WT in all measured time points (Figure 12a-e). WT plants grown on 5 mM KNO_3 formed reduced nodule numbers compared to 0 mM KNO_3 (Figure 12 a-c). *nsp3-1* mutants grown on 5 mM KNO_3 displayed reduced nodule number after 14 days post inoculation (Figure 12a) but not after later measured time points like 21 and 28 days post inoculation (Figure 12b, c), indicating compromised nitrate sensitivity. *nsp3-1* plants showed shorter primary root length under 0 mM as well as 5 mM KNO_3 compared to WT (Figure 12f). However, *nsp3-1* plants responded to nitrate availability and displayed longer primary root length under 5 mM KNO_3 than 0 mM KNO_3 (Figure 12f). *nsp3-1* mutants displayed germination problems (*nsp3-1* germination rate: 10-20 %, WT (Gifu) germination rate: 80%) as well as delayed overall development within the first 7-10 days after germination. *nsp3-1* seeds were much smaller and displayed less seed weight than wild type (Figure 12g). Taken together, *nsp3-1* plants display less nodules and nitrate dependent inhibition of nodulation is disturbed. Furthermore, *nsp3-1* mutants show several developmental problems including germination.

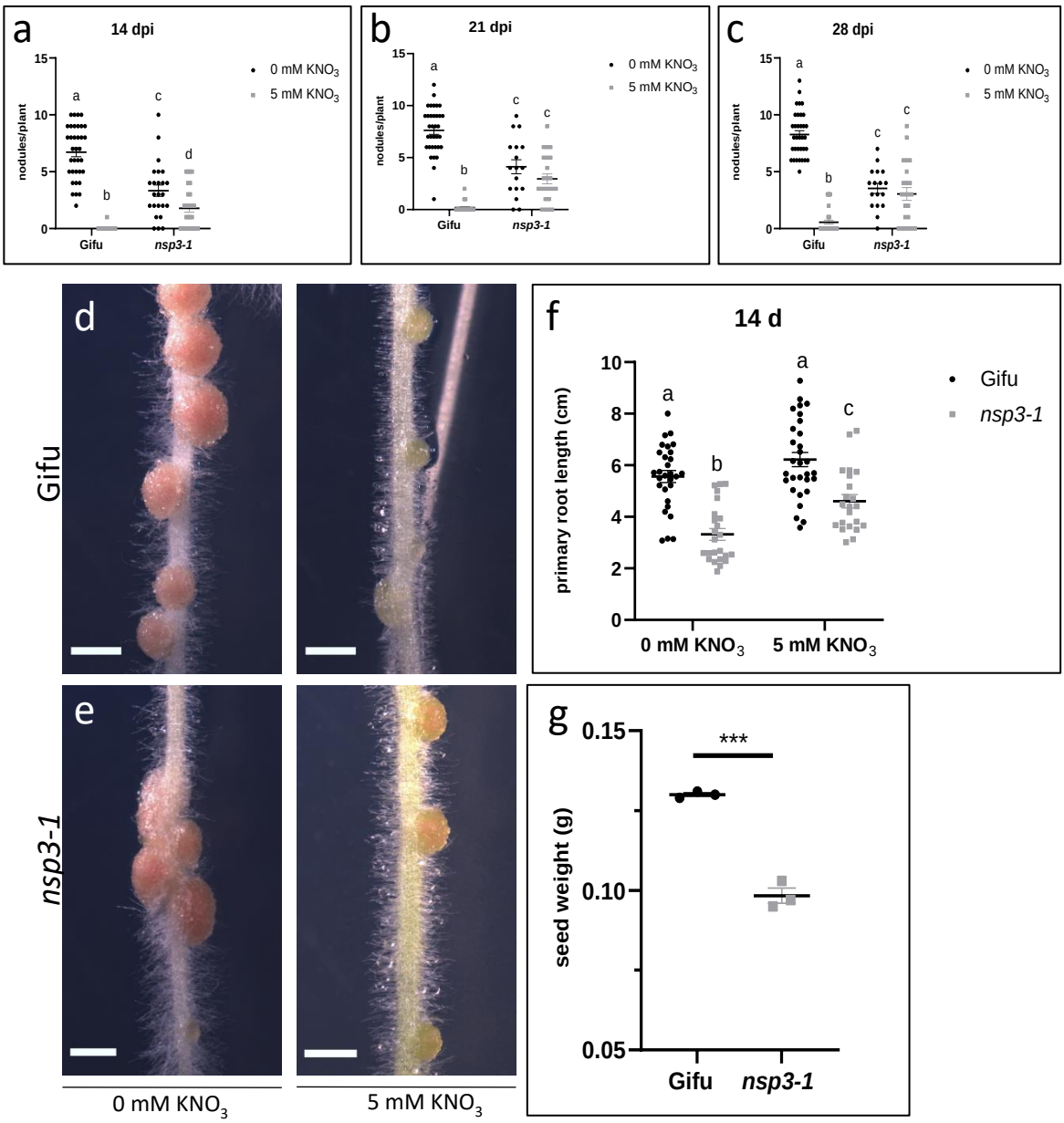

Figure 12: *nsp3-1* plants show less nodules than wild type plants and reduced nitrate sensitivity of nodulation.

a-e: Counted nodules of WT and *nsp3-1* mutants at different time points and nitrate conditions. Plants were grown on B&D plates with 0 mM or 5 mM KNO_3 and infected with *M. loti* (MAFF303099). After 14, 21 and 28 d nodules were counted. **d, e**: Pictures were taken after 14 dpi, scale bar: 1 mm. **f**: Measured primary root length of WT and *nsp3-1* mutants under different nitrate conditions. Plants were grown on B&D with 0 mM or 5 mM KNO_3. Primary root length was measured after 14d. **g**: Seed weight measurement of WT and *nsp3-1* mutants. 100 seeds were counted and weight was measured three times. Centerlines and error bars show the mean with SEM. Two-way ANOVA was performed followed by Tukey's test. $p<0.05$, significantly different values are indicated by different letters. Student's t-test ***= $p>0.001$.

Discussion

The promoter fragments used in *pNSP2::GUS* and *pNSP3::GUS* studies (3kb upstream of the gene) appear to be not functional. Therefore, addional 3kb upstream (6kb upstream of gene) were analyzed for promoter specific responsive elements. Certain promoter responisive elements like cytokinin-, nod factor- and nitrate responsive elements (NRE) as well as NIN-binding sequence were shown to be essential promoter binding sequences for transcription factors in order to induce symbiotic nodule organogenesis (Andriankaja et al., 2007; Ariel et al., 2012; Soyano et al., 2015). Within the promoter sequence of *NSP2* none of those mentioned responsive elements were found, indicating that possible elements lie further upstream than the tested 3 kb.

The analyzed 3kb (6kb upstream of *NSP3*) promoter sequence of *NSP3* showed 2 NRE and 4 ERF elements. NRE can be bound by NIN, NLP1 and NLP4 and function mainly in nitrate induced signalling, leading to inhibition of nodulation. The 2 NRE sequences might indicate a possible involvement of NSP3 in nitrate signalling, in line with the nitrate insensitivity of *nsp3-1* mutants after 21 and 28 days post inoculation (Figure 12b, c). Further, it was shown that NSP1 can directly interact with NRE of ERN1 promoter inducing the expression of ENOD11 (Hirsch et al., 2009). It could be possible that NSP1 also has the ability to bind NRE of NSP3 promoter and therefore regulate NSP3 expression. One could speculate that the NSP1/NSP2 complex induces gene expression by binding to several promoters of nodulation inducing genes including *NSP3*. It might be possible that the 4 ERF elements found in the *NSP3* promoter region, might be bound by ERF transcriptions factors belonging to the AP3/ERF familiy, which are triggered upon ethylene induction (Andriankaja et al., 2007; Middleton et al., 2007). ERF transcription factors serve as positive regulator for symbiosis (Asamizu et al., 2008; Yano et al., 2016) and might be essential for *NSP3* promoter functioning. ERF and NRE sequences within the *NSP3* promoter could indicate that at least 6kb upstream of the gene are necessary for a functional promoter of *NSP3*.

The general low nodule number in *nsp3-1* mutants suggests that NSP3 has a previously unknown role in nodulation. Furthermore, *nsp3-1* mutants grown on 5 mM KNO_3 (21 dpi and 28 dpi) do not reduce nodule number like wild type, indicating involvement of *NSP3* in nitrate dependent inhibition of nodulation (Figure 12b, c). Lauressergues et al. (2012) identified an

NSP2-like gene (Medtr5g058860), which shares amino acid homology to the *NSP3* gene in *Lotus japonicus* (Lauressergues et al., 2012). In inoculated *Medicago truncatula* plants, NSP2-like transcrip levels increased in root tissue compared to roots under mock conditions (Lauressergues et al., 2012). However Holt (2014) showed that NSP3 levels in roots gradually decrease from 1 to 4 days post inoculation, indicating a different expression pattern of NSP3 to rhizobia treatment in *Lotus japonicus* compared to *Medicago truncatula* (Holt, 2014). Holt (2014) analyzed several *nsp3* mutants from a TILLING approach regarding nodule number. None of those tested mutants showed significant reduced nodule number compared to wild type, however problems ocurred with germination and development of *nsp3* mutants (Holt, 2014). Similar problems with general unhealthiness of *nsp3-1* plants were discovered, which can also be observed in reduced seed weight compared to wild type (Figure 12g). Transient overexpression of NSP3 in *nsp2* mutants leads to partial rescue of nodulation in *nsp2* mutants, suggesting a partial functional redundancy between NSP2 and NSP3 (Holt, 2014). In order to further examine the role of NSP3, LORE insertion lines (30123453) were ordered and genotyped accordigly. With a possible better fitness in those *nsp3* mutants, more reliable plate experiments can be performed paving the way for future studies on NSP3.

2.3. Investigation of miR169bc as possible SDI candidate

2.3.1 *nf-ya1* mutant lines display defects in nodulation and infection thread formation

Apart from miR171c, miR169 is an additional SDI candidate. miR169bc and d are highly induced in CLE-RS3 OX plants and decreased in *har1-3* plants (Figure 3d). miR169 isoforms target members of the NF-YA family; transcription factors involved in nodule persistence and maintenance (Combier et al., 2006; Xu et al., 2021). In *Medicago truncatula*, miR169a overexpression leads to delayed and arrested nodule growth (Combier et al., 2006). *nf-ya1* mutants show less nodules compared to wild type, however no difference could be observed in the number of infection threads (Hossain et al., 2016; Shrestha et al., 2021). In order to examine early infection events in *Lotus japonicus*, NF-YA1 LORE lines (30162806) were infected with *M. loti* and infection threads and pockets were counted after 7 days.

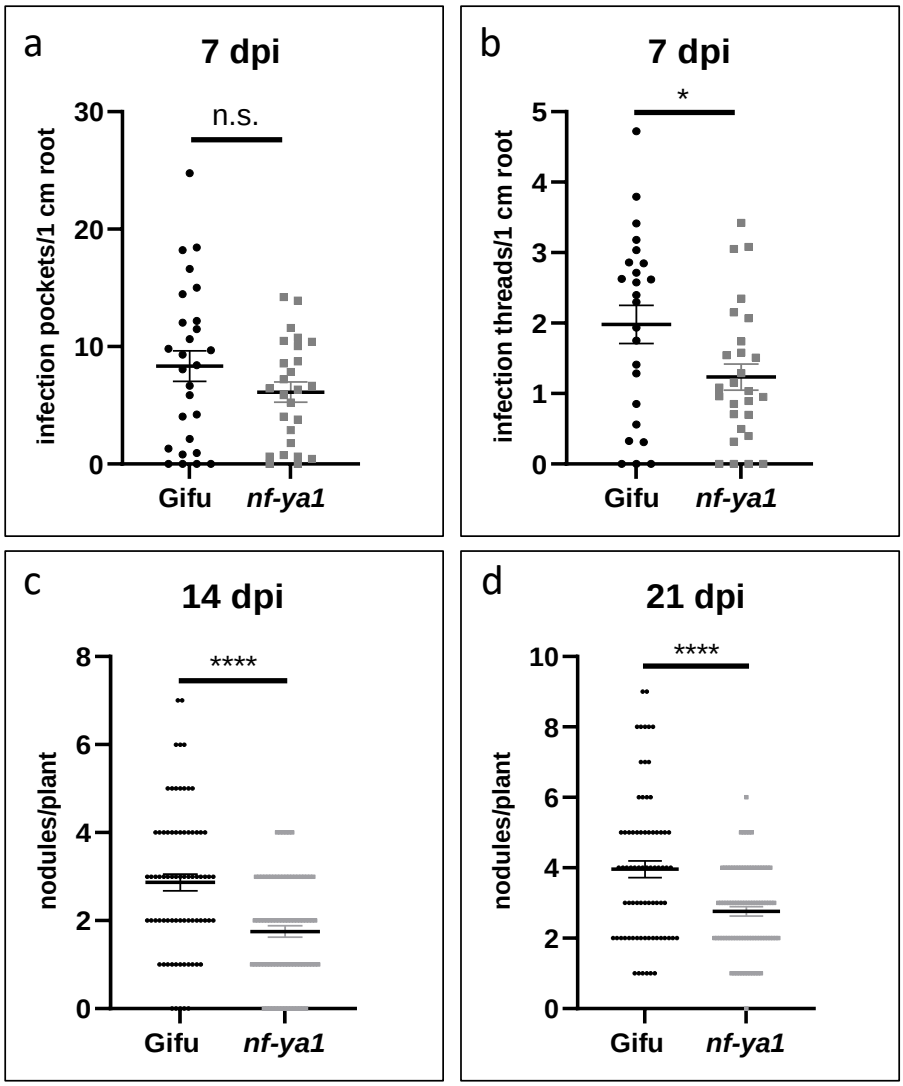

Figure 13: *nf-ya1* mutants show less nodules and infection threads than WT.

a, b: Counted infection pockets and threads of WT and *nf-ya1* mutants. Plants were grown on 0 mM KNO_3 B&D plates, infection pockets and threads were counted after 7 dpi. At least 24 biological replicates are shown. **c, d**: Counted nodules of WT and *nf-ya1* mutants. Plants were grown on 0 mM B&D plates, nodules were counted 14 and 21 dpi. At least 75 biological replicates of two independent experiments are shown. Centerlines and error bars show the mean with SEM. Student's t-test *=p< 0.05, ****=p<0.0001.

No statistically significant difference could be observed in infection pocket number between wild type and *nf-ya1* LORE lines (30162806) (Figure 13a). *nf-ya1* LORE lines (30162806) mutants displayed less infection threads (Figure 13b) and less nodules after 14 as well as 21 days compared to wild type (Figure 13c, d).

2.3.2. *pUBQ1* mediated overexpression of miR169c may be lethal

miR169bc is a potential SDI candidate, which was investigated. In order to analyze the potential nodulation phenotype, stable lines including miR169c OX and miR169 STTM were generated. Additionally, *pMIR169b::GUS* and *pMIR169c::GUS* lines were created to examine the promoter activity. miR169c OX plants died after 10-14 days, once they were transferred to pots (Supplemental figure S7). The transcript levels of the remaining miR169c OX survivor plants were examined via qPCR. All tested miR169c OX mutants displayed dramatically reduced miR169c transcript levels, indicating silencing of the transgene along with one or more endogenous *MIR169* genes (Supplemental figure S7).

Discussion

Several *nf-ya1* mutants has been studied in the past and all of them share a similar phenotype of less nodules than wild type, however no difference in early infection events was shown (Hossain et al., 2016; Soyano et al., 2019; Shrestha et al., 2021). Hossain et al. (2016) and Shrestha et al. (2021) showed that *nf-ya1* single mutants displayed less nodules but similar amount of infection events like wild type plants. *nf-ya1* LORE lines (30162806) mutants in this study carry the LORE insertion 8 bp after the ATG of the main ORF. Hossain et al. (2016) and Shrestha et al. (2021), used *nf-ya1* single mutants which were obtained through ethylmethanesulfonate (EMS). The different *nf-ya1* mutants used could explain the difference observed in early infection events.

NF-YA1 and NF-YA4 induce the expression of STYs in young nodule primordia, which in turn activate YUCCA1 and YUCCA11 (Shrestha et al., 2021). YUCCA1 and YUCCA11 encode flavin monooxygenases, which are part of the local auxin response upon inoculation (Shrestha et al., 2021). Although NF-YA1 acts partially redundantly with NF-YA4 (Hossain et al., 2016; Shrestha et al., 2021), clear nodulation and infection thread phenotypes can be observed in *nf-ya1* mutants (Figure 13). These observations indicate that the NF-YA1-STY-YUCCA node is disturbed in *nf-ya1* mutants. Auxin was shown to positively regulate nodule and infection thread formation (Suzaki et al., 2012; Suzaki et al., 2013; Breakspear et al., 2014). In mutants of the auxin responsive gene *ARF16a,* less infection threads and less infection pockets could be

shown, indicating an involvement of auxin as positive regulator in early infection events (Breakspear et al., 2014). The phenotype in *nf-ya1* mutants (Figure 13) could be caused by a disturbed NF-YA1-STY-YUCCA node and therefore less auxin availability leading to less infection threads and pockets.

Members of the miR169 family are involved in many biotic and abiotic stress responses of plants. Overexpression of miR169d in Arabidopsis leads to stress induced early flowering (Xu et al., 2014). Moreover, miR169 is expressed under nitrogen starvation as well as under drought stress (Zhao et al., 2011; Yu et al., 2019). The severe phenotype observed in miR169c OX plants (Supplemental figure S7a) can be explained by a very strong reduction of NF-YA1 transcripts in the plant tissue. It was shown that KO of NF-YA2 and NF-YA8 in *Arabidopsis thaliana* are embryonic lethal, pointing to the important function of NF-YA transcription factors in early development (Pagnussat et al., 2005; Fornari et al., 2013). Moreover, it is possible that overexpression of miR169c not only targets NF-YA1 but other members of the NF-YA cluster (6 NF-YAs exist in *Lotus japonicus*, (Jin et al., 2014)) leading to a strong downregulation of NF-YAs.

To circumvent the lethal phenotype, a different promoter for miR169 OX studies was used, and stable plants expressing miR169bc driven by *SUC2* promoter were generated. These lines provide the possibility to study phenotypic effects on roots with specific overexpression of miR169bc in shoot vasculature. Activity of the *SUC2* promoter in *L. japonicus* is light dependent (Gavrilovic et al., 2016) and therefore miR169bc expression specifically takes place in shoot vasculature, avoiding graftings. The generated stable plants including *SUC2::MIR169b*, miR169 knockdown lines (miR169-STTM), and *pMIR169c::GUS* lines provide plants for intensive nodulation studies and promoter expression analysis.

2.4. *AtSUC2* promoter activity is light dependent in *L. japonicus* roots

The demonstration of miRNA mobility was performed through graftings. However, grafting experiments are difficult to perform. The scion and rootstock part usually show a 30% merging efficiency, hence many plant replicates are needed. Therefore stable plants expressing the miRNA of interest driven by the *SUCROSE TRANSPORTER 2* (SUC2) promoter (Sauer and

Stolz, 1994) represent a useful method to avoid graftings. The *SUC2* promoter is exclusively expressed in phloem companion cells (Sauer and Stolz, 1994) and can therefore be used to drive miRNA expression in shoot phloem which is the requirement for miRNA movement (Skopelitis et al., 2018). However it is crucial that the miRNA of interest is expressed only in shoot tissue in order to examine the systemic effect of that miRNA on a possible root phenotype. Initial results by Gavrilovic et al. (2016), indicated that *SUC2::GUS* expression was only visible in roots that were exposed to light (Gavrilovic et al., 2016). In order to confirm that *SUC2* activity is exclusively light dependent and not active under dark conditions, hairy roots expressing *pAtSUC2::GUS* were generated.

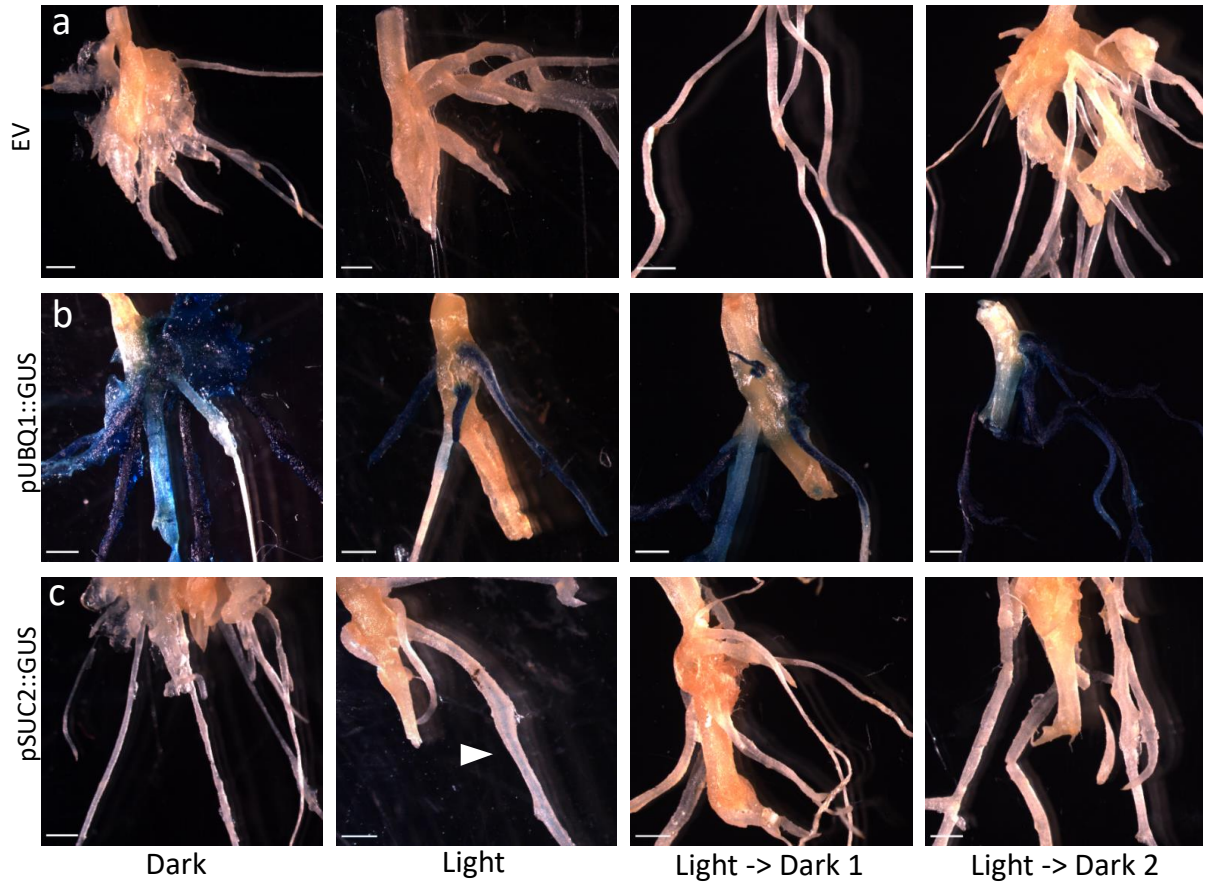

Figure 14: *AtSUC2::GUS* signal is visible in roots which are exposed to light.

a-c: GUS activity in hairy roots under different light and dark conditions. Plants were transformed with *Agrobacterium rhizogenes* AR1193 carrying the constructs, empty vector EV (**a**), *pUBQ1::GUS* (**b**) and *pAtSUC2::GUS* (**c**). Plants were grown on plate and exposed to light (**Light**) or shielded from light with combs, paper covered plates and coal agar, pipetted next to each plant (**Dark**). A subset of plants were first grown on plate exposed to light and then transferred to magenta growth boxes, where boxes were wrapped in aluminum foil and the surface covered with sand (**Light -> Dark 1**) or transferred to magenta growth boxes under normal conditions without light shielding steps (**Light -> Dark 2**). GUS staining was performed after 4 weeks. Arrowhead indicates *pAtSUC2::GUS* signal. Scale bar: 1 mm.

The empty vector control (EV) showed no GUS signal in any of the tested conditions (Figure 14a). GUS signal of hairy roots carrying *pUBQ1::GUS* was visible in all conditions (Figure 14b). Hairy roots carrying *pAtSUC2::GUS* did not display GUS signal in dark conditions (Figure 14c, Dark). *pAtSUC2::GUS* roots that were first grown on plate and later transferred to magenta growth boxes (Figure 14c, Light -> Dark 1 and 2) also do not show any GUS signal. *pAtSUC2::GUS* plants that were grown on plate and exposed to light displayed GUS signal in root stele (Figure 14c, Light, arrowhead). In order to examine if transcript levels of the *GUS* gene are detectable under dark conditions, qPCR with GUS specific primer was performed.

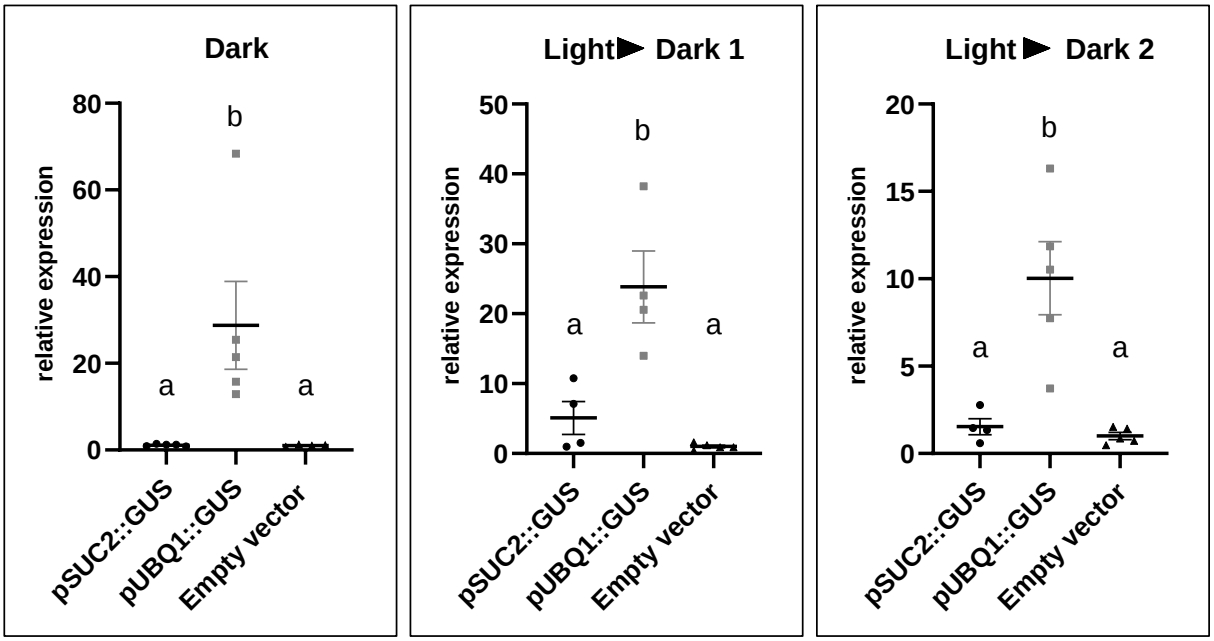

Figure 15: *pAtSUC2::GUS* expression level are low under dark conditions.

Expression level of GUS under different dark conditions. Plants were transformed with *Agrobacterium rhizogenes* AR1193 carrying the constructs *pAtSUC2::GUS*, empty vector (EV) and *pUBQ1::GUS*. Root tissue was harvested after 4 weeks. Plants were grown on plates shielded from light with combs, paper covered plates and coal agar pipetted next to each plant (**Dark**). A subset of plants were first grown on plate exposed to light (23 days) and then transferred to magenta growth boxes (5 days) where the boxes were wrapped in aluminum foil and the surface covered with sand (**Light -> Dark 1**) or transferred to magenta growth boxes without further light shielding steps (**Light-> Dark 2**). Centerlines and error bars show the mean with SEM, empty vector =1. Two-way ANOVA was performed followed by Tukey's test. $p<0.05$, significantly values letters are indicated by different letters.

In all tested conditions GUS transcript level were higher in *pUBQ1::GUS* than in empty vector plants (Figure 15). Hairy roots carrying the empty vector did not show specific GUS transcripts (Figure 15). In conditions where hairy roots were completely shielded from light GUS

transcript level driven by *AtSUC2* were near the detection limit (Figure 15, Dark). GUS expression driven by *AtSUC2* were higher in both Light -> Dark conditions (Figure 15, Light -> Dark 1 and 2) than plants carrying the empty vector. Taken together, the Arabidopsis SUC2 promoter is light dependent and remains inactive under dark conditions in *Lotus japonicus* roots. Therefore stable lines overexpressing the miRNA of interest driven by *AtSUC2* promoter can be used to perform specific phloem expression in the shoot.

Discussion

The SUC2 promoter represents a useful tool to study phloem specific expression of the gene of interest. In hairy roots expressing *pAtSUC2::GUS*, GUS signal could only be observed in roots exposed to light (Figure 14c, Light, arrowhead). In dark conditions, or conditions where plants were first exposed to light and then transferred to dark no GUS signal was visible indicating that Arabidopsis SUC2 promoter activity is light dependent in *Lotus japonicus* roots.

High light conditions allow increased photosynthesis and therefore photo-synthetically produced sucrose accumulates. The main function of SUC2 is loading of sucrose into phloem from photosynthetically active source leaves (Turgeon, 1989) from where it is transported to developing sink leaves and roots. While SUC2 is also present in roots, there it fulfills the function of sucrose retrieval during long distance transport, which has leaked out of the sieve elements (Turgeon, 1989; Stadler and Sauer, 1996). In *pAtSUC2::GUS* studies in Arabidopsis it could be shown that a strong GUS signal is present in the vasculature of source leaves and weak GUS signal in vascular cylinder of roots (Truernit and Sauer, 1995) indicating that SUC2 is highly active in source leaves. Gavrilovic et al. (2016) showed that in *pAtSUC2::GUS* transgenic *Lotus japonicus* roots, only roots exposed to light showed GUS activity, whereas in roots shielded from light the GUS signal was absent, which support the findings of this study, where GUS signal was only present when roots were exposed to light (Figure 14c).

The question how light dependent SUC2 activation functions and which factors are involved is not yet understood. It was shown that high light intensities increase SUC2 protein level (Xu et al., 2020). Two proteins namely UBIQUITIN-CONJUGATING ENZYME (UBC) 34 and WALL-ASSOCIATED KINASE LIKE (WAKL) 8 were found to regulate SUC2 activity via its

turnover rate and phosphorylation state in a light dependent manner (Xu et al., 2020). In *ubc34* mutants the SUC2 protein level as well as phloem exudate sucrose increase, implying that UBC34 controls the light-dependent turnover rate of SUC2 (Xu et al., 2020). WAKL8 however phosphorylates SUC2 in order to increase sucrose transport activity when high light intensities are present and therefore high photosynthesis activity (Xu et al., 2020). High light dependent increased SUC2 protein levels induced through an inhibited UBC34 and activated WAKL8, display light as a major trigger, however the question remains which factors are involved under dark conditions.

GUS expression level driven by *AtSUC2* in all conditions (Figure 15, Dark, Light -> Dark 1 and 2) was low compared to *pUBQ1::GUS* plants, indicating cell type specific activity of AtSUC2. However when *SUC2::GUS* plants were grown under dark conditions (Figure 15, Dark), GUS transcript levels were near the detection limit, whereas weak transcript levels could be observed in conditions where plants were first exposed to light and then kept in darkness (Figure 15, Light -> Dark 1 and 2). Although it was shown that the Arabidopsis SUC2 promoter is inactive when plants are grown under dark conditions (Wright et al., 2003; Gavrilovic et al., 2016), the underlying mechanism remains unknown. Thus, the observed weak GUS transcript levels, might indicate that *SUC2::GUS* plants were not grown long enough in darkness or roots were not completely shielded from light to completely block SUC2 promoter activity, if active SUC2 inhibition under darkness takes place which is unknown. If proteins like UBC24 and WAKL8, which are clearly involved in high light dependent SUC2 regulation (Xu et al., 2020), are also involved in dark conditions would be interesting to further address.

2.5. Plant-derived miRNAs are detectable in aphid tissue via qPCR

Most insects belonging to the order Hemiptera are pests that feed on plant sap (Grimaldi et al., 2005). In order to feed from the phloem, aphids penetrate the phloem with specialized mouth parts called stylets (Kennedy and Mittler, 1953). During the plant-aphid interaction it was shown that miRNAs are exchanged from aphid to plant and vice versa (Zhang et al., 2012; Rajwanshi et al., 2019). The detection of plant-derived miRNAs in aphid tissue provides the possibility to investigate which plant miRNAs are present in the phloem and therefore might

be possible candidates for long distance movement. Therefore aphids of the species "Planococcus citri" (Danzig and Gavrilov, 2010) were allowed to feed on *Lotus japonicus* Gifu plants for 2 weeks prior harvest. *Lotus japonicus* was treated with 1 mM KNO_3, 5 mM KNO_3 or 1 mM KNO_3 and *M. loti* inoculation and miRNA levels of miR2111 were measured.

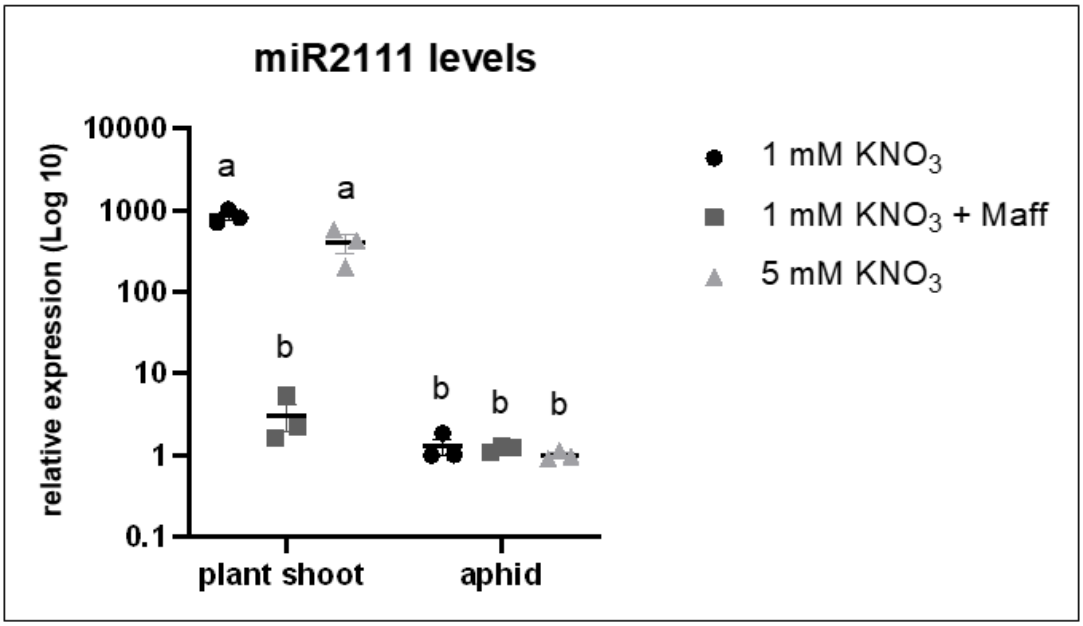

Figure 16: **Plant-derived miR2111 levels are detectable in aphid tissue.**

Expression levels of miR2111 in *Lotus japonicus* and aphid tissue. Plants were grown in magenta growth boxes and treated with 1 mM KNO_3, 5 mM KNO_3 or 1mM KNO_3 and *M. loti* (MAFF 303099) inoculation. Aphids fed on plants for 2 weeks prior harvest. Centerlines and error bars show the mean with SEM, aphid 5 mM KNO_3 =1. Two-way ANOVA was performed followed by Tukey's test. $p<0.05$, significantly different values are indicated by different letters.

High miR2111 levels were observed in plant shoots treated with 1mM KNO_3 and 5 mM KNO_3 (Figure 16). Low transcript levels of miR2111 were observed in plants treated with 1 mM KNO_3 and *M. loti* inoculation. Aphids that were harvested alongside plant shoot tissue did not show a difference in miR2111 level and are in general low. In the same experiment miR171c levels were measured, however problems with melt curve and primer specificity occurred. Overall, it is possible to detect plant-derived miRNAs in aphids with common Trizol-mediated RNA extraction followed by qPCR (5.9. RNA extraction, 5.10 cDNA synthesis and qPCR).

Discussion

Plant-derived miRNA detection in aphid tissue enables a first hint of evaluation of the phloem sap and the respective miRNAs present. In general, miRNA detection in aphids follows the same procedure in RNA extraction and qPCR (5.9. RNA extraction, 5.10 cDNA synthesis and qPCR) like from plant tissue however; some problems still need to be solved. In general the amount of plant-derived miRNAs in aphid is low, therefor a lot of aphid tissue is needed (at least 150 mg, these are between 10-20 aphids depending on their size). Grinding the aphid material after freezing in liquid nitrogen works best with either a pistil and the corresponding tube or crushing with several metal beads. The harvest time point of 2 weeks after onset of feeding were chosen, corresponding to the time frame needed for aphids to colonize the plant (Figure 16). The question remains if at a later time point the amount of plant miRNAs in aphids further accumulate or if plant miRNAs in general are degraded in aphids after a certain time or excreted. As symbiosis activator, miR2111 enables the plant to enter symbiosis by targeting the symbiosis inhibitor TML (Takahara et al., 2013; Tsikou et al., 2018). Thus, high miR2111 default levels could be observed upon 1 mM KNO_3 conditions (Figure 16). Plants treated with rhizobia displayed low miR2111 levels (Figure 16) because of AON induction and HAR1-mediated downregulation of miR2111 (Tsikou et al., 2018; Okuma et al., 2020). Sexauer et al. unpublished (2022) showed nitrate dependent downregulation of miR2111 in *Lotus japonicus.* Intermediate miR2111 transcript levels upon nitrate treatment (Figure 16) could be caused by false nitrate concentration or in general wrong nitrate treatment. Specific pattern of miR2111 in plant tissue due to different treatments cannot be observed in aphid tissue (Figure 16). These observation would indicate that in general plant-derived miRNAs are degraded in aphids or excreted from their bodies, however it is not clear when and how fast.

3 Conclusion

The aim of this work was to test the hypothesis that miRNAs act as shoot-derived inhibitors in nodulation symbiosis, and to identify and test candidate miRNA-target nodes. miR171c fulfills the criteria postulated for SDI-activity (Lin et al., 2010). miR171c expression in shoots is dependent on the LRR-RLK gene *HAR1* and is specifically expressed in shoot phloem cells. Moreover, this work shows that miR171c is systemically mobile. Overabundance of miR171c in miR171c OX plants partially inhibits nodulation. Notably, miR171c OX and miR171c KO plants showed nitrate dependent phenotypes: miR171c OX plants react hypersensitively and KO plants insensitively to nitrate, suggesting a role of miR171c in nitrate dependent inhibition of nodulation. This work reveals that miR171c is not only involved in rhizobia triggered AON but also in nitrate induced AON signaling as a systemic and local inhibitor of symbiosis. Further, NSP3 as target of miR171c (besides NSP2) was shown to be involved in nodulation and possibly acts in nitrate dependent inhibition of nodulation. miR169 was shown to qualify as additional SDI candidate and needs to be further investigated. Small RNA sequencing revealed several other miRNAs including miR5111 and miR5205 as promising candidates for future AON studies.

4 Outlook

Albeit miR171c qualifies as SDI, it is possible that several other small RNAs act complementarily conferring a specific regulatory downstream response in the presence of compatible rhizobia. Small RNA sequencing revealed several other miRNA candidates with promising SDI profiles. Further, other small RNAs like phasiRNAs could be involved in SDI signaling which needs to be further addressed.

miR171c OX and KO plants show a nitrate dependent phenotype compared to wild type plants. However it is not known where exactly in this signaling pathway miR171c is active. Under high nitrate conditions NLP1 and NLP4 (Nishida and Suzaki, 2018; Nishida et al., 2021) are two key players in nitrate signaling; however the downstream factors are not yet understood. It could be possible that NLP1 and NLP4 directly activate miR171c locally, which

in turn targets NSP2 (and NSP3) and therefore induces downstream responses. The question remains how two signaling pathways (rhizobia triggered AON and nitrate induced AON) having a common factor like miR171c are interlinked.

One possibility for such an interlinkage could be HAR1-mediated response together with other shoot factors like CORYNE, CLAVATA2 or KLAVIER (Oka-Kira et al., 2005; Miyazawa et al., 2010; Krusell et al., 2011; Crook et al., 2016). With the possibility of several homo- or hetero complexes and therefore different outputs, a specific response to either rhizobia or nitrate might be imaginable. Moreover, the different receptor kinases active in the shoot could induce several miRNAs or in general small RNAs acting as SDI and therefore guarantee a specific downstream response.

Another factor, which might be involved in miR171c regulation upon rhizobia and nitrate treatment are miRNA encoded peptides (miPEPs). The involvement of miPEPs in regulation of mtr-miR171b were shown (Lauressergues et al., 2015). These peptides translated from small ORFs upstream of the *MIR* gene can enhance the accumulation of mature miRNAs. If those miPEPs influence the accumulation of miR171c in *Lotus japonicus* needs to be addressed with overexpression studies or external application of miPEPs.

The specific regulation of miR171c raises the question of a possible involvement of C-terminally encoded peptides (CEP) which function in *Medicago truncatula* as a hunger signal under low nitrogen conditions (Imin et al., 2013; Tabata et al., 2014). These CEPs travel from root to shoot where they interact with its CEP receptor (CEPR) (Imin et al., 2013; Tabata et al., 2014; Taleski et al., 2018). The induction of CEP peptides positively regulate the levels of miR2111 and therefore degradation of its target TML conferring symbiosis susceptibility (Takahara et al., 2013; Gautrat et al., 2020). If CEP and CEPR interact with miR171c is not known. Basic expression levels of miR171c can be observed under low N conditions. It could be possible that CEPR regulates the transcript level of miR171c in shoots when plants are in a symbiosis susceptible state. In future experiments miR171c expression levels in *cepr* mutants could provide further insights. Furthermore, miR171c is induced locally in roots upon rhizobia presence and nitrate application. In *Medicago truncatula* CEP4 and CEP5 are upregulated in roots (but not in shoots) under low N conditions (Zhu et al., 2021). These CEPs could inhibit the expression of miR171c enabling the plant to enter into symbiosis.

Besides CEPs in *Medicago truncatula*, CLE peptides were shown to act in AON as systemic signal (Reid et al., 2011; Imin et al., 2013; Tabata et al., 2014). While CLE-RS1, CLE-RS2 and CLE-RS3 are induced systemically during rhizobial presence, CLE-RS2, CLE-RS3 and CLE40 are mainly active when nitrate is applied (Okamoto et al., 2009; Nishida et al., 2016). However if CLE peptides and miR171c act in the same pathway has not been studied so far. CLE-RS1, CLE-RS2 and CLE-RS3 were shown to suppress nodulation in a HAR1-dependent manner (Okamoto et al., 2009; Nishida et al., 2016). Although, it is assumed that these CLE peptides travel from root to shoot, direct HAR1 interaction was only shown for CLE-RS2 (Okamoto et al., 2013). Because miR171c expression in shoots is HAR1 dependent (in both, rhizobia- and nitrate-induced AON) it can be assumed that rhizobia and nitrate induced CLE peptides interact with HAR1 which then induce miR171c expression in shoots, resulting in inhibition of nodulation. One could speculate that HAR1 translates the incoming specific CLE peptides into miR171c induction which functions as systemic inhibitor of AON. However it is unknown if besides miR171c other miRNAs are induced. One possible candidate could be miR169 which was shown to be highly induced in CLE-RS3 OX shoots. In order to test if miR169 expression in shoots is HAR1 dependent, miR169 levels could be investigated in *har1-3* mutants upon rhizobia presence and nitrate application. Further, besides HAR1 other receptor-like kinases could be tested for possible involvement in CLE peptide signaling. However miR171c is induced in shoots as well as in roots which raises the question if CLE peptides induce miR171c expression locally in roots. Therefore, CLE-RS1, CLE-RS2 and CLE-RS3 expression levels could be tested in miR171c KO mutants and vice versa test miR171c expression levels in *cle-rs1*, *cle-rs2* and *cle-rs3* mutants to determine which factor induces the other.

miR171c targets NSP2 as well as NSP3 in *Lotus japonicus*. NSP2 has been extensively studied (Kaló et al., 2005; Heckmann et al., 2006; Murakami et al., 2006), however the function of NSP3 remained unknown. We show that NSP3 is involved in nodulation and also has a role in nitrate dependent inhibition of nodulation. However it is not known where, when and how NSP3 is active. It might be possible that NSP3 is part of the NSP1-NSP2 complex (Hirsch et al., 2009). NSP3 could act as stabilizing part enabling optimal DNA binding affinity and therefore transcription of nodulation and nitrate specific genes. *nsp3-1* mutants displayed less nodules than WT. However, *nsp2* mutants are non-nodulating (Kaló et al., 2005; Heckmann et al., 2006) and *nsp1* mutants show dramatically reduced nodule number (Smit et al., 2005; Heckmann et

al., 2006) indicating that NSP2 as well as NSP1 are crucial and required during nodulation and NSP3 could have a supporting/stabilizing role. Future NSP3 interaction studies with NSP1 and NSP2 could reveal new insights. Moreover, because NSP3 shows a moderate phenotype compared to NSP2 and NSP1, one could speculate that NSP3 has a fine tuning role during symbiosis. It might be possible that NSP1-NSP2 regulate NSP3 expression and depending on NSP3 levels, specific nodulation and nitrate inducible genes are triggered. In this context it would be interesting to examine NSP3 expression levels in nitrate signaling mutants like *nlp* (Nishida and Suzaki, 2018; Nishida et al., 2021) and vice versa test NLP transcript levels in *nsp3* mutants to investigate where NSP3 is active. It needs to be further investigated which role NSP3 fulfills during nodulation and nitrate signaling and if/how interaction with NSP1 and NSP2 takes place.

5 Material and Methods

5.1. Plant and bacterial resources

For all plate experiments as well as RNA sequencing *Lotus japonicus* ecotype Gifu B-12 9 (Handberg and Stougaard, 1992) and *har1-3* (Krusell et al., 2002b) was used. *nf-ya1* mutants (LORE number: 30162806) were isolated from the LORE1 insertion mutant resource (Małolepszy et al., 2016) and genotyped accordingly. Furthermore *nsp3-1* mutants which were isolated from a TILLING population (Perry et al., 2009) approach were used.

Plants were infected with the rhizobial strain *Mesorhizobium loti* MAFF303099 expressing *DsRED* (Maekawa et al., 2009b). For construct generation *E. coli* strain TOP10 (Invitrogen, Fisher Scientific) were used. Whole plant transformation was performed with *Agrobacterium tumefaciens* strain AGL1 (Lazo et al., 1991) and transgenic hairy root transformation with *Agrobacterium rhizogenes* AR12 or AR1193 (Stougaard et al., 1987; Hansen et al., 1989).

5.2. Seed sterilization

Seeds were scarified with sandpaper and sterilized with sodium-hypochloride (0.8%) for 8 min. After washing with ddH2O (6x) seeds were imbibed in "conserve" solution (Corteva, 450 nM) for 2-3h at room temperature. Seeds were placed on quarter-strength Broughton and Dilworth (B&D) (Broughton and Dilworth, 1971; modified 80uM FE-EDTA instead of Fe-Citrate), agar plates and stratified for 1-3 days. Plates were kept in dark for 3 days at room temperature allowing the plants to germinate.

5.3. Plant growth and infection

After germination, seedlings were placed on quarter-strength B&D agar plates grown at 21°C (16h light, 8h dark). Plant roots were shielded from light. For nitrate responsive plate experiments, B&D agar was supplemented with 5 mM KNO_3.

For phenotypic analysis of infection threads and nodules plants were infected with MAFF303099 (Maekawa et al., 2009a) . To this end, MAFF303099 strain was picked from a fresh culture plate and grown in YMB media for 2-3 days. The liquid culture was centrifuged at 3000g for 10 min and resuspended in 5 ml 1/4 B&D media. The bacterial suspension was diluted to a final OD of 0.01 for plates and 0.001 for magentas growth boxes, and applied directly to the roots (10 – 20µl per root). Infection threads were counted 7 days and nodules 14, 21 and 28 days post inoculation.

For long-term experiments where plants grew older than 21 days, plants were transferred to Magenta growth boxes (SacO2) containing a mixture of clay granules and vermiculite of the ratio 3:1 (1500 - 2000 g of granules/vermiculite mixture). Plants in magenta growth boxes were watered with 200-300 ml 1/4 B&D medium.

5.4. Plant experiments

5.4.1. Split root assay

After germination, roots of the seedlings were cut (2 – 5 mm from root tip) and the upper parts of the seedlings were transferred to B&D plates supplemented with 5 mM KNO_3. After 14 days plants with two developed secondary roots were transferred to B&D 1.5% agar patches. Plant roots were positioned on two different agar patches containing different concentrations of KNO_3 or the same concentrations as control. For infection experiments, one agar patch was infected with *M. loti* MAFF303099. After 14 days root and shoot tissue was harvested for RNA extractions.

5.4.2. Graftings

After germination (WT Gifu: 3 days, miR171c KO: 6 days) plants were transferred to B&D plates containing 1 mM KNO_3 and kept in dark for 2 days. Plants were grown for additional 8 days in light (16h light, 8h dark) then graftings were carried out. Plants were cut at the hypocotyl and transferred to sterile millipore water to prevent drying of the cutting site.

Shoots and roots of the respected genotype were transplanted on each other and were fixed by a 5 mm section of a 0.025 inch silicone tube (Reichelt). Grafted plants were transferred to B&D plates containing 1 mM or 5 mM KNO_3. After 2-3 weeks grafting success can be observed and plants were transferred to magenta growth boxes and inoculated with *M. loti* MAFF303099. After 28 days post inoculation nodules were counted.

5.4.3. GUS staining

GUS staining and fixation was performed as described (Gavrilovic et al., 2016). After fixation, plants were incubated twice in buffer containing acetic acid, glycerol and ethanol (ratio 1:1:3) for 30 min at 60°C. GUS stained plants were photographed (Leica MZFLIII).

For semi thin sections, GUS-stained plant tissue was embedded in resin (Kulzer technovit) and cut with Leica RM 2065 (6 µm). Sections were stained with 0.1% ruthenium red (Sigma) and de-stained several times in H_2O. Semi thin section were pictured with the Keyence microscope BZ-8000K or Epifluorescence microscope Zeiss Imager M2. Embedding and semi thin sections were performed by Ulrike Herzog.

5.5. Cloning

5.5.1 Constructs generated by gateway cloning system

For constructs cloned via the gateway cloning system (Invitrogen, FisherScientific; Table 2) the gene of interest was amplified from *Lotus japonicus* Gifu genomic DNA or synthesized (BaseClear). Specific primers (Table 3) with attb overhang enable the integration of the gene of interest into pDONOR vector via BP reaction. After confirmation with restriction digest, an LR reaction was performed in order to integrate the gene of interest into the respective expression clone. Constructs were confirmed by restriction digest and sequencing.

5.5.2. Constructs generated with Golden Gate system

For constructs cloned via the Golden Gate system (Weber et al., 2011; Castel et al., 2019; Table 2) The gene of interest was amplified with specific primers (Table 3) carrying a BsaI overhang

from *Lotus japonicus* Gifu genomic DNA or available clones. A level 1 reaction was performed where the gene of interest was assembled together with a suitable promoter and terminator to form a functional expression cassette. After confirmation with restriction digest, a level 2 reaction was performed where different expression cassettes are assembled into the respective expression clone. Constructs were confirmed with restriction digest and sequencing.

Table 2: Overview of generated constructs

Construct	Construct reference	Cloning system	Purpose	Template	Expression vector
pUBQ1:miR171c:tNOS	Agro 52/53 A-075	Gateway	Stable line generation	Genomic Gifu DNA	PMC69
miR171c KO	Agro 54/55	GG (Castel et al., 2019)	Stable line generation	BCJJ433A template for gRNAs	pAGM4673
pMIR171c:GUS:tNOS	Agro 64/65 A-090	Gateway	Stable line generation	Genomic Gifu DNA	PMDC163
pSUC2:miR171c:t35s	Agro 101/102 A-036	GG (Castel et al., 2019)	Stable line generation	Genomic Gifu DNA	pAGM4673
pUBQ1:miR169 STTM:tNOS	Agro 97/98 A-034	Gateway STTM construct (Yan et al., 2012)	Stable line generation	Genomic Gifu DNA	PMC69
pSUC2:miR169b:t35s	Agro 132 A-040	GG (Castel et al., 2019)	Stable line generation	synthesized	pAGM4673
pMIR169b:GUS:tNOS	Agro 91/92 A-031	Gateway	Stable line generation	Synthesized	PMC790
pMIR169c:GUS:tNOS	Agro 93/94 A-032	Gateway	Stable line generation	synthesized	PMC790
UBQ1:miR169c :tNOS	Agro 89/90 A-030	Gateway	Stable line generation	Genomic Gifu DNA	PMC69
pSUC2:miR172:t35s	Agro 103/104 A-037	GG (Castel et al., 2019)	Stable line generation	Genomic Gifu DNA	pAGM4673
pNSP2:GUS:t35s	Agro 125 A-047	Gateway	Hairy root generation	synthesized	PMC0076
pNSP3:GUS:t35s	Agro 126 A-048	Gateway	Hairy root generation	synthesized	PMC0076
pSUC2:GUS:t35s	Agro 127 A-049	Gateway	Hairy root generation	PMC0094	PMC1270
pUBQ1:CLE-RS3:tNOS	Agro 56/57 A-043	GG (Weber et al., 2011)	Hairy root generation	Genomic Gifu DNA	PMC1270
pUBQ1:miR169b:tNOS	Agro 113/114 A-091	GG (Weber et al., 2011)	Hairy root generation	Synthesized	PMC1270
pUBQ1:miR169c:tNOS	Agro 115/116 A-094	GG (Weber et al., 2011)	Hairy root generation	Synthesized	PMC1270
pUBQ1:miR169 STTM:tNOS	Agro 111/112 A-046	GG (Weber et al., 2011)	Hairy root generation	Genomic Gifu DNA	PMC1270

5.5.3. Primers used for cloning

Table 3: Primers used for cloning

construct	Primer
pUBQ1:miR171c:tNOS	oKM226 **GGGGACAAGTTTGTACAAAAAAGCAGGCT**ATAGGAGGGAGAAGTTGT oKM227 **GGGGACCACTTTGTACAAGAAAGCTGGGT**GAACGTGAAGTTATGCGG
miR171c KO	oKM174 tgtggtctcaATTGGACATGGCGTGATGTTGATCGTTTAAGAGCTATGCTGGAA oKM176 tgtggtctcaATTGAGACAAGAGTGATATTGATTGTTTAAGAGCTATGCTGGAA
pMIR171c:GUS:tNOS	oKM350 **GGGGACAAGTTTGTACAAAAAAGCAGGCTTA**CAATGTCCTCCTTCTTCGTCA oKM351 **GGGGACCACTTTGTACAAGAAAGCTGGGTC**CTTTTGCAGAAGGAAGCTAC
pSUC2:miR171c:t35s	oKM407 gcgaggtctcGaatgATAGGAGGGAGAAGTTGT oKM408 ccatggtctcGaagcGAACGTGAAGTTATGCGG
pUBQ1:miR169 STTM:tNOS	oKM470 **GGGGACAAGTTTGTACAAAAAAGCAGGCTTA**AGGCAACTCATctaTC oKM472 **GGGGACCACTTTGTACAAGAAAGCTGGGTC**TAGCCAAGAtagATG
pSUC2:miR169b:t35s	oKM458 tattgcggtctcaaatgAGCAGACAGCATATATGG oKM459 gcaataggtctctaagcATAAAAAGGGAGATTGGTC
pMIR169b:GUS:tNOS	Synthesized (SF2)
pMIR169c:GUS:tNOS	Synthesized (SF3)
pUBQ1:miR169c :tNOS	oKM421 **GGGGACAAGTTTGTACAAAAAAGCAGGCTTA**GAGACTTCCTTTTTGCTG oKM422 **GGGGACCACTTTGTACAAGAAAGCTGGGTC**GAGTTGAGGTTGAGAGATG
SUC2:miR172:t35s	Template clone PM1501
pNSP2:GUS:t35s	Synthesized (SF8)
pNSP3:GUS:t35s	Synthesized (SF9)
pSUC2:GUS:t35s	Template clone PM964
pUBQ1:CLE-RS3:tNOS	oKM319 tattgcggtctcaaatgATGGCGAATGCAAGTAGA oKM320 gcaataggtctctaagctcaACCATGACCCTGCT
pUBQ1:miR169b:tNOS	oKM458 tattgcggtctcaaatgAGCAGACAGCATATATGG oKM459 gcaataggtctctaagcATAAAAAGGGAGATTGGTC
pUBQ1:miR169c:tNOS	oKM460 tattgcggtctcaaatgGAGACTTCCTTTTTGCTG oKM461 gcaataggtctctaagcGAGTTGAGGTTGAGAGATG
pUBQ1:miR169 STTM:tNOS	oKM466 tattgcggtctcaaatgAGGCAACTCATctaTCTTGGCTAgttgttgttgttatggtctaATTTAAATatggtctaaaga

5.5. Conjugational transfer of integration vectors into *Agrobacterium rhizogenes*

Constructs used for hairy root generation were cloned via the gateway system into a PIV10-based expression clone. *E.coli* cells harboring pIV10 were crossed with helper *E.coli* strain GJ23 and mated to *Agrobacterium rhizogenes* strain AR1193 or AR12 as described in Stougaard 1995 (Stougaard and protocols, 1995). All bacteria were tested for correct inserts by PCR amplification.

5.6. Plant transformation

Whole plant transformation for stable lines were performed by Caterina Brancato as described in Handberg 1994 (Handberg et al., 1994).

5.7. Genotyping of stable lines

Stable lines of miR171c, miR169bc and miR172 as well as the *nf-ya1* LORE insertion mutant were genotyped with specific primer (Table 4). For miR171c KO lines, genomic primer spanning the miR171c precursor region were used to detect CAS-9 mediated deletion.

Table 4: Primers used for genotyping

Construct	Sequence
miR171c OX (UBQ1 promoter)	oKM434 TCCAAGCGTTAATTAGGG oKM435 TGTATAATTGCGGGACTC
miR171c KO	**oKM226** **GGGGACAAGTTTGTACAAAAAAGCAGGCT**ATAGGAGGGAGAAGTTGT
pMIR171c::GUS	oKM450 AACAACGAACTGAACTGG oKM451 TAATGCGAGGTACGGTAG
miR171c OX (SUC2 promoter)	oKM298 TCCCTCCTTGTTCTCTCC oKM299 TGGGTGTGGTTGATGAAG
miR169 STTM	oKM475 TCGTTCAAACATTTGGC oKM476 AACATAGATGACACCGC
miR169b OX (SUC2 promoter)	oKM298 TCCCTCCTTGTTCTCTCC oKM299 TGGGTGTGGTTGATGAAG
pMIR169b::GUS	oKM450 AACAACGAACTGAACTGG oKM451 TAATGCGAGGTACGGTAG
pMIR169c::GUS	oKM450 AACAACGAACTGAACTGG oKM451 TAATGCGAGGTACGGTAG
miR169c OX (UBQ1 promoter)	oKM434 TCCAAGCGTTAATTAGGG oKM435 TGTATAATTGCGGGACTC
miR172 OX (SUC2 promoter)	oKM298 TCCCTCCTTGTTCTCTCC oKM299 TGGGTGTGGTTGATGAAG
***nf-ya1* (30162806)**	oKM454 TGTGTACGGTTGTCTGGCCGACAGTT oKM455 CAGCAGCCTGTGAATCCTTAGTGGCA

5.8. Sequence-specific amplification polymorphism (SSAP)

In order to identify homozygous miR171c OX mutants, SSAP was carried out as described in Urbansky (Urbański et al., 2013). Basically, DNA from transgenic plants was digested with a multi cutter enzyme. Then specific adapters are ligated to the restriction sites. With primers (Table 5) binding to the adapters PCR is performed creating fragments of various lengths. Fragments are separated on agarose gels, isolated and purified. Via sequencing, the genomic location of fragments spanning part of the vector backbone and the genomic region can be identified. The insert location of miR171c OX #4 was determined as at Ljchr1 21492223-21492322, and miR171c OX #35 is located at Ljchr3 8352697-8352440.

Table 5: Primers used for SSAP

Name	Sequence
Splink 1	oKM498 CGAAGAGTAACCGTTGCTAGGAGAGACC
Splink 2	oKM499 GTGGCTGAATGAGACTGGTGTCGAC
SSAP RB out PMC69	oKM504 GGCACTGGCCGTCGTTTTA
SSAP RB in PMC69	oKM505 TTGCAGCACATCCCCCTTTC
SSAP LB out PMC69	oKM506 AGGGTTTCGCTCATGTGTTGAG
SSAP LB in PMC69	oKM507 CAGTACTAAAATCCAGATCCCCCGAA
SSAP adapter TaqI overhang	oKM508 CGACCACTAGTGTCGACACCAGTCTCTAATTTTTTTTTTCAAAAAAA
SSAP #4 fw	oKM583 CCACCATAAAAGACCTTG
oKM584 SSAP #4 rev	oKM584TCTTGTCCTGTTTGTTGG
oKM599 SSAP nr35 fw	oKM599 TCCATGCGTCTCTACTTA
oKM600 SSAP nr35 rev	oKM600 TACTTTGTGCTGTTGTGC

5.9. RNA extraction

RNA was extracted using a modified Lithium Chloride – TRIZOL LS based method. Plant and aphid tissue was shock frozen in liquid nitrogen and ground to fine powder with metal beads. DNA and protein were removed with chloroform extraction and RNA was dissolved in LoTE buffer (3 mM Tris-HCl pH7.5, 0.2 mM EDTA pH7.5) or DEPC water and stored at -80 (detailed protocol attached in appendix).

5.10. cDNA synthesis and qPCR

In order to target small RNAs a "pulsed" reverse transcription reaction (Varkonyi-Gasic et al., 2007) was performed. miRNAs are targeted with stemloop primers that carry 6 bp overhang which can bind specifically to the 3'end of the respective mature miRNAs. To each reaction oligodT primer were added to target mRNAs of the reference genes. The reverse transcription conditions were: 16°C for 30 minutes, 60 cycles (30°C for 30 seconds, 42°C for 30 seconds, 50°C for 1 second) and 85°C for 5 minutes. As reverse transcriptase enzyme we used: Revert aid (FisherScientific) or Superscript IV (FisherScientific).

For qPCR, cDNA with specific primers for the respective reference genes and mature RNAs were mixed with Mastermix of the SensiFAST SYBR No-ROX Kit (Bioline). The qPCR reaction conditions were 40x 95°C 15s, specific annealing temperature of primer 15s, 72°C 15s, specific acquisitions (AQ) point (72°C-82°C) 1s followed by the melt curve. Primers were designed to span exon/exon border and product length was between 80 bp and 200 bp. Additionally, annealing temperature (AT) of the primer were examined by gradient PCR. qPCR reaction was performed on a lightcycler (Biorad CFX384) and products were checked with sequencing. Two reference genes were used namely PP2A and ATP synthase. All qPCR reactions were performed in three technical replicates. Standard error of the Mean was calculated from biological replicates only, using mean values of technical replicates. Raw data was exported into LinRegPCR program (Ramakers et al., 2003; Ruijter et al., 2009) which is calculating the primer efficiency. Data was then exported to excel and mean values were calculated.

Table 6: Primers used for RT and qPCR with annealing temperature (AT) and acquisition (AQ)

Name	Sequence	AT/AQ
qPCR Universal Reverse	qCW1 AGTGCAGGGTCCGAGGTATTC	
miR169b,c_loopRT	qCW21 GTCGTATCCAGTGCAGGGTCCGAGGTATTCGCACTGGATACGAC**AGGCAA**	
miR169b,c_qpcr	qCW22 gagtca**T**AGCCAAGGATG	AT: 56 AQ: 82
DH64_mi171c2_loopRT	qCW25 GTCGTATCCAGTGCAGGGTCCGAGGTATTCGCACTGGATACGAC**GAGTGA**	
miR171c_qcr	qCW26 ctgtgcgaTGAGCCGAATCAA	AT: 66 AQ: 78

LjATP Synthase_qpcr	qCW27 AACACCACTCTCGATCATTTCTCTG	AT: 60 AQ: 79
LjATP Synthase_qpcr	qCW28 CAATGTCGCCAAGGCCCATGGTG	AT: 60 AQ: 79
PP2A_qpcr_fw	qCW41 GTAAATGCGTCTAAAGATAGGGTCC	AT: 68 AQ: 78
PP2A_qpcr_rev	qCW42 ACTAGACTGTAGTGCTTGAGAGGC	AT: 68 AQ: 78
TUBa_qpcr_fw (Zheng et al., 2019)	qCW53 GGTTCGACAACAGCGGTAGA	AT: 56 AQ: 72
TUBa_qpcr_rev (Zheng et al., 2019)	qCW54 GTGGCACCGGATCAGGATTT	AT: 56 AQ: 72
miR2111b_loopRT	qCW59 GTCGTATCCAGTGCAGGGTCCGAGGTATTCGCACTGGATACGAC**TACACC**	
miR2111b_qpcr	qCW60 GCGCGTAATCTGCATCCTGAG	AT: 60 AQ: 75
GUS_qpcr_fw	qCW61 CGGGAAAAGTGTACGTAtcac	AT: 56 AQ: 72
GUS_qpcr_rev	qCW62 aggtgttcggcgtggtgta	AT: 56 AQ: 72

5.11. Small RNA sequencing

Gifu WT, *har1-3* and plants transiently overexpressing CLE-RS3 were first grown on B&D plates for 3 weeks. Then plants were transferred to magenta growth boxes and a subset of plants was infected with rhizobial strain MAFF303099 (Maekawa et al., 2009a). After 14 days the second and the third leaf from top of the plant was harvested and shock frozen in liquid nitrogen. RNA extraction was carried out as described. In order to prepare samples for shipping, RNA was precipitated with sodium acetate. Different genotypes and treatments were analyzed in two biological replicates.

Small RNA sequencing was performed at GeneXPro GmbH (Frankfurt, Germany) using the True Quant small RNA-Seq Kit for ultra- low input. The kit is based on the ligation of two UMI- containing adapters and does not involve gel-purification. The libraries were sequenced on an Illumina NextSeq500 instrument. Duplicate reads were eliminated based on the UMI using an in-house software (GeneXPro). The reads were hereafter annotated to the "Lotus japonicus "entries in the "miRbase": all non-annotated reads where hereafter annotated by mapping to all miRBase "plant" entries. Small RNA transcripts were quantified and pairwise comparisons were performed using DESeq2 (Love et al., 2014b; Love et al., 2014d) for p-value

calculation of differentially expressed small RNAs. Analysis of small RNA sequencing data was performed by GeneXPro.

6 Appendix

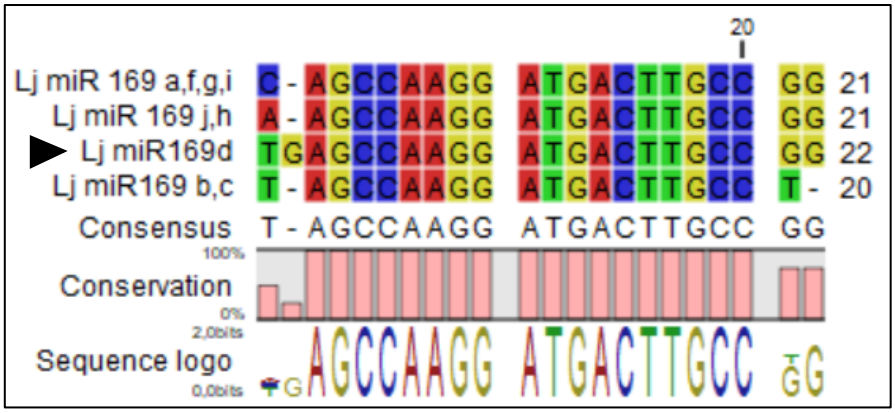

Supplemental figure S 1: Alignment of *Lotus japonicus* mature miR169 isoforms.

Alignment was performed with CLC main workbench 8 with the following settings, gap open cost: 10, gap extension cost: 1. The newly identified miRNA isoform miR169d is labelled with an arrowhead.

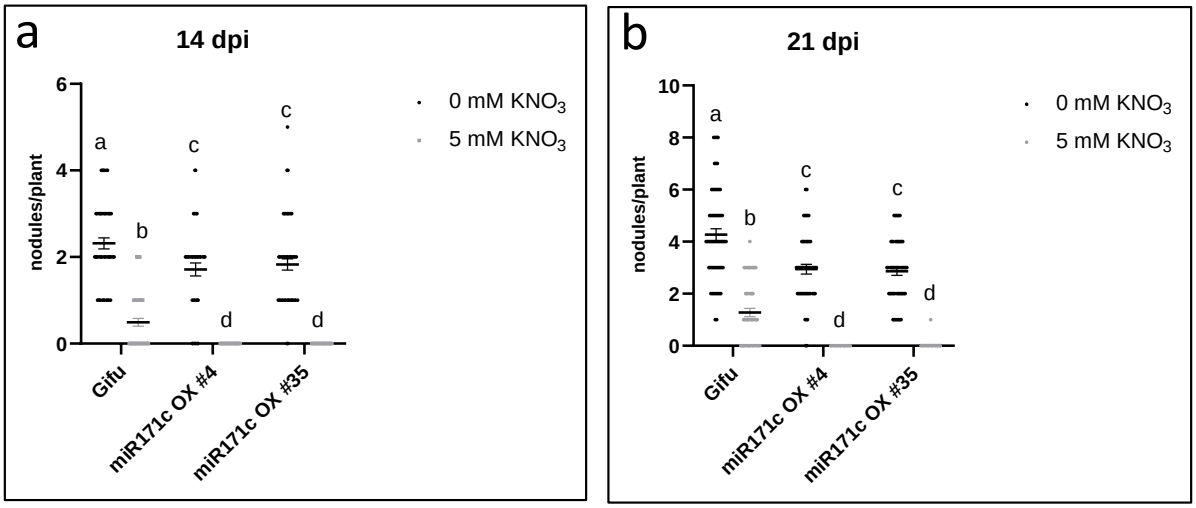

Supplemental figure S 2: miR171c OX plants partially inhibit nodulation and are hypersensitive to nitrate.

.**a-b**: Nodule count of wild type (Gifu), miR171c OX#4 and miR171c OX#35 under different nitrate conditions. Plants were grown on B&D media containing 0 mM or 5 mM KNO_3, nodules were counted after 14d (**a**) and 21d (**b**), at least 52 plants (of two independent experiments) were used for each condition. Two-way ANOVA was performed followed by Tukey's test. $p<0.05$, significantly different values are indicated by different letters. Centerline and error bars show the mean with SEM

.

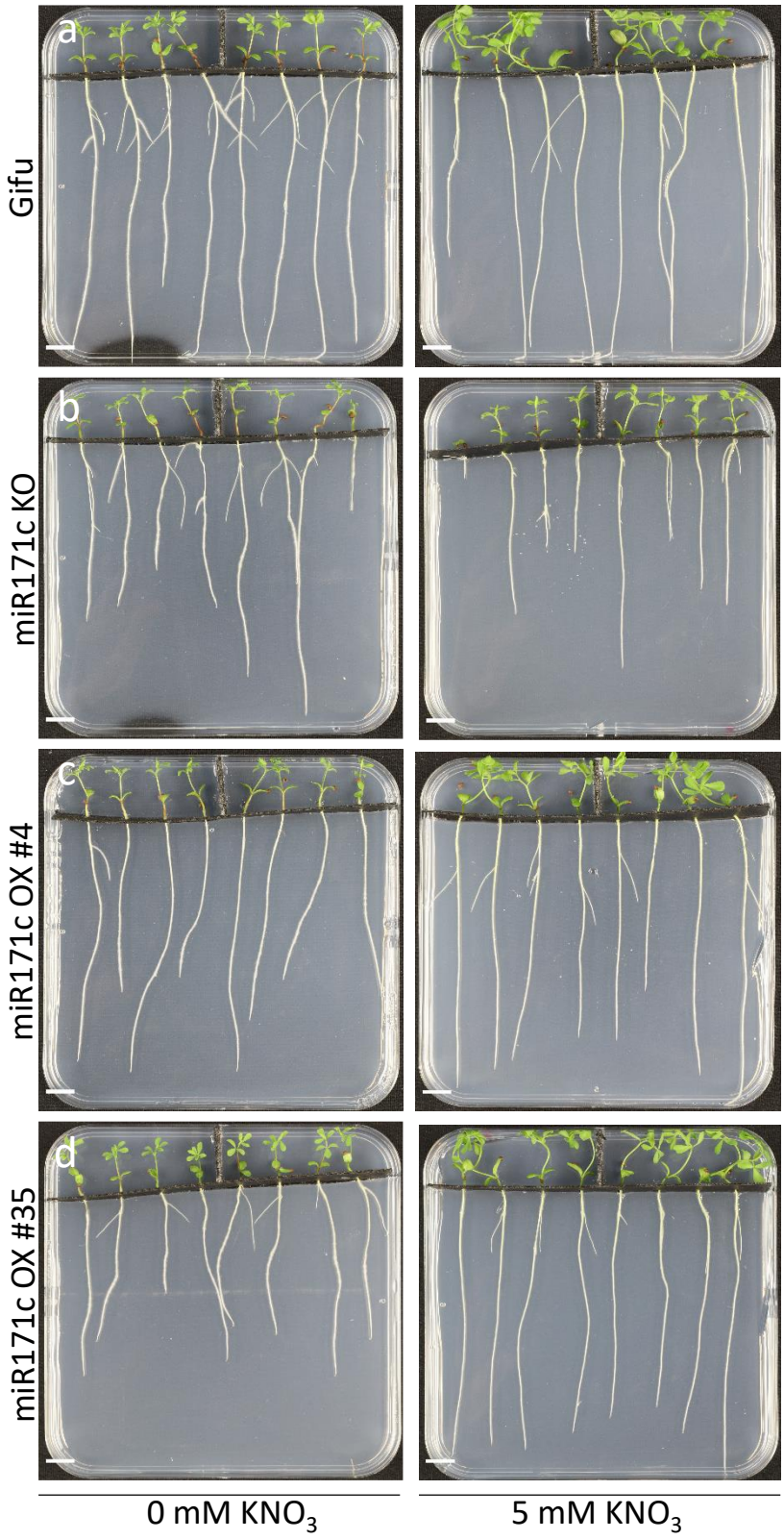

Supplemental figure S 3: miR171c OX shoots respond to nitrate supply, miR171c KO shoots are nitrate insensitive.

a- d: Phenotypic analysis of Gifu (**a**), miR171c KO (**b**), two homozygous isolated miR171c OX lines #4 (**c**), #35 (**d**) plants to nitrate supply. Plants were grown on B&D plates containing 0 mM KNO_3 or 5 mM KNO_3. Pictures were taken 14d post transfer. Scale bar: 1cm

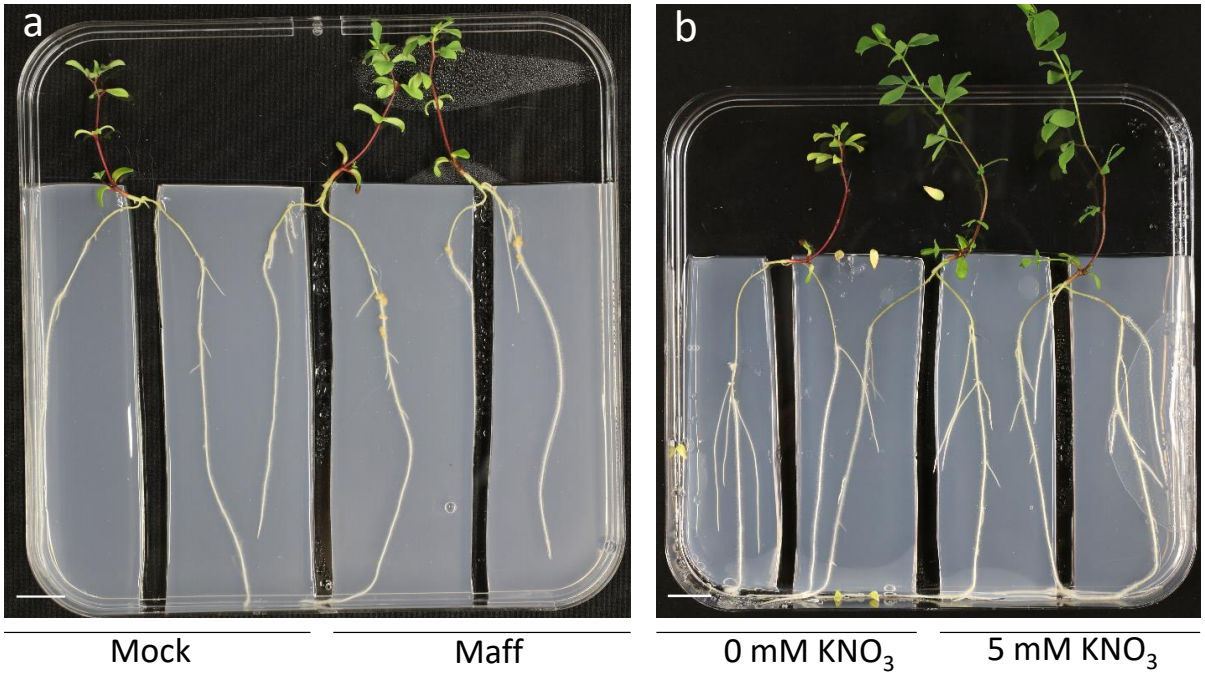

Supplemental figure S 4: Shoots of nitrate treated split roots are bigger than shoots of rhizobia treated split roots.

a-b: Rhizobia- and nitrate-treated split root assay of wild type (Gifu) plants. After secondary root growth, plants were transferred to agar patches and treated with *M. loti* MAFF303099 (**a**), or with 5 mM KNO_3 (**b**). Tissue was harvested after 14 dpi (**a**) or 17 d (**b**). Scale bar: 1 cm

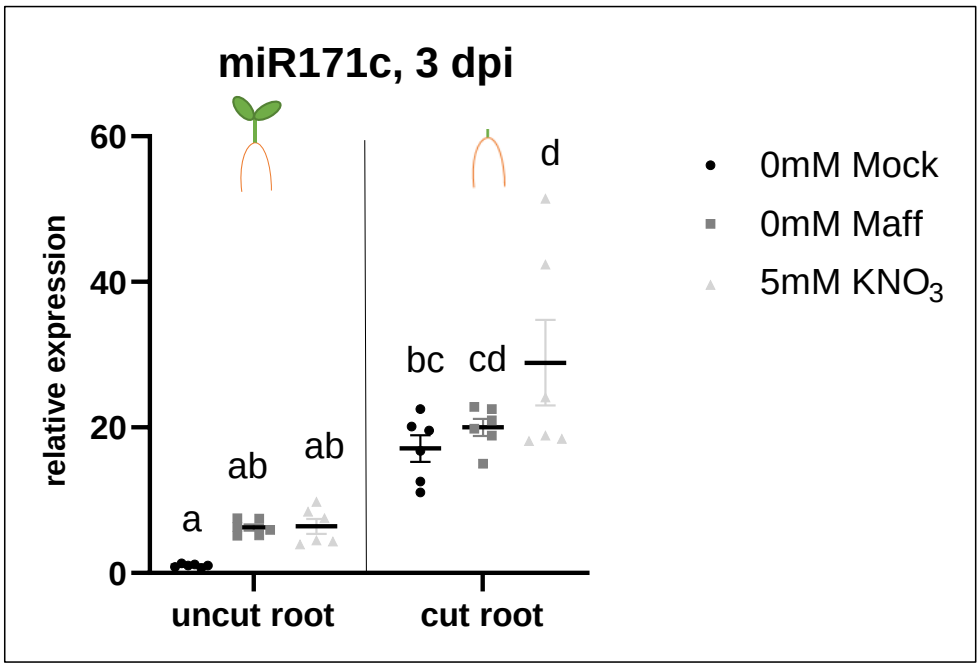

Supplemental figure S 5: A general shoot inhibitor might control miR171c induction in roots.

qRT-PCR based expression levels of miR171c in shootless root assay. After shoot removal, cut roots were treated with *M. loti* MAFF303099 or transferred to B&D plates containing 5 mM KNO_3. Control plants (uncut) were treated the same way. Root tissue was harvested 3 dpi. Two-way ANOVA was performed followed by Tukey's test. $p<0.05$, significantly different values are indicated by different letters. Centerline and error bars show the mean with SEM, uncut root 0mM Mock =1.

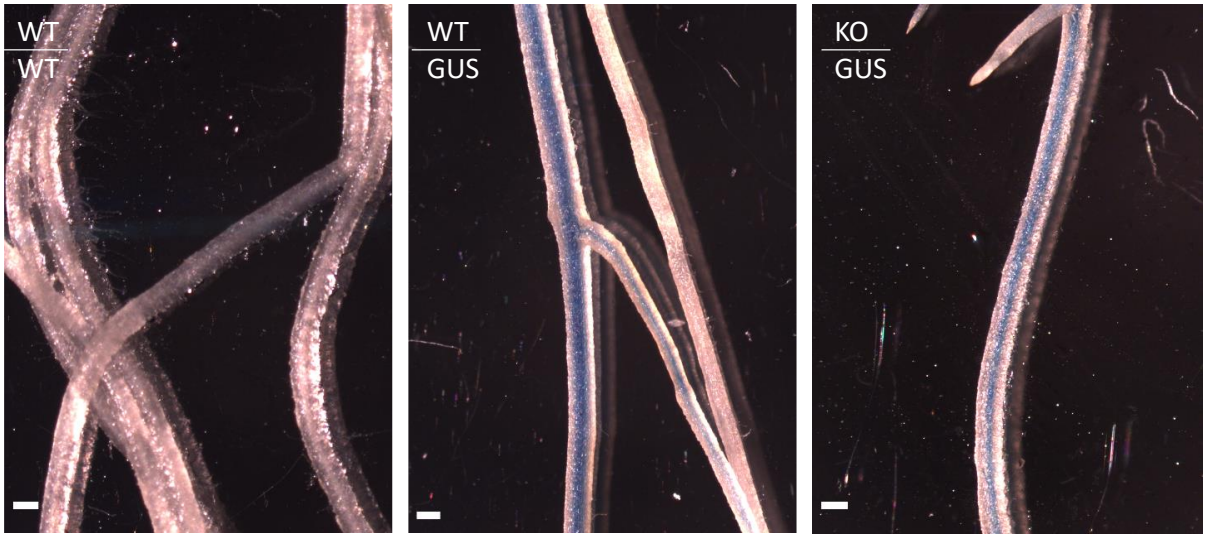

Supplemental figure S 6: *pMIR171c::GUS* activity in roots is independent of shoot miR171c presence.

GUS activity of WT/GUS and KO/GUS grafts (scion/rootstock). After 4 weeks successful grafted plants (WT/WT, WT/*pMIR171c::GUS*, miR171c KO/*pMIR171c::GUS*) were stained with X-Gluc-staining buffer and pictures were taken. Scale bar: 1 mm.

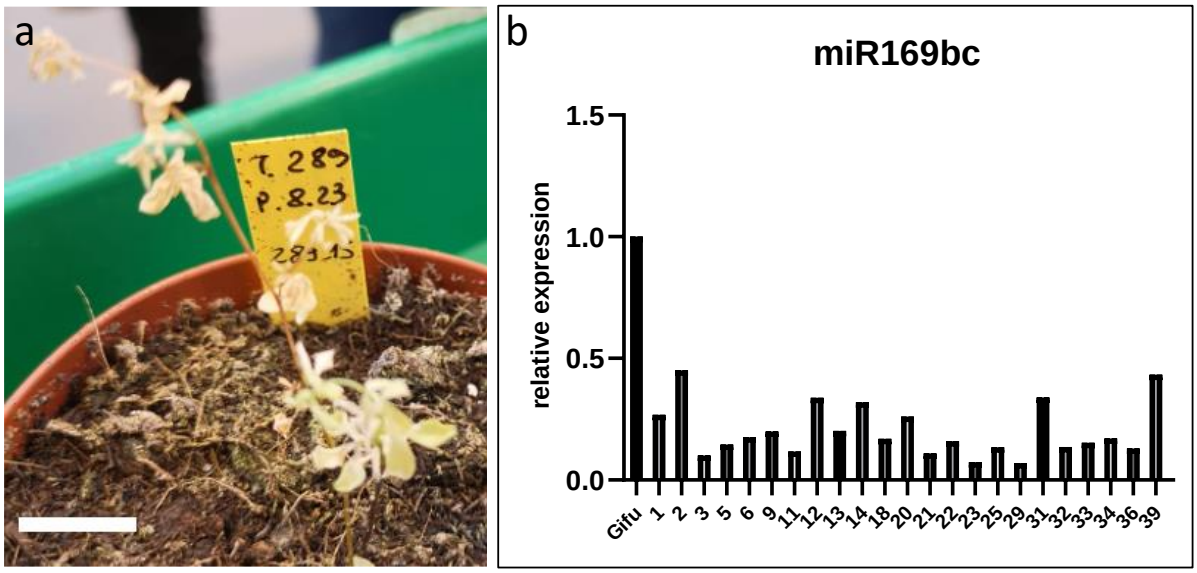

Supplemental figure S 7: Overexpression of miR169bc driven by *pUBQ1* appears to be lethal.

a: Stable lines of *pUBQ1::miR169bc* expressing plants died shortly after transfer to soil (10-14 days). **b**: Expression levels of miR169bc in miR169bc OX plants. *pUBQ1::miR169bc* survivor plants display reduced miR169bc transcript level (**b**). Scale bar 1cm.

Trizol-Chloroform RNA Isolation optimized by Moritz Sexauer Version 31.03.22 (Original version: Franziska Krajinski's group, MPI Golm)

Buffers and chemicals needed:

- Lysis buffer (100mM Tris-HCL (pH7.5), 0,5 M LiCl, 10 mM EDTA (pH8.0), 1% LiDS,

5 mM DTT (after autoclave))

- Homemade Trizol
- Chloroform
- 1M Acetic Acid
- 3M Sodium Acetate pH 5.6 (adjusted with pure Acetic Acid)
- 70/100% EtOH
- DEPC water

Autoclave Lysis buffers and material if possible, use DEPC water for all buffers (Diethylpyrocarbonate) work on ice if not stated differently, all Trizol steps take place in the fume hood (no ice)

Homemade Trizol:

- 38% saturated Phenol (Roti Aqua Phenol)
- Guanidine Thiocyanate 0.8 M
- Ammonium Thiocyanate 0.4 M
- Sodium Acetate pH 5.6 (3M solution) 0.1 M
- Glycerol 5 %

Weight in Thiocyanates, add Sodium Acetate adjust volume to 57% with DEPC water. Add 5% Glycerol, Add 38% Phenol take the lower Phase using a single use 10ml+ pipette.

Procedure:

- collect plant material in 2 ml safelock tube freeze in liquid N2
- Add pre-cooled steel beads and homogenize by vortex; keep on LN2
- Transfer max 60 mg in N2 frozen ground tissue (30 mg for shoot samples) to a 2 ml tube
- Add 600 µl Lysis/binding buffer, mix and vortex well and fast
- Centrifuge 10 min at 4 °C at 21000 g
- carefully transfer supernatant into new tube containing 900 µl of Trizol
- vortex min. 30 sec and leave at room temperature for 5 min
- spin for 10 seconds to remove trizol from lid (this step is for safety reasons)
- add 400µl chloroform and mix by shaking (works better than vortexing)
- Spin 5 min at 16000 g
- Carefully take the upper phase to a new tube (you should be able to get 1100 µl) add 600µl chloroform
- and mix by shaking and leave at RT for 2 min
- Centrifuge 5 min at 16000g
- Carefully take the upper (water) phase without touching the other phase and divide into 2 new tubes (= 1 vol.) (should be around 2x 500 µl)

- Add 0.1 vol 3 M NaOAc (50µl), mix by inverting
- Add 0.1 vol acitic acid (50µl), mix by inverting
- Add 2.5 vol 100% EtOH (4 degC) (1300µl), mix by inverting and incubate over night at -20°C
- Centrifuge at 21000 g at 4 degree for 1 h, carefully decant supernatant
- Wash the pellet with 1000 µl cold 80 % EtOH, flick the tube, but do not resuspend the pellet, centrifuge at full speed for 10 min and decant the supernatant
- Repeat the washing and decant the supernatant
- optional: add 100 µl 100% EtOH (this will help drying the pellet later)
- Centrifuge again for 30 s and remove remaining EtOH by pipetting
- Dry the pellet for 7-10 min. (if you have trouble drying the pellet you can heat the tube to 65°C for max 20s to dry it.)
- Resuspend pellet in 20 µl per tube (DEPC water/) LoTE buffer (work at 4°C; use cold water; pipetting)
- 2 min. at 65°C to aid RNA dissolution vortex shortly and put it on ice directly
- Spin the tube shortly to collect RNA solution at the bottom
- Transfer resuspended RNA into RNAse free, labelled tubes (1.5ml or smaller)
- Measure RNA concentration
- Store RNA at -80°C

7 Literature

Andriankaja, A., Boisson-Dernier, A., Frances, L., Sauviac, L., Jauneau, A., Barker, D.G., and de Carvalho-Niebel, F. (2007). AP2-ERF transcription factors mediate Nod factor–dependent Mt ENOD11 activation in root hairs via a novel cis-regulatory motif. The Plant cell **19,** 2866-2885.

Ané, J.-M., Kiss, G.B., Riely, B.K., Penmetsa, R.V., Oldroyd, G.E., Ayax, C., Lévy, J., Debellé, F., Baek, J.-M., and Kalo, P. (2004). Medicago truncatula DMI1 required for bacterial and fungal symbioses in legumes. Science (New York, N.Y.) **303,** 1364-1367.

Ángel Martín-Rodríguez, J., Ariani, A., Leija, A., Elizondo, A., Fuentes, S.I., Ramirez, M., Gepts, P., Hernández, G., and Formey, D. (2021). Phaseolus vulgaris MIR1511 genotypic variations differentially regulate plant tolerance to aluminum toxicity. The Plant Journal **105,** 1521-1533.

Ariel, F., Brault-Hernandez, M., Laffont, C., Huault, E., Brault, M., Plet, J., Moison, M., Blanchet, S., Ichanté, J.L., and Chabaud, M. (2012). Two direct targets of cytokinin signaling regulate symbiotic nodulation in Medicago truncatula. The Plant cell **24,** 3838-3852.

Asamizu, E., Shimoda, Y., Kouchi, H., Tabata, S., and Sato, S. (2008). A Positive Regulatory Role for LjERF1 in the Nodulation Process Is Revealed by Systematic Analysis of Nodule-Associated Transcription Factors of Lotus japonicus Plant physiology **147,** 2030-2040.

Aung, K., Lin, S.-I., Wu, C.-C., Huang, Y.-T., Su, C.-l., and Chiou, T.-J. (2006). pho2, a phosphate overaccumulator, is caused by a nonsense mutation in a microRNA399 target gene. Plant physiology **141,** 1000-1011.

Barbulova, A., Rogato, A., D'Apuzzo, E., Omrane, S., and Chiurazzi, M. (2007). Differential effects of combined N sources on early steps of the nod factor–dependent transduction pathway in Lotus japonicus. Molecular plant-microbe interactions **20,** 994-1003.

Baumberger, N., and Baulcombe, D. (2005). Arabidopsis ARGONAUTE1 is an RNA Slicer that selectively recruits microRNAs and short interfering RNAs. Proceedings of the National Academy of Sciences **102,** 11928-11933.

Benkovics, A.H., and Timmermans, M.C. (2014). Developmental patterning by gradients of mobile small RNAs. Current opinion in genetics & development **27,** 83-91.

Bolaños-Vásquez, M.C., and Werner, D. (1997). Effects of Rhizobium tropici, R. etli, and R. leguminosarum bv. phaseoli on nod gene-inducing flavonoids in root exudates of Phaseolus vulgaris. Molecular plant-microbe interactions **10,** 339-346.

Boualem, A., Laporte, P., Jovanovic, M., Laffont, C., Plet, J., Combier, J.P., Niebel, A., Crespi, M., and Frugier, F. (2008). MicroRNA166 controls root and nodule development in Medicago truncatula. The Plant Journal **54,** 876-887.

Branscheid, A., Devers, E.A., May, P., and Krajinski, F. (2011). Distribution pattern of small RNA and degradome reads provides information on miRNA gene structure and regulation. Plant signaling & behavior **6,** 1609-1611.

Breakspear, A., Liu, C., Roy, S., Stacey, N., Rogers, C., Trick, M., Morieri, G., Mysore, K.S., Wen, J., and Oldroyd, G.E. (2014). The root hair "infectome" of Medicago truncatula uncovers changes in cell cycle genes and reveals a requirement for auxin signaling in rhizobial infection. The Plant cell **26,** 4680-4701.

Breedveld, M., Cremers, H., Batley, M., Posthumus, M., Zevenhuizen, L., Wijffelman, C., and Zehnder, A. (1993). Polysaccharide synthesis in relation to nodulation behavior of Rhizobium leguminosarum. Journal of bacteriology **175,** 750-757.

Brodersen, P., Sakvarelidze-Achard, L., Bruun-Rasmussen, M., Dunoyer, P., Yamamoto, Y.Y., Sieburth, L., and Voinnet, O. (2008). Widespread translational inhibition by plant miRNAs and siRNAs. Science (New York, N.Y.) **320,** 1185-1190.

Broghammer, A., Krusell, L., Blaise, M., Sauer, J., Sullivan, J.T., Maolanon, N., Vinther, M., Lorentzen, A., Madsen, E.B., and Jensen, K.J. (2012). Legume receptors perceive the rhizobial lipochitin oligosaccharide signal molecules by direct binding. Proceedings of the National Academy of Sciences **109,** 13859-13864.

Broughton, W., and Dilworth, M.J.B.j. (1971). Control of leghaemoglobin synthesis in snake beans **125,** 1075-1080.

Buhtz, A., Springer, F., Chappell, L., Baulcombe, D.C., and Kehr, J. (2008). Identification and characterization of small RNAs from the phloem of Brassica napus. The Plant Journal **53,** 739-749.

Bustos-Sanmamed, P., Mao, G., Deng, Y., Elouet, M., Khan, G.A., Bazin, J., Turner, M., Subramanian, S., Yu, O., and Crespi, M. (2013). Overexpression of miR160 affects root growth and nitrogen-fixing nodule number in Medicago truncatula. Functional Plant Biology **40,** 1208-1220.

Caba, J., Recalde, L., and Ligero, F. (1998). Nitrate-induced ethylene biosynthesis and the control of nodulation in alfalfa. Plant, Cell & Environment **21,** 87-93.

Caba, J.M., Centeno, M.L., Fernández, B., Gresshoff, P.M., and Ligero, F. (2000). Inoculation and nitrate alter phytohormone levels in soybean roots: differences between a supernodulating mutant and the wild type. Planta **211,** 98-104.

Caetano-Anollés, G., and Gresshoff, P.M. (1991). Plant genetic control of nodulation. Annual review of microbiology **45,** 345-382.

Carroll, B.J., and Mathews, A. (2018). Nitrate inhibition of nodulation in legumes. In Molecular biology of symbiotic nitrogen fixation (CRC Press), pp. 159-180.

Carroll, B.J., McNeil, D.L., and Gresshoff, P.M. (1985). Isolation and properties of soybean [Glycine max (L.) Merr.] mutants that nodulate in the presence of high nitrate concentrations. Proceedings of the National Academy of Sciences **82,** 4162-4166.

Castel, B., Tomlinson, L., Locci, F., Yang, Y., and Jones, J.D. (2019). Optimization of T-DNA architecture for Cas9-mediated mutagenesis in Arabidopsis. PloS one **14,** e0204778.

Catoira, R., Galera, C., de Billy, F., Penmetsa, R.V., Journet, E.-P., Maillet, F., Rosenberg, C., Cook, D., Gough, C., and Dénarié, J. (2000). Four genes of Medicago truncatula controlling components of a Nod factor transduction pathway. The Plant cell **12,** 1647-1665.

Cerri, M.R., Wang, Q., Stolz, P., Folgmann, J., Frances, L., Katzer, K., Li, X., Heckmann, A.B., Wang, T.L., and Downie, J.A. (2017). The ERN 1 transcription factor gene is a target of the CC a MK/CYCLOPS complex and controls rhizobial infection in Lotus japonicus. New Phytologist **215,** 323-337.

Charpentier, M., Bredemeier, R., Wanner, G., Takeda, N., Schleiff, E., and Parniske, M. (2008). Lotus japonicus CASTOR and POLLUX are ion channels essential for perinuclear calcium spiking in legume root endosymbiosis. The Plant cell **20,** 3467-3479.

Charpentier, M., Sun, J., Martins, T.V., Radhakrishnan, G.V., Findlay, K., Soumpourou, E., Thouin, J., Véry, A.-A., Sanders, D., and Morris, R.J. (2016). Nuclear-localized cyclic nucleotide–gated channels mediate symbiotic calcium oscillations. Science (New York, N.Y.) **352,** 1102-1105.

Chen, T., Zhu, H., Ke, D., Cai, K., Wang, C., Gou, H., Hong, Z., and Zhang, Z. (2012). A MAP kinase kinase interacts with SymRK and regulates nodule organogenesis in Lotus japonicus. The Plant cell **24,** 823-838.

Cheng, H.-P., and Walker, G.C. (1998). Succinoglycan is required for initiation and elongation of infection threads during nodulation of alfalfa by Rhizobium meliloti. Journal of bacteriology **180,** 5183-5191.

Cho, M.-J., and Harper, J.E. (1991). Effect of localized nitrate application on isoflavonoid concentration and nodulation in split-root systems of wild-type and nodulation-mutant soybean plants. Plant physiology **95,** 1106-1112.

Combier, J.-P., Frugier, F., de Billy, F., Boualem, A., El-Yahyaoui, F., Moreau, S., Vernié, T., Ott, T., Gamas, P., and Crespi, M. (2006). MtHAP2-1 is a key transcriptional regulator of symbiotic nodule development regulated by microRNA169 in Medicago truncatula. Genes & development **20,** 3084-3088.

Coronado, C., Zuanazzi, J.S., Sallaud, C., Quirion, J.-C., Esnault, R., Husson, H.-P., Kondorosi, A., and Ratet, P. (1995). Alfalfa root flavonoid production is nitrogen regulated. Plant physiology **108,** 533-542.

Crespi, M., and Frugier, F. (2008). De novo organ formation from differentiated cells: root nodule organogenesis. Science Signaling **1,** re11-re11.

Crook, A.D., Schnabel, E.L., and Frugoli, J.A. (2016). The systemic nodule number regulation kinase SUNN in Medicago truncatula interacts with Mt CLV 2 and Mt CRN. The Plant Journal **88,** 108-119.

Danzig, E., and Gavrilov, I. (2010). Mealybugs of the genera Planococcus and Crisicoccus (Sternorrhyncha: Pseudococcidae) of Russia and adjacent countries. Zoosystematica Rossica **19,** 39-49.

Dart, P., and Wildon, D. (1970). Nodulation and nitrogen fixation by Vigna sinensis and Vicia atropurpurea: The influence of concentration, form, and site of application of combined nitrogen. Australian Journal of Agricultural Research **21,** 45-56.

De Luis, A., Markmann, K., Cognat, V., Holt, D.B., Charpentier, M., Parniske, M., Stougaard, J., and Voinnet, O. (2012). Two microRNAs linked to nodule infection and nitrogen-fixing ability in the legume Lotus japonicus. Plant physiology **160,** 2137-2154.

Delves, A., Higgins, A., and Gresshoff, P. (1987). Shoot control of supernodulation in a number of mutant soybeans, Glycine max (L.) Merr. Functional Plant Biology **14,** 689-694.

Delves, A., Higgins, A., and Gresshoff, P. (1992). Shoot apex removal does not alter autoregulation of Modulation in soybean. Plant, Cell & Environment **15,** 249-254.

Delves, A.C., Mathews, A., Day, D.A., Carter, A.S., Carroll, B.J., and Gresshoff, P.M. (1986). Regulation of the soybean-Rhizobium nodule symbiosis by shoot and root factors. Plant physiology **82,** 588-590.

Devers, E.A. (2019). MiR 171 h restricts root symbioses and shows, like its target NSP 2, a complex transcriptional regulation in Medicago truncatula. The Model Legume Medicago truncatula**,** 975-986.

Din, M., Barozai, M.Y., and Baloch, I.A. (2014). Identification and functional analysis of new conserved microRNAs and their targets in potato (Solanum tuberosum L.). Turkish Journal of Botany **38,** 1199-1213.

Dong, Z., Han, M.-H., and Fedoroff, N. (2008). The RNA-binding proteins HYL1 and SE promote accurate in vitro processing of pri-miRNA by DCL1. Proceedings of the National Academy of Sciences **105,** 9970-9975.

Duc, G., Trouvelot, A., Gianinazzi-Pearson, V., and Gianinazzi, S. (1989). First report of non-mycorrhizal plant mutants (Myc−) obtained in pea (Pisum sativum L.) and fababean (Vicia faba L.). Plant science **60,** 215-222.

Farazi, T.A., Juranek, S.A., and Tuschl, T. (2008). The growing catalog of small RNAs and their association with distinct Argonaute/Piwi family members. Development **135,** 1201-1214.

Fornari, M., Calvenzani, V., Masiero, S., Tonelli, C., and Petroni, K. (2013). The Arabidopsis NF-YA3 and NF-YA8 genes are functionally redundant and are required in early embryogenesis. PLoS One **8,** e82043.

Gautrat, P., Laffont, C., and Frugier, F. (2020). Compact root architecture 2 promotes root competence for nodulation through the miR2111 systemic effector. Current Biology **30,** 1339-1345. e1333.

Gavrilovic, S., Yan, Z., Jurkiewicz, A.M., Stougaard, J., and Markmann, K. (2016). Inoculation insensitive promoters for cell type enriched gene expression in legume roots and nodules. Plant Methods **12,** 1-14.

Grimaldi, D., Engel, M.S., Engel, M.S., and Engel, M.S. (2005). Evolution of the Insects. (Cambridge University Press).

Groth, M., Takeda, N., Perry, J., Uchida, H., Dräxl, S., Brachmann, A., Sato, S., Tabata, S., Kawaguchi, M., and Wang, T.L. (2010). NENA, a Lotus japonicus homolog of Sec13, is required for rhizodermal infection by arbuscular mycorrhiza fungi and rhizobia but dispensable for cortical endosymbiotic development. The Plant cell **22,** 2509-2526.

Hadri, A.-E., Spaink, H.P., Bisseling, T., and Brewin, N.J. (1998). Diversity of root nodulation and rhizobial infection processes. In The Rhizobiaceae (Springer), pp. 347-360.

Han, J., Xie, H., Kong, M., Sun, Q., Li, R., and Pan, J. (2014). Computational identification of miRNAs and their targets in Phaseolus vulgaris. Genet Mol Res **13,** 310-322.

Han, J., Kong, M., Xie, H., Sun, Q., Nan, Z., Zhang, Q., and Pan, J. (2013). Identification of miRNAs and their targets in wheat (Triticum aestivum L.) by EST analysis. Genet Mol Res **12,** 805.

Handberg, K., and Stougaard, J. (1992). Lotus japonicus, an autogamous, diploid legume species for classical and molecular genetics **2,** 487-496.

Handberg, K., Stiller, J., Thykjær, T., and Stougaard, J. (1994). Transgenic plants: Agrobacterium-mediated transformation of the diploid legume Lotus japonicus. In Cell Biology (Elsevier), pp. 119-127.

Hanemian, M., Barlet, X., Sorin, C., Yadeta, K.A., Keller, H., Favery, B., Simon, R., Thomma, B.P.H.J., Hartmann, C., Crespi, M., Marco, Y., Tremousaygue, D., and Deslandes, L. (2016). Arabidopsis CLAVATA1 and CLAVATA2 receptors contribute to Ralstonia solanacearum pathogenicity through a miR169-dependent pathway. New Phytologist **211,** 502-515.

Haney, C.H., and Long, S.R. (2010). Plant flotillins are required for infection by nitrogen-fixing bacteria. Proceedings of the National Academy of Sciences **107,** 478-483.

Hansen, J., Jørgensen, J.E., Stougaard, J., and Marcker, K.A. (1989). Hairy roots - a short cut to transgenic root nodules. Plant Cell Rep **8,** 12-15.

Hastwell, A. (2018). Functional characterisation of novel peptide hormones in legume nodulation and plant development. PhD Thesis, 241.

Heckmann, A.B., Lombardo, F., Miwa, H., Perry, J.A., Bunnewell, S., Parniske, M., Wang, T.L., and Downie, J.A. (2006). Lotus japonicus nodulation requires two GRAS domain regulators, one of which is functionally conserved in a non-legume. Plant physiology **142,** 1739-1750.

Heckmann, A.B., Sandal, N., Bek, A.S., Madsen, L.H., Jurkiewicz, A., Nielsen, M.W., Tirichine, L., and Stougaard, J. (2011). Cytokinin induction of root nodule primordia in Lotus japonicus is regulated by a mechanism operating in the root cortex. Molecular plant-microbe interactions **24,** 1385-1395.

Held, M., Hou, H., Miri, M., Huynh, C., Ross, L., Hossain, M.S., Sato, S., Tabata, S., Perry, J., and Wang, T.L. (2014). Lotus japonicus cytokinin receptors work partially redundantly to mediate nodule formation. The Plant cell **26,** 678-694.

Hirsch, S., Kim, J., Muñoz, A., Heckmann, A.B., Downie, J.A., and Oldroyd, G.E. (2009). GRAS proteins form a DNA binding complex to induce gene expression during nodulation signaling in Medicago truncatula. The Plant cell **21,** 545-557.

Holt, D.B. (2014). Small RNAs involved in bacterial root symbiosis in *Lotus Japonicus* (Aarhus University).

Holt, D.B., Gupta, V., Meyer, D., Abel, N.B., Andersen, S.U., Stougaard, J., and Markmann, K. (2015). micro RNA 172 (miR172) signals epidermal infection and is expressed in cells primed for bacterial invasion in Lotus japonicus roots and nodules. New Phytologist **208,** 241-256.

Hossain, M.S., Shrestha, A., Zhong, S., Miri, M., Austin, R.S., Sato, S., Ross, L., Huebert, T., Tromas, A., and Torres-Jerez, I. (2016). Lotus japonicus NF-YA1 plays an essential role during nodule differentiation and targets members of the SHI/STY gene family. Molecular plant-microbe interactions **29,** 950-964.

Imaizumi-Anraku, H., Takeda, N., Charpentier, M., Perry, J., Miwa, H., Umehara, Y., Kouchi, H., Murakami, Y., Mulder, L., and Vickers, K. (2005). Plastid proteins crucial for symbiotic fungal and bacterial entry into plant roots. Nature **433,** 527-531.

Imin, N., Mohd-Radzman, N.A., Ogilvie, H.A., and Djordjevic, M.A. (2013). The peptide-encoding CEP1 gene modulates lateral root and nodule numbers in Medicago truncatula. J Exp Bot **64,** 5395-5409.

Iwakawa, H.-o., and Tomari, Y. (2013). Molecular insights into microRNA-mediated translational repression in plants. Molecular cell **52,** 591-601.

Jeudy, C., Ruffel, S., Freixes, S., Tillard, P., Santoni, A.L., Morel, S., Journet, E.P., Duc, G., Gojon, A., and Lepetit, M. (2010). Adaptation of Medicago truncatula to nitrogen limitation is modulated via local and systemic nodule developmental responses. New Phytologist **185,** 817-828.

Jin, J., Zhang, H., Kong, L., Gao, G., and Luo, J. (2014). PlantTFDB 3.0: a portal for the functional and evolutionary study of plant transcription factors. Nucleic acids research **42,** D1182-D1187.

Jones-Rhoades, M.W., Bartel, D.P., and Bartel, B. (2006). MicroRNAs and their regulatory roles in plants. Annu. Rev. Plant Biol. **57,** 19-53.

Kaló, P., Gleason, C., Edwards, A., Marsh, J., Mitra, R.M., Hirsch, S., Jakab, J., Sims, S., Long, S.R., and Rogers, J. (2005). Nodulation signaling in legumes requires NSP2, a member of the GRAS family of transcriptional regulators. Science (New York, N.Y.) **308,** 1786-1789.

Kanamori, N., Madsen, L.H., Radutoiu, S., Frantescu, M., Quistgaard, E.M., Miwa, H., Downie, J.A., James, E.K., Felle, H.H., and Haaning, L.L. (2006). A nucleoporin is required for induction of Ca2+ spiking in legume nodule development and essential for rhizobial and fungal symbiosis. Proceedings of the National Academy of Sciences **103,** 359-364.

Kawaharada, Y., James, E.K., Kelly, S., Sandal, N., and Stougaard, J. (2017a). The ethylene responsive factor required for nodulation 1 (ERN1) transcription factor is required for infection-thread formation in Lotus japonicus. Molecular plant-microbe interactions **30,** 194-204.

Kawaharada, Y., Kelly, S., Nielsen, M.W., Hjuler, C., Gysel, K., Muszyński, A., Carlson, R., Thygesen, M., Sandal, N., and Asmussen, M. (2015). Receptor-mediated exopolysaccharide perception controls bacterial infection. Nature **523,** 308-312.

Kawaharada, Y., Nielsen, M.W., Kelly, S., James, E.K., Andersen, K.R., Rasmussen, S.R., Füchtbauer, W., Madsen, L.H., Heckmann, A.B., and Radutoiu, S. (2017b). Differential regulation of the Epr3 receptor coordinates membrane-restricted rhizobial colonization of root nodule primordia. Nature communications **8,** 1-11.

Kawashima, C.G., Yoshimoto, N., Maruyama-Nakashita, A., Tsuchiya, Y.N., Saito, K., Takahashi, H., and Dalmay, T. (2009). Sulphur starvation induces the expression of microRNA-395 and one of its target genes but in different cell types. The Plant Journal **57,** 313-321.

Kennedy, J., and Mittler, T. (1953). A method of obtaining phloem sap via the mouth-parts of aphids. Nature **171,** 528-528.

Kim, Y.J., Zheng, B., Yu, Y., Won, S.Y., Mo, B., and Chen, X. (2011). The role of Mediator in small and long noncoding RNA production in Arabidopsis thaliana. The EMBO journal **30,** 814-822.

Krusell, L., Madsen, L.H., Sato, S., Aubert, G., Genua, A., Szczyglowski, K., Duc, G., Kaneko, T., Tabata, S., and De Bruijn, F. (2002a). Shoot control of root development and nodulation is mediated by a receptor-like kinase. Nature **420,** 422-426.

Krusell, L., Madsen, L.H., Sato, S., Aubert, G., Genua, A., Szczyglowski, K., Duc, G., Kaneko, T., Tabata, S., and De Bruijn, F.J.N. (2002b). Shoot control of root development and nodulation is mediated by a receptor-like kinase **420,** 422-426.

Krusell, L., Sato, N., Fukuhara, I., Koch, B.E., Grossmann, C., Okamoto, S., Oka-Kira, E., Otsubo, Y., Aubert, G., and Nakagawa, T. (2011). The Clavata2 genes of pea and Lotus japonicus affect autoregulation of nodulation. The Plant Journal **65,** 861-871.

Kurihara, Y., and Watanabe, Y. (2004). Arabidopsis micro-RNA biogenesis through Dicer-like 1 protein functions. Proceedings of the National Academy of Sciences **101,** 12753-12758.

Kurihara, Y., Takashi, Y., and Watanabe, Y. (2006). The interaction between DCL1 and HYL1 is important for efficient and precise processing of pri-miRNA in plant microRNA biogenesis. Rna **12,** 206-212.

Kushwaha, H.R., Singh, A.K., Sopory, S.K., Singla-Pareek, S.L., and Pareek, A. (2009). Genome wide expression analysis of CBS domain containing proteins in Arabidopsis thaliana (L.) Heynh and Oryza sativa L. reveals their developmental and stress regulation. BMC Genomics **10,** 200.

Lauressergues, D., Couzigou, J.-M., San Clemente, H., Martinez, Y., Dunand, C., Bécard, G., and Combier, J.-P. (2015). Primary transcripts of microRNAs encode regulatory peptides. Nature **520,** 90-93.

Lauressergues, D., Delaux, P.M., Formey, D., Lelandais-Brière, C., Fort, S., Cottaz, S., Bécard, G., Niebel, A., Roux, C., and Combier, J.P. (2012). The microRNA miR171h modulates arbuscular mycorrhizal colonization of Medicago truncatula by targeting NSP2. The Plant Journal **72,** 512-522.

Lazo, G.R., Stein, P.A., and Ludwig, R.A.J.B.t. (1991). A DNA transformation–competent Arabidopsis genomic library in Agrobacterium **9,** 963-967.

Lefebvre, B., Timmers, T., Mbengue, M., Moreau, S., Hervé, C., Tóth, K., Bittencourt-Silvestre, J., Klaus, D., Deslandes, L., and Godiard, L. (2010). A remorin protein interacts with symbiotic receptors and regulates bacterial infection. Proceedings of the National Academy of Sciences **107,** 2343-2348.

Lerouge, P., Roche, P., Faucher, C., Maillet, F., Truchet, G., Promé, J.C., and Dénarié, J. (1990). Symbiotic host-specificity of Rhizobium meliloti is determined by a sulphated and acylated glucosamine oligosaccharide signal. Nature **344,** 781-784.

Li, J., Yang, Z., Yu, B., Liu, J., and Chen, X. (2005). Methylation protects miRNAs and siRNAs from a 3′-end uridylation activity in Arabidopsis. Current biology **15,** 1501-1507.

Li, S., Wang, X., Xu, W., Liu, T., Cai, C., Chen, L., Clark, C.B., and Ma, J. (2021). Unidirectional movement of small RNAs from shoots to roots in interspecific heterografts. Nature Plants **7,** 50-59.

Li, Y., Zhao, S.-L., Li, J.-L., Hu, X.-H., Wang, H., Cao, X.-L., Xu, Y.-J., Zhao, Z.-X., Xiao, Z.-Y., and Yang, N. (2017). Osa-miR169 negatively regulates rice immunity against the blast fungus Magnaporthe oryzae. Frontiers in plant science **8,** 2.

Li, Z., Xu, H., Li, Y., Wan, X., Ma, Z., Cao, J., Li, Z., He, F., Wang, Y., and Wan, L. (2018). Analysis of physiological and miRNA responses to Pi deficiency in alfalfa (Medicago sativa L.). Plant molecular biology **96,** 473-492.

Ligero, F., Caba, J.M., Lluch, C., and Olivares, J. (1991). Nitrate inhibition of nodulation can be overcome by the ethylene inhibitor aminoethoxyvinylglycine. Plant physiology **97,** 1221-1225.

Limpens, E., Franken, C., Smit, P., Willemse, J., Bisseling, T., and Geurts, R. (2003). LysM domain receptor kinases regulating rhizobial Nod factor-induced infection. Science (New York, N.Y.) **302,** 630-633.

Lin, J., Roswanjaya, Y.P., Kohlen, W., Stougaard, J., and Reid, D. (2021). Nitrate restricts nodule organogenesis through inhibition of cytokinin biosynthesis in Lotus japonicus. Nature communications **12,** 1-12.

Lin, Y.H., Ferguson, B.J., Kereszt, A., and Gresshoff, P.M. (2010). Suppression of hypernodulation in soybean by a leaf-extracted, NARK-and Nod factor-dependent, low molecular mass fraction. New Phytologist **185,** 1074-1086.

Liu, C.-W., and Murray, J.D. (2016). The role of flavonoids in nodulation host-range specificity: an update. Plants **5,** 33.

Liu, C.-W., Breakspear, A., Stacey, N., Findlay, K., Nakashima, J., Ramakrishnan, K., Liu, M., Xie, F., Endre, G., and de Carvalho-Niebel, F. (2019). A protein complex required for polar growth of rhizobial infection threads. Nature communications **10,** 1-17.

Love, M., Anders, S., and Huber, W. (2014a). Differential analysis of count data–the DESeq2 package. Genome Biol **15,** 10-1186.

Love, M., Anders, S., and Huber, W.J.G.B. (2014b). Differential analysis of count data–the DESeq2 package **15,** 10-1186.

Love, M.I., Huber, W., and Anders, S. (2014c). Moderated estimation of fold change and dispersion for RNA-seq data with DESeq2. Genome biology **15,** 1-21.

Love, M.I., Huber, W., and Anders, S.J.G.b. (2014d). Moderated estimation of fold change and dispersion for RNA-seq data with DESeq2 **15,** 1-21.

Luo, Z., Jin, L., and Qiu, L. (2012). MiR1511 co-regulates with miR1511* to cleave the GmRPL4a gene in soybean. Chinese Science Bulletin **57,** 3804-3810.

Madsen, E.B., Madsen, L.H., Radutoiu, S., Olbryt, M., Rakwalska, M., Szczyglowski, K., Sato, S., Kaneko, T., Tabata, S., and Sandal, N. (2003). A receptor kinase gene of the LysM type is involved in legumeperception of rhizobial signals. Nature **425,** 637-640.

Maekawa, T., Maekawa-Yoshikawa, M., Takeda, N., Imaizumi-Anraku, H., Murooka, Y., and Hayashi, M. (2009a). Gibberellin controls the nodulation signaling pathway in Lotus japonicus. The Plant Journal **58,** 183-194.

Maekawa, T., Maekawa-Yoshikawa, M., Takeda, N., Imaizumi-Anraku, H., Murooka, Y., and Hayashi, M.J.T.P.J. (2009b). Gibberellin controls the nodulation signaling pathway in Lotus japonicus **58,** 183-194.

Maillet, F., Poinsot, V., André, O., Puech-Pagès, V., Haouy, A., Gueunier, M., Cromer, L., Giraudet, D., Formey, D., and Niebel, A. (2011). Fungal lipochitooligosaccharide symbiotic signals in arbuscular mycorrhiza. Nature **469,** 58-63.

Małolepszy, A., Mun, T., Sandal, N., Gupta, V., Dubin, M., Urbański, D., Shah, N., Bachmann, A., Fukai, E., Hirakawa, H., Tabata, S., Nadzieja, M., Markmann, K., Su, J., Umehara, Y., Soyano, T., Miyahara, A., Sato, S., Hayashi, M., Stougaard, J., and Andersen, S.U. (2016). The LORE1 insertion mutant resource. The Plant journal : for cell and molecular biology **88,** 306-317.

Markmann, K., and Parniske, M. (2009). Evolution of root endosymbiosis with bacteria: how novel are nodules? Trends in plant science **14,** 77-86.

Matamoros, M.A., Baird, L.M., Escuredo, P.R., Dalton, D.A., Minchin, F.R., Iturbe-Ormaetxe, I., Rubio, M.C., Moran, J.F., Gordon, A.J., and Becana, M. (1999). Stress-induced legume root nodule senescence. Physiological, biochemical, and structural alterations. Plant physiology **121,** 97-112.

Mi, S., Cai, T., Hu, Y., Chen, Y., Hodges, E., Ni, F., Wu, L., Li, S., Zhou, H., and Long, C. (2008). Sorting of small RNAs into Arabidopsis argonaute complexes is directed by the 5′ terminal nucleotide. Cell **133,** 116-127.

Middleton, P.H., Jakab, J., Penmetsa, R.V., Starker, C.G., Doll, J., Kaló, P., Prabhu, R., Marsh, J.F., Mitra, R.M., and Kereszt, A. (2007). An ERF transcription factor in Medicago truncatula that is essential for Nod factor signal transduction. The Plant cell **19,** 1221-1234.

Miri, M., Janakirama, P., Huebert, T., Ross, L., McDowell, T., Orosz, K., Markmann, K., and Szczyglowski, K. (2019). Inside out: root cortex-localized LHK1 cytokinin receptor limits epidermal infection of Lotus japonicus roots by Mesorhizobium loti. New Phytologist **222,** 1523-1537.

Miyata, K., Kawaguchi, M., and Nakagawa, T. (2013). Two distinct EIN2 genes cooperatively regulate ethylene signaling in Lotus japonicus. Plant and cell physiology **54,** 1469-1477.

Miyazawa, H., Oka-Kira, E., Sato, N., Takahashi, H., Wu, G.-J., Sato, S., Hayashi, M., Betsuyaku, S., Nakazono, M., and Tabata, S. (2010). The receptor-like kinase KLAVIER mediates systemic regulation of nodulation and non-symbiotic shoot development in Lotus japonicus. Development **137,** 4317-4325.

Moling, S., Pietraszewska-Bogiel, A., Postma, M., Fedorova, E., Hink, M.A., Limpens, E., Gadella, T.W., and Bisseling, T. (2014). Nod factor receptors form heteromeric complexes and are essential for intracellular infection in Medicago nodules. The Plant cell **26,** 4188-4199.

Montgomery, T.A., Howell, M.D., Cuperus, J.T., Li, D., Hansen, J.E., Alexander, A.L., Chapman, E.J., Fahlgren, N., Allen, E., and Carrington, J.C. (2008). Specificity of ARGONAUTE7-miR390 interaction and dual functionality in TAS3 trans-acting siRNA formation. Cell **133,** 128-141.

Murakami, Y., Miwa, H., Imaizumi-Anraku, H., Kouchi, H., Downie, J.A., Kawaguchi, M., and Kawasaki, S. (2006). Positional cloning identifies Lotus japonicus NSP2, a putative transcription factor of the GRAS family, required for NIN and ENOD40 gene expression in nodule initiation. DNA research **13,** 255-265.

Murray, J.D., Karas, B.J., Sato, S., Tabata, S., Amyot, L., and Szczyglowski, K. (2007). A cytokinin perception mutant colonized by Rhizobium in the absence of nodule organogenesis. Science (New York, N.Y.) **315,** 101-104.

Murray, J.D., Muni, R.R.D., Torres-Jerez, I., Tang, Y., Allen, S., Andriankaja, M., Li, G., Laxmi, A., Cheng, X., and Wen, J. (2011). Vapyrin, a gene essential for intracellular progression of arbuscular mycorrhizal symbiosis, is also essential for infection by rhizobia in the nodule symbiosis of Medicago truncatula. The Plant Journal **65,** 244-252.

Nishida, H., and Suzaki, T. (2018). Nitrate-mediated control of root nodule symbiosis. Current opinion in plant biology **44,** 129-136.

Nishida, H., Handa, Y., Tanaka, S., Suzaki, T., and Kawaguchi, M. (2016). Expression of the CLE-RS3 gene suppresses root nodulation in Lotus japonicus. Journal of plant research **129,** 909-919.

Nishida, H., Ito, M., Miura, K., Kawaguchi, M., and Suzaki, T. (2020). Autoregulation of nodulation pathway is dispensable for nitrate-induced control of rhizobial infection. Plant signaling & behavior **15,** 1733814.

Nishida, H., Tanaka, S., Handa, Y., Ito, M., Sakamoto, Y., Matsunaga, S., Betsuyaku, S., Miura, K., Soyano, T., and Kawaguchi, M. (2018). A NIN-LIKE PROTEIN mediates nitrate-induced control of root nodule symbiosis in Lotus japonicus. Nature communications **9,** 1-14.

Nishida, H., Nosaki, S., Suzuki, T., Ito, M., Miyakawa, T., Nomoto, M., Tada, Y., Miura, K., Tanokura, M., and Kawaguchi, M. (2021). Different DNA-binding specificities of NLP and NIN transcription factors underlie nitrate-induced control of root nodulation. The Plant cell.

Nishimura, R., Hayashi, M., Wu, G.-J., Kouchi, H., Imaizumi-Anraku, H., Murakami, Y., Kawasaki, S., Akao, S., Ohmori, M., and Nagasawa, M. (2002). HAR1 mediates systemic regulation of symbiotic organ development. Nature **420,** 426-429.

Nizampatnam, N.R., Schreier, S.J., Damodaran, S., Adhikari, S., and Subramanian, S. (2015). micro RNA 160 dictates stage-specific auxin and cytokinin sensitivities and directs soybean nodule development. The Plant Journal **84,** 140-153.

Nova-Franco, B., Íñiguez, L.P., Valdés-López, O., Alvarado-Affantranger, X., Leija, A., Fuentes, S.I., Ramírez, M., Paul, S., Reyes, J.L., and Girard, L. (2015). The micro-RNA172c-APETALA2-1 node as a key regulator of the common bean-Rhizobium etli nitrogen fixation symbiosis. Plant physiology **168,** 273-291.

Oka-Kira, E., Tateno, K., Miura, K.i., Haga, T., Hayashi, M., Harada, K., Sato, S., Tabata, S., Shikazono, N., and Tanaka, A. (2005). klavier (klv), a novel hypernodulation mutant of Lotus japonicus affected in vascular tissue organization and floral induction. The Plant Journal **44,** 505-515.

Okamoto, S., Shinohara, H., Mori, T., Matsubayashi, Y., and Kawaguchi, M. (2013). Root-derived CLE glycopeptides control nodulation by direct binding to HAR1 receptor kinase. Nature communications **4,** 1-7.

Okamoto, S., Ohnishi, E., Sato, S., Takahashi, H., Nakazono, M., Tabata, S., and Kawaguchi, M. (2009). Nod factor/nitrate-induced CLE genes that drive HAR1-mediated systemic regulation of nodulation. Plant and Cell Physiology **50,** 67-77.

Okuma, N., Soyano, T., Suzaki, T., and Kawaguchi, M. (2020). MIR2111-5 locus and shoot-accumulated mature miR2111 systemically enhance nodulation depending on HAR1 in Lotus japonicus. Nature communications **11,** 1-13.

Oldroyd, G.E., Engstrom, E.M., and Long, S.R. (2001). Ethylene inhibits the Nod factor signal transduction pathway of Medicago truncatula. The Plant cell **13,** 1835-1849.

Oldroyd, G.E., Murray, J.D., Poole, P.S., and Downie, J.A. (2011). The rules of engagement in the legume-rhizobial symbiosis. Annual review of genetics **45,** 119-144.

Pagnussat, G.C., Yu, H.-J., Ngo, Q.A., Rajani, S., Mayalagu, S., Johnson, C.S., Capron, A., Xie, L.-F., Ye, D., and Sundaresan, V. (2005). Genetic and molecular identification of genes required for female gametophyte development and function in Arabidopsis. Development.

Pant, B.D., Musialak-Lange, M., Nuc, P., May, P., Buhtz, A., Kehr, J., Walther, D., and Scheible, W.-R. (2009). Identification of nutrient-responsive Arabidopsis and rapeseed microRNAs by comprehensive real-time polymerase chain reaction profiling and small RNA sequencing. Plant physiology **150,** 1541-1555.

Park, M.Y., Wu, G., Gonzalez-Sulser, A., Vaucheret, H., and Poethig, R.S. (2005). Nuclear processing and export of microRNAs in Arabidopsis. Proceedings of the National Academy of Sciences **102,** 3691-3696.

Parniske, M. (2008). Arbuscular mycorrhiza: the mother of plant root endosymbioses. Nature Reviews Microbiology **6,** 763-775.

Penmetsa, R.V., and Cook, D.R. (1997). A legume ethylene-insensitive mutant hyperinfected by its rhizobial symbiont. Science (New York, N.Y.) **275,** 527-530.

Perry, J., Brachmann, A., Welham, T., Binder, A., Charpentier, M., Groth, M., Haage, K., Markmann, K., Wang, T.L., and Parniske, M. (2009). TILLING in Lotus japonicus identified large allelic series for symbiosis genes and revealed a bias in functionally defective ethyl methanesulfonate alleles toward glycine replacements. Plant physiology **151,** 1281-1291.

Peters, N.K., Frost, J.W., and Long, S.R. (1986). A plant flavone, luteolin, induces expression of Rhizobium meliloti nodulation genes. Science (New York, N.Y.), 977-980.

Pumplin, N., Mondo, S.J., Topp, S., Starker, C.G., Gantt, J.S., and Harrison, M.J. (2010). Medicago truncatula Vapyrin is a novel protein required for arbuscular mycorrhizal symbiosis. The Plant Journal **61,** 482-494.

Radutoiu, S., Madsen, L.H., Madsen, E.B., Felle, H.H., Umehara, Y., Grønlund, M., Sato, S., Nakamura, Y., Tabata, S., and Sandal, N. (2003). Plant recognition of symbiotic bacteria requires two LysM receptor-like kinases. Nature **425,** 585-592.

Rajwanshi, R., Devi, K.J., Sharma, G.R., and Lal, B. (2019). Role of miRNAs in plant-microbe interaction. In In vitro Plant Breeding towards Novel Agronomic Traits (Springer), pp. 167-195.

Ramakers, C., Ruijter, J.M., Deprez, R.H.L., and Moorman, A.F.J.N.l. (2003). Assumption-free analysis of quantitative real-time polymerase chain reaction (PCR) data **339,** 62-66.

Reid, D., Liu, H., Kelly, S., Kawaharada, Y., Mun, T., Andersen, S.U., Desbrosses, G., and Stougaard, J. (2018). Dynamics of ethylene production in response to compatible Nod factor. Plant physiology **176,** 1764-1772.

Reid, D.E., Ferguson, B.J., and Gresshoff, P.M. (2011). Inoculation-and nitrate-induced CLE peptides of soybean control NARK-dependent nodule formation. Molecular Plant-Microbe Interactions **24,** 606-618.

Reid, D.E., Heckmann, A.B., Novák, O., Kelly, S., and Stougaard, J. (2016). CYTOKININ OXIDASE/DEHYDROGENASE3 maintains cytokinin homeostasis during root and nodule development in Lotus japonicus. Plant physiology **170,** 1060-1074.

Reyero-Saavedra, M.D.R., Qiao, Z., Sánchez-Correa, M.D.S., Díaz-Pineda, M.E., Reyes, J.L., Covarrubias, A.A., Libault, M., and Valdés-López, O. (2017). Gene silencing of Argonaute5 negatively affects the establishment of the legume-rhizobia symbiosis. Genes **8,** 352.

Ruijter, J., Ramakers, C., Hoogaars, W., Karlen, Y., Bakker, O., Van den Hoff, M., and Moorman, A.J.N.a.r. (2009). Amplification efficiency: linking baseline and bias in the analysis of quantitative PCR data **37,** e45-e45.

Saito, K., Yoshikawa, M., Yano, K., Miwa, H., Uchida, H., Asamizu, E., Sato, S., Tabata, S., Imaizumi-Anraku, H., and Umehara, Y. (2007). NUCLEOPORIN85 is required for calcium spiking, fungal and bacterial symbioses, and seed production in Lotus japonicus. The Plant cell **19,** 610-624.

Sarkies, P., and Miska, E.A. (2014). Small RNAs break out: the molecular cell biology of mobile small RNAs. Nature Reviews Molecular Cell Biology **15,** 525-535.

Sasaki, T., Suzaki, T., Soyano, T., Kojima, M., Sakakibara, H., and Kawaguchi, M. (2014). Shoot-derived cytokinins systemically regulate root nodulation. Nature communications **5,** 1-9.

Sauer, N., and Stolz, J. (1994). SUC1 and SUC2: two sucrose transporters from Arabidopsis thaliana; expression and characterization in baker's yeast and identification of the histidine-tagged protein. The Plant Journal **6,** 67-77.

Schauser, L., Roussis, A., Stiller, J., and Stougaard, J. (1999). A plant regulator controlling development of symbiotic root nodules. Nature **402,** 191-195.

Sexauer, M., Bhasin, H., Schön, M., Roitsch, E., Herzog, U., and Markmann, K. (2022). A micro RNA mediates shoot control of root branching T.U. Centre for Molecular Biology of Plants, ed (Nature Communications), pp. 17.

Shrestha, A., Zhong, S., Therrien, J., Huebert, T., Sato, S., Mun, T., Andersen, S.U., Stougaard, J., Lepage, A., and Niebel, A. (2021). Lotus japonicus Nuclear Factor YA1, a nodule emergence stage-specific regulator of auxin signalling. The New Phytologist **229,** 1535.

Singh, S., Katzer, K., Lambert, J., Cerri, M., and Parniske, M. (2014). CYCLOPS, a DNA-binding transcriptional activator, orchestrates symbiotic root nodule development. Cell host & microbe **15,** 139-152.

Skopelitis, D.S., Hill, K., Klesen, S., Marco, C.F., von Born, P., Chitwood, D.H., and Timmermans, M.C. (2018). Gating of miRNA movement at defined cell-cell interfaces governs their impact as positional signals. Nature communications **9,** 1-10.

Smit, P., Raedts, J., Portyanko, V., Debellé, F., Gough, C., Bisseling, T., and Geurts, R. (2005). NSP1 of the GRAS protein family is essential for rhizobial Nod factor-induced transcription. Science (New York, N.Y.) **308,** 1789-1791.

Soyano, T., Shimoda, Y., and Hayashi, M. (2015). NODULE INCEPTION antagonistically regulates gene expression with nitrate in Lotus japonicus. Plant and Cell Physiology **56,** 368-376.

Soyano, T., Kouchi, H., Hirota, A., and Hayashi, M. (2013). Nodule inception directly targets NF-Y subunit genes to regulate essential processes of root nodule development in Lotus japonicus. PLoS genetics **9,** e1003352.

Soyano, T., Shimoda, Y., Kawaguchi, M., and Hayashi, M. (2019). A shared gene drives lateral root development and root nodule symbiosis pathways in Lotus. Science (New York, N.Y.) **366,** 1021-1023.

Soyano, T., Hirakawa, H., Sato, S., Hayashi, M., and Kawaguchi, M. (2014). NODULE INCEPTION creates a long-distance negative feedback loop involved in homeostatic regulation of nodule organ production. Proceedings of the National Academy of Sciences **111,** 14607-14612.

Spaink, H.P., Sheeley, D.M., van Brussel, A.A., Glushka, J., York, W.S., Tak, T., Geiger, O., Kennedy, E.P., Reinhold, V.N., and Lugtenberg, B.J. (1991). A novel highly unsaturated fatty acid moiety of lipo-oligosaccharide signals determines host specificity of Rhizobium. Nature **354,** 125-130.

Stadler, R., and Sauer, N. (1996). The Arabidopsis thaliana AtSUC2 gene is specifically expressed in companion cells. Botanica Acta **109,** 299-306.

Stougaard, J., Abildsten, D., and Marcker, K.A. (1987). The Agrobacterium rhizogenes pRi TL-DNA segment as a gene vector system for transformation of plants. Molecular and General Genetics MGG **207,** 251-255.

Stougaard, J.J.P.g.t., and protocols, e. (1995). Agobacterium rhizogenes as a vector for transforming higher plants**,** 49-61.

Stracke, S., Kistner, C., Yoshida, S., Mulder, L., Sato, S., Kaneko, T., Tabata, S., Sandal, N., Stougaard, J., and Szczyglowski, K. (2002). A plant receptor-like kinase required for both bacterial and fungal symbiosis. Nature **417,** 959-962.

Streeter, J., and Wong, P.P. (1988). Inhibition of legume nodule formation and N2 fixation by nitrate. Critical Reviews in Plant Sciences **7,** 1-23.

Suzaki, T., Ito, M., and Kawaguchi, M. (2013). Induction of localized auxin response during spontaneous nodule development in Lotus japonicus. Plant signaling & behavior **8,** e23359.

Suzaki, T., Yano, K., Ito, M., Umehara, Y., Suganuma, N., and Kawaguchi, M. (2012). Positive and negative regulation of cortical cell division during root nodule development in Lotus japonicus is accompanied by auxin response. Development **139,** 3997-4006.

Suzaki, T., Takeda, N., Nishida, H., Hoshino, M., Ito, M., Misawa, F., Handa, Y., Miura, K., and Kawaguchi, M. (2019). LACK OF SYMBIONT ACCOMMODATION controls intracellular symbiont accommodation in root nodule and arbuscular mycorrhizal symbiosis in Lotus japonicus. PLoS genetics **15,** e1007865.

Suzuki, K., Oguro, H., Yamakawa, T., Yamamoto, A., Akao, S., and Saeki, Y. (2008). Diversity and distribution of indigenous soybean-nodulating rhizobia in the Okinawa islands, Japan. Soil Science & Plant Nutrition **54,** 237-246.

Syed, N.H., and Flavell, A.J. (2006). Sequence-specific amplification polymorphisms (SSAPs): a multi-locus approach for analyzing transposon insertions. Nature Protocols **1,** 2746-2752.

Tabata, R., Sumida, K., Yoshii, T., Ohyama, K., Shinohara, H., and Matsubayashi, Y. (2014). Perception of root-derived peptides by shoot LRR-RKs mediates systemic N-demand signaling. Science (New York, N.Y.) **346,** 343-346.

Takahara, M., Magori, S., Soyano, T., Okamoto, S., Yoshida, C., Yano, K., Sato, S., Tabata, S., Yamaguchi, K., and Shigenobu, S. (2013). Too much love, a novel Kelch repeat-containing F-box protein, functions in the long-distance regulation of the legume–Rhizobium symbiosis. Plant and cell physiology **54,** 433-447.

Takeda, A., Iwasaki, S., Watanabe, T., Utsumi, M., and Watanabe, Y. (2008). The mechanism selecting the guide strand from small RNA duplexes is different among argonaute proteins. Plant and cell physiology **49,** 493-500.

Taleski, M., Imin, N., and Djordjevic, M.A. (2018). CEP peptide hormones: key players in orchestrating nitrogen-demand signalling, root nodulation, and lateral root development. Journal of Experimental Botany **69,** 1829-1836.

Timmers, A. (2008). The role of the plant cytoskeleton in the interaction between legumes and rhizobia. Journal of microscopy **231,** 247-256.

Tirichine, L., Sandal, N., Madsen, L.H., Radutoiu, S., Albrektsen, A.S., Sato, S., Asamizu, E., Tabata, S., and Stougaard, J. (2007). A gain-of-function mutation in a cytokinin receptor triggers spontaneous root nodule organogenesis. Science (New York, N.Y.) **315,** 104-107.

Tirichine, L., Imaizumi-Anraku, H., Yoshida, S., Murakami, Y., Madsen, L.H., Miwa, H., Nakagawa, T., Sandal, N., Albrektsen, A.S., and Kawaguchi, M. (2006). Deregulation of a Ca 2+/calmodulin-dependent kinase leads to spontaneous nodule development. Nature **441,** 1153-1156.

Truernit, E., and Sauer, N. (1995). The promoter of the Arabidopsis thaliana SUC2 sucrose-H+ symporter gene directs expression of β-glucuronidase to the phloem: evidence for phloem loading and unloading by SUC2. Planta **196,** 564-570.

Tsikou, D., Yan, Z., Holt, D.B., Abel, N.B., Reid, D.E., Madsen, L.H., Bhasin, H., Sexauer, M., Stougaard, J., and Markmann, K. (2018). Systemic control of legume susceptibility to rhizobial infection by a mobile microRNA. Science (New York, N.Y.) **362,** 233-236.

Turgeon, R. (1989). The sink-source transition in leaves. Annual review of plant biology **40,** 119-138.

Urbański, D.F., Małolepszy, A., Stougaard, J., and Andersen, S.U. (2013). High-throughput and targeted genotyping of Lotus japonicus LORE1 insertion mutants. In Legume Genomics (Springer), pp. 119-146.

Valdés-López, O., Yang, S.S., Aparicio-Fabre, R., Graham, P.H., Reyes, J.L., Vance, C.P., and Hernández, G. (2010). MicroRNA expression profile in common bean (Phaseolus vulgaris) under nutrient deficiency stresses and manganese toxicity. New Phytologist **187,** 805-818.

Van Spronsen, P., Bakhuizen, R., Van Brussel, A., and Kijne, J. (1994). Cell wall degradation during infection thread formation by the root nodule bacterium Rhizobium leguminosarum is a two-step process. European journal of cell biology **64,** 88-94.

Varkonyi-Gasic, E., Wu, R., Wood, M., Walton, E.F., and Hellens, R.P.J.P.m. (2007). Protocol: a highly sensitive RT-PCR method for detection and quantification of microRNAs **3,** 1-12.

Vazquez, F., Vaucheret, H., Rajagopalan, R., Lepers, C., Gasciolli, V., Mallory, A.C., Hilbert, J.-L., Bartel, D.P., and Crété, P. (2004). Endogenous trans-acting siRNAs regulate the accumulation of Arabidopsis mRNAs. Molecular cell **16,** 69-79.

Vigue, J., Harper, J., Hageman, R., and Peters, D. (1977). Nodulation of Soybeans Grown Hydroponically on Urea 1. Crop Science **17,** 169-172.

Wang, B., Yeun, L.H., Xue, J.Y., Liu, Y., Ané, J.M., and Qiu, Y.L. (2010). Presence of three mycorrhizal genes in the common ancestor of land plants suggests a key role of mycorrhizas in the colonization of land by plants. New phytologist **186,** 514-525.

Wang, C., Zhu, H., Jin, L., Chen, T., Wang, L., Kang, H., Hong, Z., and Zhang, Z. (2013a). Splice variants of the SIP1 transcripts play a role in nodule organogenesis in Lotus japonicus. Plant molecular biology **82,** 97-111.

Wang, Y., Zhang, C., Hao, Q., Sha, A., Zhou, R., Zhou, X., and Yuan, L. (2013b). Elucidation of miRNAs-mediated responses to low nitrogen stress by deep sequencing of two soybean genotypes. PLoS One **8,** e67423.

Weber, E., Engler, C., Gruetzner, R., Werner, S., and Marillonnet, S. (2011). A modular cloning system for standardized assembly of multigene constructs. PloS one **6,** e16765.

Wopereis, J., Pajuelo, E., Dazzo, F.B., Jiang, Q., Gresshoff, P.M., De Bruijn, F.J., Stougaard, J., and Szczyglowski, K. (2000). Short root mutant of Lotus japonicus with a dramatically altered symbiotic phenotype. The Plant Journal **23,** 97-114.

Wright, K.M., Roberts, A.G., Martens, H.J., Sauer, N., and Oparka, K.J. (2003). Structural and Functional Vein Maturation in Developing Tobacco Leaves in Relation to AtSUC2 Promoter Activity. Plant physiology **131,** 1555-1565.

Xiao, T.T., Schilderink, S., Moling, S., Deinum, E.E., Kondorosi, E., Franssen, H., Kulikova, O., Niebel, A., and Bisseling, T. (2014). Fate map of Medicago truncatula root nodules. Development **141,** 3517-3528.

Xie, F., Murray, J.D., Kim, J., Heckmann, A.B., Edwards, A., Oldroyd, G.E., and Downie, J.A. (2012). Legume pectate lyase required for root infection by rhizobia. Proceedings of the National Academy of Sciences **109,** 633-638.

Xu, H., Li, Y., Zhang, K., Li, M., Fu, S., Tian, Y., Qin, T., Li, X., Zhong, Y., and Liao, H. (2021). miR169c-NFYA-C-ENOD40 modulates nitrogen inhibitory effects in soybean nodulation. New Phytologist **229,** 3377-3392.

Xu, M.Y., Zhang, L., Li, W.W., Hu, X.L., Wang, M.-B., Fan, Y.L., Zhang, C.Y., and Wang, L. (2014). Stress-induced early flowering is mediated by miR169 in Arabidopsis thaliana. Journal of experimental botany **65,** 89-101.

Xu, Q., Yin, S., Ma, Y., Song, M., Song, Y., Mu, S., Li, Y., Liu, X., Ren, Y., and Gao, C. (2020). Carbon export from leaves is controlled via ubiquitination and phosphorylation of sucrose transporter SUC2. Proceedings of the National Academy of Sciences **117,** 6223-6230.

Yamashino, T., Yamawaki, S., Hagui, E., Ishida, K., Ueoka-Nakanishi, H., Nakamichi, N., and Mizuno, T. (2013). Clock-controlled and FLOWERING LOCUS T (FT)-dependent photoperiodic pathway in Lotus japonicus II: characterization of a microRNA implicated in the control of flowering time. Bioscience, biotechnology, and biochemistry, 120872.

Yan, J., Gu, Y., Jia, X., Kang, W., Pan, S., Tang, X., Chen, X., and Tang, G. (2012). Effective small RNA destruction by the expression of a short tandem target mimic in Arabidopsis. The Plant cell **24,** 415-427.

Yano, K., Yoshida, S., Müller, J., Singh, S., Banba, M., Vickers, K., Markmann, K., White, C., Schuller, B., and Sato, S. (2008). CYCLOPS, a mediator of symbiotic intracellular accommodation. Proceedings of the National Academy of Sciences **105,** 20540-20545.

Yano, K., Aoki, S., Liu, M., Umehara, Y., Suganuma, N., Iwasaki, W., Sato, S., Soyano, T., Kouchi, H., and Kawaguchi, M. (2016). Function and evolution of a Lotus japonicus AP2/ERF family transcription factor that is required for development of infection threads. DNA Research **24,** 193-203.

Yashima, H., Fujikake, H., Sato, T., Ohtake, N., Sueyoshi, K., and Ohyama, T. (2003). Systemic and local effects of long-term application of nitrate on nodule growth and N2 fixation in soybean (Glycine max [L.] Merr.). Soil Science and Plant Nutrition **49,** 825-834.

Yokota, K., Fukai, E., Madsen, L.H., Jurkiewicz, A., Rueda, P., Radutoiu, S., Held, M., Hossain, M.S., Szczyglowski, K., and Morieri, G. (2009). Rearrangement of actin cytoskeleton mediates invasion of Lotus japonicus roots by Mesorhizobium loti. The Plant cell **21,** 267-284.

Yoro, E., Nishida, H., Ogawa-Ohnishi, M., Yoshida, C., Suzaki, T., Matsubayashi, Y., and Kawaguchi, M. (2019). PLENTY, a hydroxyproline O-arabinosyltransferase, negatively regulates root nodule symbiosis in Lotus japonicus. Journal of experimental botany **70,** 507-517.

Yu, B., Yang, Z., Li, J., Minakhina, S., Yang, M., Padgett, R.W., Steward, R., and Chen, X. (2005). Methylation as a crucial step in plant microRNA biogenesis. Science (New York, N.Y.) **307,** 932-935.

Yu, Y., Ni, Z., Wang, Y., Wan, H., Hu, Z., Jiang, Q., Sun, X., and Zhang, H. (2019). Overexpression of soybean miR169c confers increased drought stress sensitivity in transgenic Arabidopsis thaliana. Plant Science **285,** 68-78.

Yuan, S., Zhu, H., Gou, H., Fu, W., Liu, L., Chen, T., Ke, D., Kang, H., Xie, Q., and Hong, Z. (2012). A ubiquitin ligase of symbiosis receptor kinase involved in nodule organogenesis. Plant physiology **160,** 106-117.

Zhang, Y., Wiggins, B.E., Lawrence, C., Petrick, J., Ivashuta, S., and Heck, G. (2012). Analysis of plant-derived miRNAs in animal small RNA datasets. BMC genomics **13,** 381-381.

Zhao, M., Ding, H., Zhu, J.K., Zhang, F., and Li, W.X. (2011). Involvement of miR169 in the nitrogen-starvation responses in Arabidopsis. New phytologist **190,** 906-915.

Zheng, L.-y., Zhang, Z.-j., Zhang, J.-m., Li, X.-w., Huang, J., Lin, W.-c., Li, W.-d., Li, C.-r., and Lu, Y.-b. (2019). Selection of reference genes for RT-qPCR analysis of Phenacoccus solenopsis (Hemiptera: Pseudococcidae) sex-dimorphic development. Journal of Integrative Agriculture **18,** 854-864.

Zhu, F., Ye, Q., Chen, H., Dong, J., and Wang, T. (2021). Multigene editing reveals that MtCEP1/2/12 redundantly control lateral root and nodule number in Medicago truncatula. Journal of Experimental Botany **72,** 3661-3676.

Zhu, H., Chen, T., Zhu, M., Fang, Q., Kang, H., Hong, Z., and Zhang, Z. (2008). A novel ARID DNA-binding protein interacts with SymRK and is expressed during early nodule development in Lotus japonicus. Plant physiology **148,** 337-347.

Zhu, H., Hu, F., Wang, R., Zhou, X., Sze, S.-H., Liou, L.W., Barefoot, A., Dickman, M., and Zhang, X. (2011). Arabidopsis Argonaute10 specifically sequesters miR166/165 to regulate shoot apical meristem development. Cell **145,** 242-256.